Characterization of Dissolved Organic Matter and Reduced Sulfur in Coastal Marine and Estuarine Environments: Implications for Protective Effects on Acute Copper Toxicity

by

Sarah G.S. DePalma

A thesis
presented to the University of Waterloo
in fulfillment of the
thesis requirement for the degree of
Master of Science
in
Biology

Waterloo, Ontario, Canada, 2009

I hereby declare that I am the sole author of this thesis. This is a true copy of the thesis, including any required final revisions, as accepted by my examiners.

I understand that my thesis may be made electronically available to the public.

Abstract

Copper-induced toxicity in aqueous systems depends on its speciation and bioavailability. Dissolved organic matter (DOM) and reduced sulfur species can complex copper, influencing speciation and decreasing bioavailability. DOM composition in estuaries can vary, depending on allochthonous, autochthonous, or wastewater source. At a molecular level, variability in DOM quality potentially results in different copper binding affinities. The aim of this study was to characterize and quantify DOM and reduced sulfur in estuaries and investigate possible correlations between these parameters and the capacity to complex copper, reducing its toxicity. This study will have implications on the development of marine-specific toxicity prediction models. DOM was characterized in seventy-one estuarine samples through DOC concentration and fluorescence measurements, combined with spectral resolution techniques, to quantify humic-, fulvic-, tryptophan-, and tyrosine-like fractions. Reduced sulfur was measured by the chromium-reducible sulfide (CRS) technique. Acute copper toxicity tests were done on a subset of samples expressing extreme DOC, fluorescent allochthonous, autochthonous, and CRS concentrations. The results showed significant differences in DOM quality, independent of DOC concentration. In terms of total fluorescent material, humic-like material ranged from 9.48% to 66.1%, followed by fulvic-like with a range of 14.5% to 63.2%, and 0.00% to 36.5% for tryptophan-like and 0.64% to 25.2% for tyrosine-like material. CRS was widely variable among the samples; concentrations ranging from 0.5 nM to 7800 nM. The toxicity results suggested DOC was a very good predictive measure of copper EC_{50} in estuaries ($r^2 = 0.84$) independent of DOM quality. Furthermore, CRS was saturated at low copper concentrations indicating strong binding sites for copper, suggesting that while CRS is protective, it does not bind copper at toxicologically relevant concentrations and therefore is not a good predictive measure of copper toxicity.

Acknowledgements

I am deeply grateful to my supervisor, Dr. Scott Smith, for giving me the opportunity to work on this project and to learn so much along the way. I am thankful for his encouragement, patience (especially with my stubbornness at times), and experiences aplenty. His positive outlook and enthusiasm from a scientific perspective has made me a strong believer that chemistry can be sexy. I feel very privileged to have worked under his supervision.

My appreciation extends to Dr. Ray Arnold. Thanks to his continuous encouragement and invaluable advice on life after school, I have a clearer outlook on what I careers I can attain with my education. Thank you for all the exciting experiences in San Francisco and Napa Valley, I will not forget it.

I would also like to sincerely thank Dr. Jim McGeer for the long discussions that helped me sort out the technical toxicology details of my work. I am also thankful to him for challenging me to look at at my research from a different perspective. His detailed comments, feedback, and insights were incredibly helpful.

I am grateful to Dr. George Dixon and Dr. Mark Servos whom have generously given their time and expertise to better my work. I thank them for their contribution and their good-natured support.

I am indebted to numerous others with whom I have interacted during the course of my graduate studies. Particularly, I would like to acknowledge Dr. Russell Bell and Dr. Jim Kramer for use of the CRS apparatus and for looking out for me in Sydney. I am also thankful to Jeff Cotsifas and everyone at Pacific EcoRisk for teaching me how to run my toxicity assays, in perfect detail. These tests went very smoothly because of their instructions. My sincere thanks to Bob Santore at HydroQual for calculating the free copper concentrations. I am grateful for the help from Dr. R.J. O'Hara Hines and Ximena Camacho from the University of Waterloo Statistical Consulting Department for development of the partial factorial design and assistance with the t-test analysis. Many thanks to Linda Zepf from the University of Waterloo Biology Department for going over and above her duties when I had an endless supply of administrative questions and concerns. I would also like to thank the Copper Development Association for funding and to the University of Waterloo for my financial assistance through scholarships, bursaries, and the teaching assistant positions.

I am appreciative of the friends I made along the way, who kept me sane through the stressful patches and were there to share the fun times: Phil Lynett for keeping my social life active and successfully persuading me to spend Friday evenings at Wilf's with all the hilarious organic chemists (ps. good luck at Queens!), Jane Gohl for all the wonderful talks, both happy and sad ones, and all the invaluable advice, and to all my lab-mates in the CLEAR lab, especially Becky Gilmore for the recipe-swapping, wine and cheese parties (maybe we are Suzy-homemakers), and being my gym buddy. It was really nice working and sharing stories with you

these past two years and I hope it continues (minus the thesis-related stress, of course).

To my family for all the love and emotional support. Especially my mom for always being there for me. Hearing her voice over the phone always made my day. I did this for you.

Most importantly, I want to thank Ken Maly for not only proof-reading practically everything I wrote and providing many stylistic suggestions to help me improve my presentations and clarify my arguments, but also for being very understanding, fully supportive, and a loving, caring, man in my life. I love you.

For my Babcia, Svitlana Yurkiv, my mom, Marie DePalma, and my sister, Nati.

Contents

List of Tables

List of Figures

Chapter 1

Introduction

1.1 Copper in Coastal Marine and Estuarine Environments

Copper is naturally found in rocks and sediment which contribute dissolved copper into surface waters through natural erosion and runoff. Natural runoff has been reported to contribute between 0.03 μg Cu·L^{-1} and 0.23 μg Cu·L^{-1} (0.0005 μM to 0.004 μM) into surface coastal seawater (Bowen, 1985). With its durability, malleability, and conductivity benefits, elemental copper is widely used in numerous industrial processes, which increases dissolved copper concentrations via wastewater runoff. In addition, antifouling paints on the hulls of recreational vessels has been a major concern in coastal waters, releasing an average of 3.7 to 4.3 μg Cu·cm^{-2}·day^{-1} (Schiff et al., 2004). With over 53% of the US population living along the coast, growing by 1.1 million per year (NOAA, 2004), it is important to research the toxicity of copper in these environments. Although it is an essential element, with a recommended daily allowance of 0.9 mg·day^{-1} for adult men and women (Food and Nutrition Board and Institute of Medicine, 2001), elevated concentrations of copper by way of industrial output increase its potential detrimental impact on aquatic life.

As copper enters estuarine systems, it undergoes a complex set of reactions

influenced by pH, salinity, and other various ions, which results in heterogeneity of aqueous copper species. An equilibrium model of Cu(II) species with respect to salinity is illustrated in Figure 1.1.

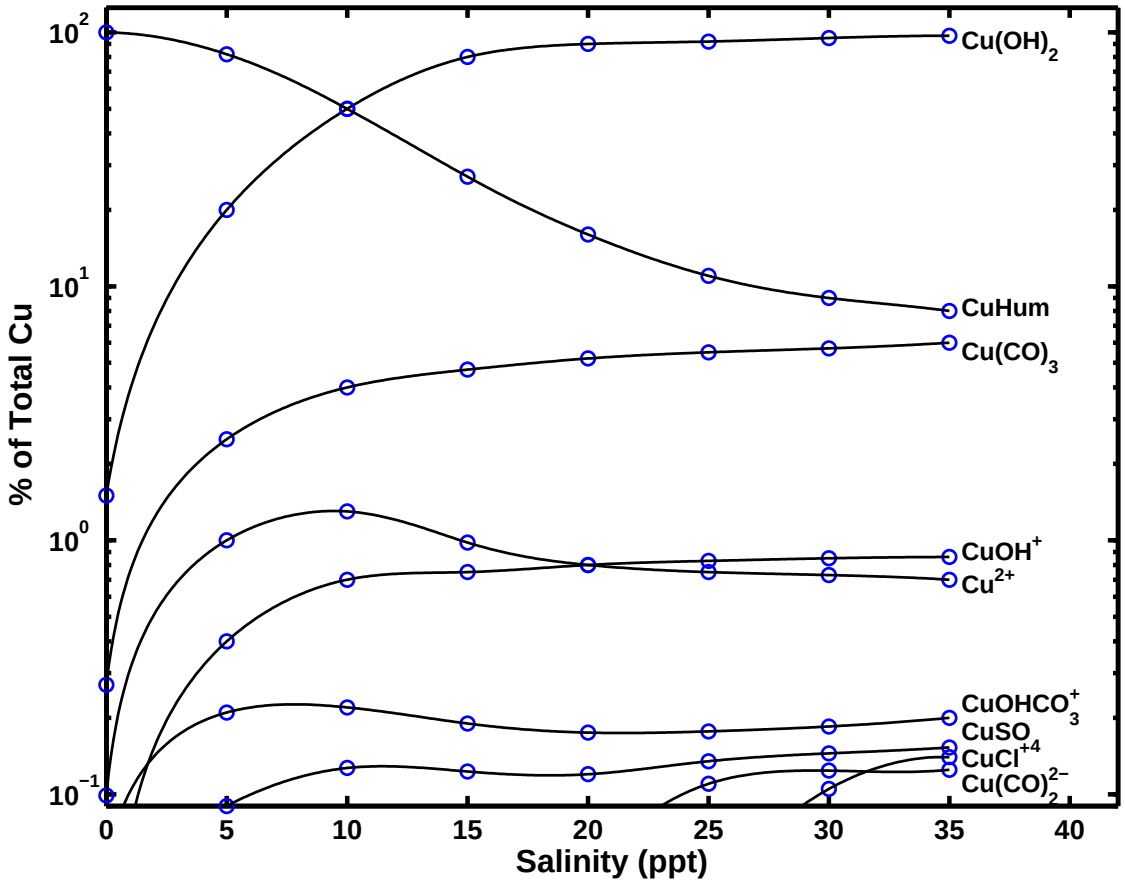

Figure 1.1: Proposed equilibrium model describing the change in Cu(II) speciation across a salinity gradient from 0 to 35 ‰ with a pH of 8 (Adapted from: Leppäkoski and Bonsdorff (1989)). 'CuHum' represents copper-humic complexation, signifying copper bound to organic matter across the salinity gradient seen here.

For marine systems, in terms of water chemistry conditions, pH has the least effect because seawater is a natural buffer system with a relatively constant pH between 7.8 and 8.3 in coastal marine waters (Millero, 2001) and 7.5 to 8.8 in estuaries (Day et al., 1989). At equilibrium, copper speciation varies among free copper ions, complexation by dissolved natural ligands (possibly $Cu(OH)_2$, copper-humic (CuHum), $Cu(CO)_3$, $CuOH^+$, $CuOHCO_3^+$, $CuSO_4$,

$CuCl^+$, $Cu(CO)_2^{2-}$), and adsorption on particulate or colloidal matter (possibly CuHum) across the salinity gradient, as seen in Figure 1.1. The copper species readily available for biotic uptake, known as 'bioavailable' species, typically refer to free Cu^{2+} and $CuOH^+$ (Figure 1.1) (De Schamphelaere and Janssen, 2002). Therefore, copper toxicity in estuaries is influenced by the chemical characteristics of the site in which the copper is found. Furthermore, these chemical characteristics potentially vary over time and by location. This suggests that copper toxicity may have both spatial and temporal dependence. In particular, bioavailability of copper in estuarine waters is influenced by both natural and anthropogenic input from surrounding coastal environments. In the development of a marine-specific biotic ligand model (BLM), these measurements would be used as input parameters for a computerized chemistry-based BLM, similar to existing freshwater BLMs. Freshwater BLMs, such as the HydroQual© BLM, is a numerical approach to predicting metal toxicity through complex chemical equilibrium modelling (DiToro et al., 2001; Santore et al., 2001; Paquin et al., 2002).

The focus of this thesis project is to determine the protective effects of two potential input parameters for a marine-specific BLM: dissolved organic matter (DOM) and chromium(II) reducible sulfide (CRS). DOM is known to vary in concentration and molecular composition with respect to its origin such as watershed runoff, autotroph activity in the water column, and wastewater effluent. Similarly, CRS is thought to vary with source in addition to naturally-occurring hydrolysis and reduction reactions in marine waters. Both DOM and CRS are known to complex copper and so have the potential to mitigate copper toxicity in coastal marine and estuarine environments. DOM (represented as dissolved organic carbon concentrations) is predictive of copper EC_{50} (Arnold et al., 2006), but the correlation between copper EC_{50} and CRS is unknown.

1.2 Dissolved Organic Matter

One of the most common measures of DOM is done by quantifying dissolved organic carbon (DOC) concentrations in mg $C{\cdot}L^{-1}$. Increases in the concentration of DOC will decrease the bioavailability and toxicity of copper in marine water (Arnold, 2005). Typical DOC concentrations in the open ocean range from about 0.7 mg $C{\cdot}L^{-1}$ to 0.9 mg $C{\cdot}L^{-1}$, coastal zones are around 2 mg $C{\cdot}L^{-1}$, and river estuaries have been reported with concentrations that may reach 10 mg $C{\cdot}L^{-1}$ and higher (Dafner and Wangersky, 2002b, and references therein).

DOM can be characterized based on differences in molecular size, shape, and reactive functional moities. In terms of molecular size, DOM can be considered a subset of total organic matter (total OM). Total OM describes a broad classification of organic molecules in aquatic systems. Further classification has been done on total OM based on molecular size, as illustrated in Figure 1.2.

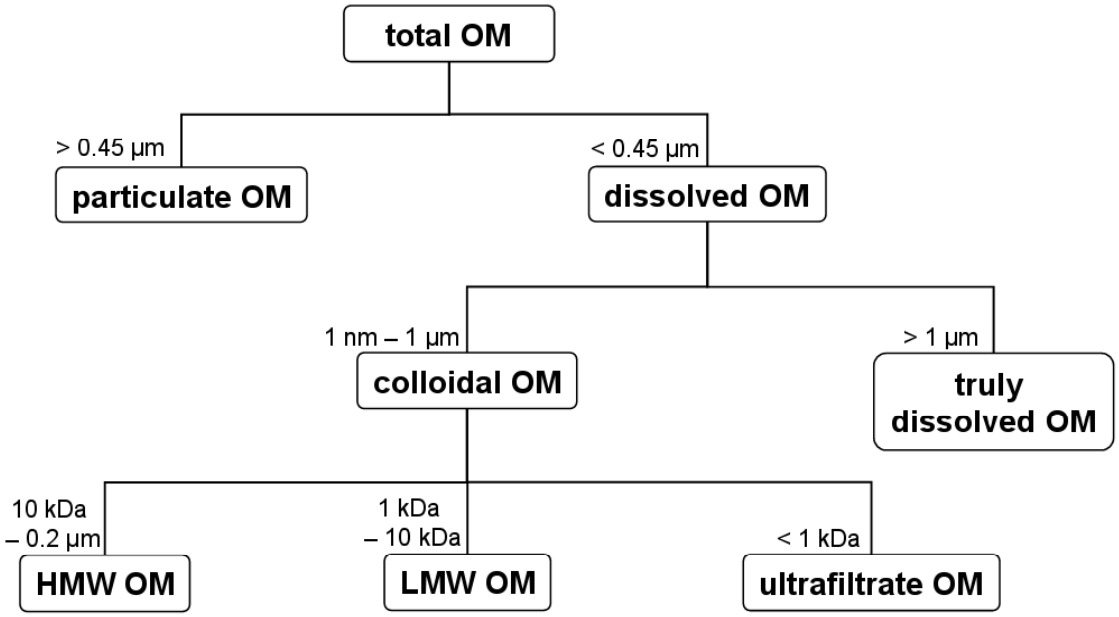

Figure 1.2: Classification of organic matter, based on molecular size (Adapted from: Dafner and Wangersky (2002b)). OM = organic matter, HMW = high molecular weight, LMW = low molecular weight.

Total OM is commonly separated into particulate OM and DOM (Figure 1.2). This initial separation is based on filtration through a 0.45 μm membrane filter. Further classification of DOM separates colloidal OM (1 nm to 1 μm) from truly dissolved OM (>1 μm) (Dafner and Wangersky, 2002b). Colloidal OM can be further separated into three classes: high molecular weight colloidal OM (10 kDa to 0.2 μm), low molecular weight colloidal OM (10 kDa to 1 kDa), and ultrafiltrate OM (<1 kDa) (Dafner and Wangersky, 2002b). In this study, DOM is operationally defined as OM that passes through a 0.45 μm membrane filter.

Characterization of DOM based on molecular shape and reactive functional groups is especially important with respect to copper complexation. The nature, or 'quality' of marine DOM, is influenced by input sources. In the open ocean, DOM is predominantly aliphatic (Harvey et al., 1983) where most of it originates from marine microorganisms and rainwater input (Dafner and Wangersky, 2002b). Furthermore, marine DOM from the open ocean has been found to exist as large macromolecular structures linking lipids, carbohydrates, acetates and proteins (Aluwihare et al., 1997; Dafner and Wangersky, 2002b). Amino acids, as macromolecular protein structures, are found to contribute about 20% DOC, which was seen in Chesapeake Bay (Sigleo and Means, 1990). This amount of amino acids may be a significant contribution of amine functional groups capable of reacting with Cu(II). The molecular structures of tryptophan and tyrosine, which are easily characterized amino acids, are illustrated in Figure 1.3.

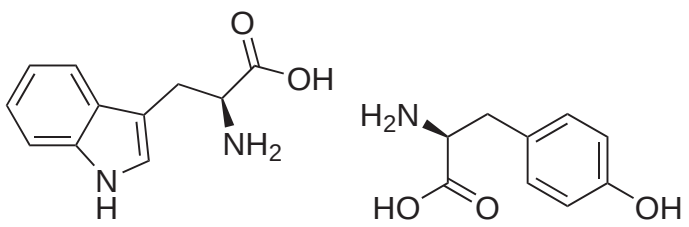

Figure 1.3: Molecular structures of tryptophan (left) and tyrosine (right).

In contrast, coastal marine and estuaries contain more aromatic DOM, originating from terrestrial degradation and lignin oxidation (Harvey et al., 1983). Examples of highly aromatic DOM are humic structures primarily consisting of humic and fulvic acids, as illustrated with representative structures in Figure 1.4. Both humic and fulvic material contain aromatic structural groups with an abundance of carboxylic and phenolic reactive functional groups, followed by amine, and sulfidic reactive functional groups to a lesser extent, all of which could potentially bind to metals (Malcolm, 1990).

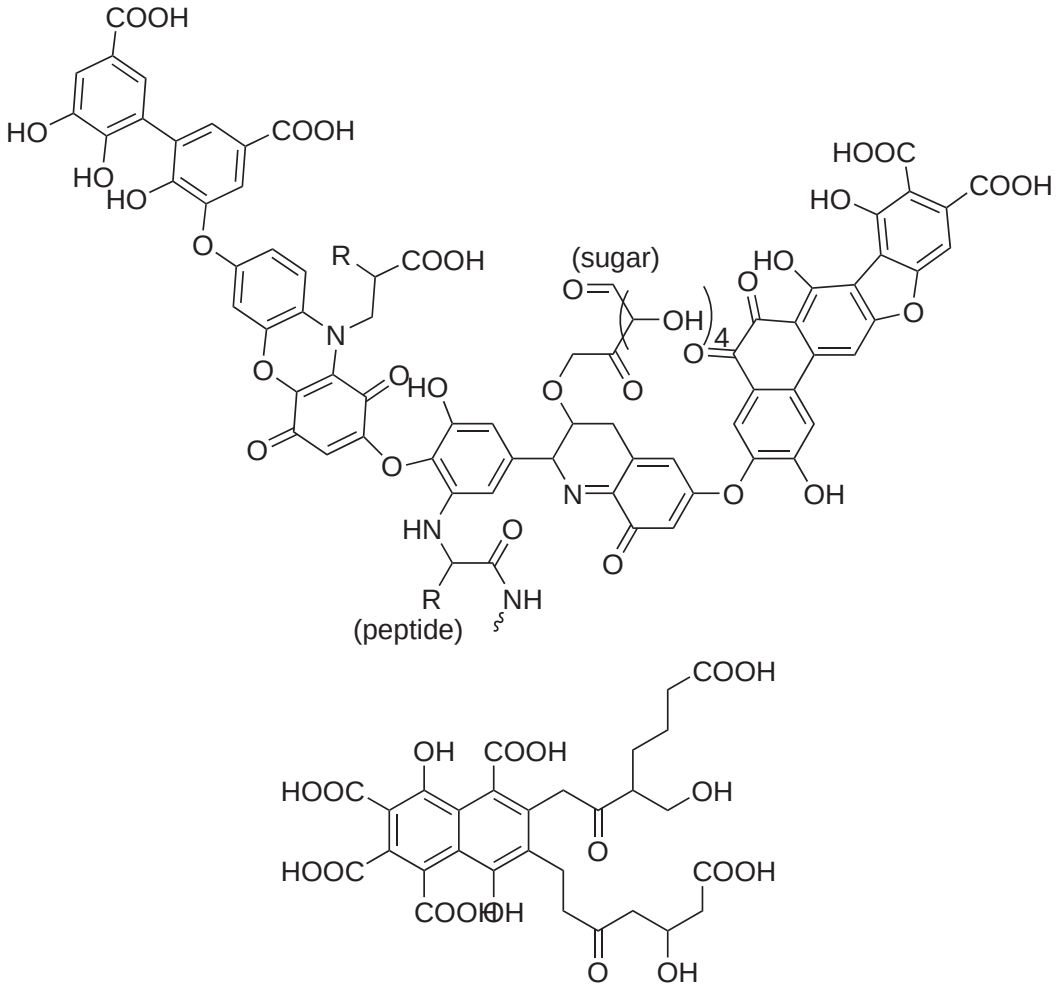

Figure 1.4: Representative fragment structures of humic acid (top) and fulvic acid (bottom).

The difference between humic and fulvic material is twofold. Humic material is typically considered higher in molecular weight ranging from 1,500 kDa to 5,000 kDa, whereas fulvic acid ranges from about 600 to 1,000 kDa (Malcolm, 1990). However, there is some ambiguity in these values since the actual structures that make up humic and fulvic material have not been fully characterized (Hessen and Tranvik, 1998). The second and more commonly accepted difference is that humic material is insoluble in solutions below pH 2, which was operationally-defined with origins in soil chemistry (Ma et al., 2001; McDonald et al., 2004, and references therein). In coastal marine and estuarine waters where the pH is approximately 8.0, the high abundance of carboxylic functional groups in gives these humic substances a net negative charge via deprotonation, resulting in available sites for copper complexation (Harvey et al., 1983).

A high population along the coast results in higher amounts of anthropogenic effluent, which contributes higher quantities of both terrestrial and proteinaceous material through increased wastewater runoff and algal activity. Sedlak et al. (1997) proposed that a large percentage of copper found in wastewater effluent is complexed with strong ligands ($\log K > 10$), as opposed to humic substances that otherwise contribute moderately-strong binding sites. Furthermore, van Veen et al. (2002) found that the complexation capacity of wastewater DOM with copper decreased copper toxicity by 4-fold in both fresh and estuarine waters. Since characterization of DOM in coastal marine and estuarine waters is a focus of this study, the variation in DOM quality with respect to site location is key and may influence the bioavailability of copper in these environments.

1.2.1 DOM Quality

In terms of organic matter quality based on input source, DOM can be initially categorized by two broad end-member classes: allochthonous carbon and autochthonous carbon (McKnight et al., 2001). However, there is considerable

variability within the nature of these two end-members themselves. A simple diagram illustrating the range of organic matter quality by input source can be found in Figure 1.5.

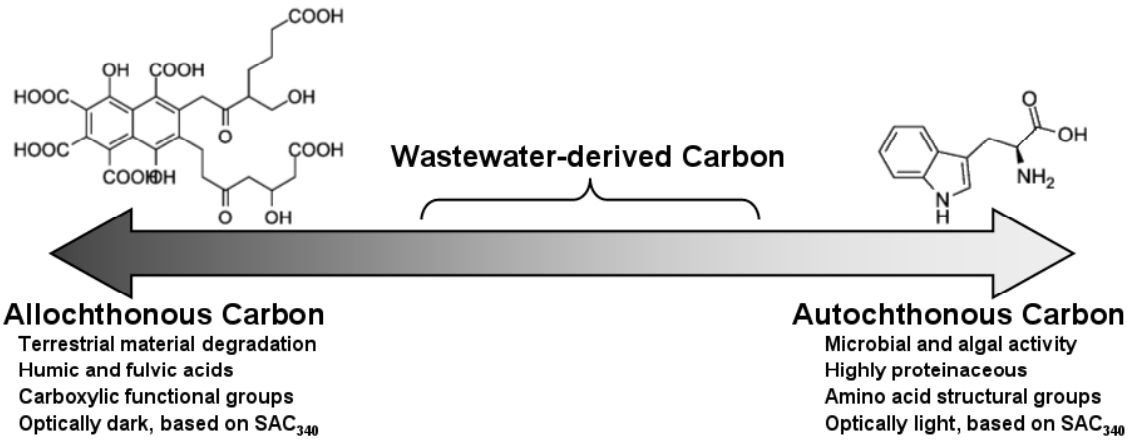

Figure 1.5: Scale of organic matter quality with respect to input source (Schwartz et al., 2004; Winter et al., 2007).

Allochthonous carbon is derived from terrestrial input, consisting primarily of humic and fulvic material (McKnight et al., 2001), representative structures shown in Figure 1.4. In contrast, autochthonous carbon is generated in the water column through microbial and algal activity (McKnight et al., 2001). It is highly proteinaceous in nature and is characterized by amino acid structural groups. Example structures of amino acid binding blocks are shown in Figure 1.3. Intermediate between the two end-member classes is wastewater-derived organic matter, which include material of both humic and proteinaceous fractions in different proportions. Baker (2001) reported distinct fluorescent signatures of tryptophan and fulvic acid in approximately equal intensity ratios present in sewage wastewater effluent.

Relative amounts of allochthonous and autochthonous carbon can be approximated by their specific absorption coefficient at 340 nm (SAC_{340}). Schwartz et al. (2004) quantified the influence of allochthonous and autochthonous carbon on metal

toxicity to rainbow trout in freshwater systems based on the optical characteristics of these end-members at 340 nm. Toxicity studies reported that both optically-dark allochthonous and optically-light autochthonous material significantly decreased copper bioavailability, however the former had a greater protective effect than the latter (Schwartz et al., 2004). Winter et al. (2007) further characterized DOM in freshwater via fluorescence spectroscopy, where qualitative separation of allochthonous carbon into humic- and fulvic-like fractions and autochthonous carbon into tryptophan- and tyrosine-like fractions was performed. Fluorescence, in combination with parallel factor analysis (PARAFAC) has been a useful tool in quantifying a defined number of fluorescent fractions in both fresh and marine water (Mopper and Schultz, 1993; Coble, 1996; Stedmon and Markager, 2005; Hall and Kenny, 2007).

1.2.2 DOM Quality Characterized by Fluorescence

Fluorescence spectroscopy is a highly sensitive and selective technique that can elucidate molecules from a heterogeneous system based on their aromatic structural groups. When the molecules are excited with a wavelength of UV or visible light (high energy) some of the energy is absorbed to produce a short-lived (order of 10^{-9} s) excited state. The excited molecule can release energy by re-emitting heat or light of longer wavelengths (lower energy). A Jablonski Diagram can be used to illustrate the energy-level transition from excitation to emission, as seen in Figure 1.6.

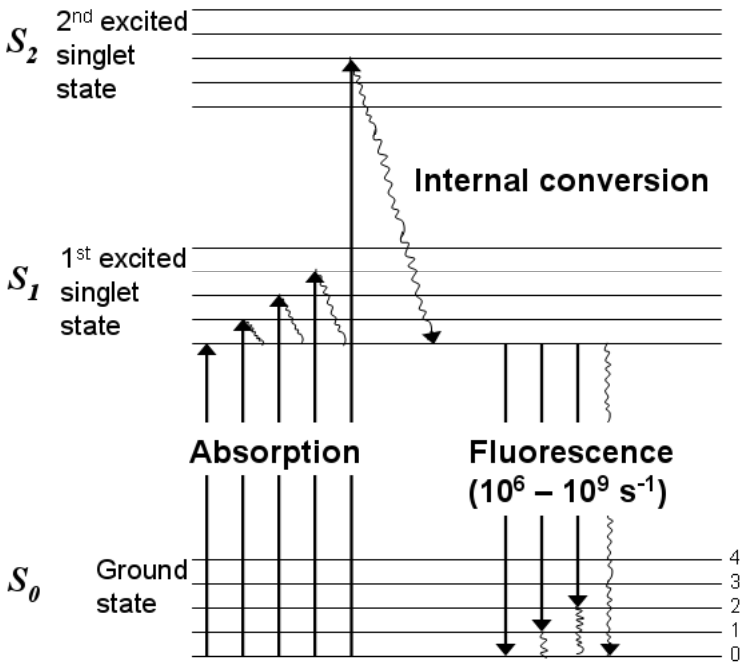

Figure 1.6: A Jablonski diagram indicating the absorption of energy once the molecule is excited, followed by emission between 10^{-6} and 10^{-9} seconds, unique to fluorescence.

The difference in energy between the ground state (S_0) and the excited singlet states (S_1, S_2,...S_n) identifies the wavelengths of the energy absorbed. Following absorption (or excitation), vibrational relaxation to the lowest energy sublevel of S_n occurs, which is considered radiationless that converts light to heat (Figure 1.6). At this point, one of three scenarios can take place: radiationless internal conversion back down to S_0, radiationless intersystem crossing between other singlet or triplet states ($S_1 \longleftarrow S_2$ for example), or fluorescence. Fluorescence describes the emission of radiation as a photon corresponding to $S_0 \longleftarrow S_1$ transition (Figure 1.6). The wavelength of fluorescence emission is dependent on the energy difference between the S_0 and S_1 states where a lesser (less energy) difference returns a longer fluorescence wavelength.

Simple fluorophores typically have a unique emission maximum, however may absorb more than one excitation wavelength. The fluorescent emission spectral shape is independent of the excitation wavelengths, resulting in excitation/emission

(Ex/Em) pairs for different fluorophores. A fluorescence excitation-emission matrix (FEEM) is the result of compiling data from simultaneous scanning of excitation and emission wavelengths over the fluorescence spectrum. When observed as a contour plot, FEEMs provide qualitative information on the molecular structures of fluorophores based on their peak positions. Therefore distinctions can be made between fluorophores in a complex mixture in solution, based on their fluorescing characteristics. An example of a fluorescence contour plot can be found in Figure 1.7.

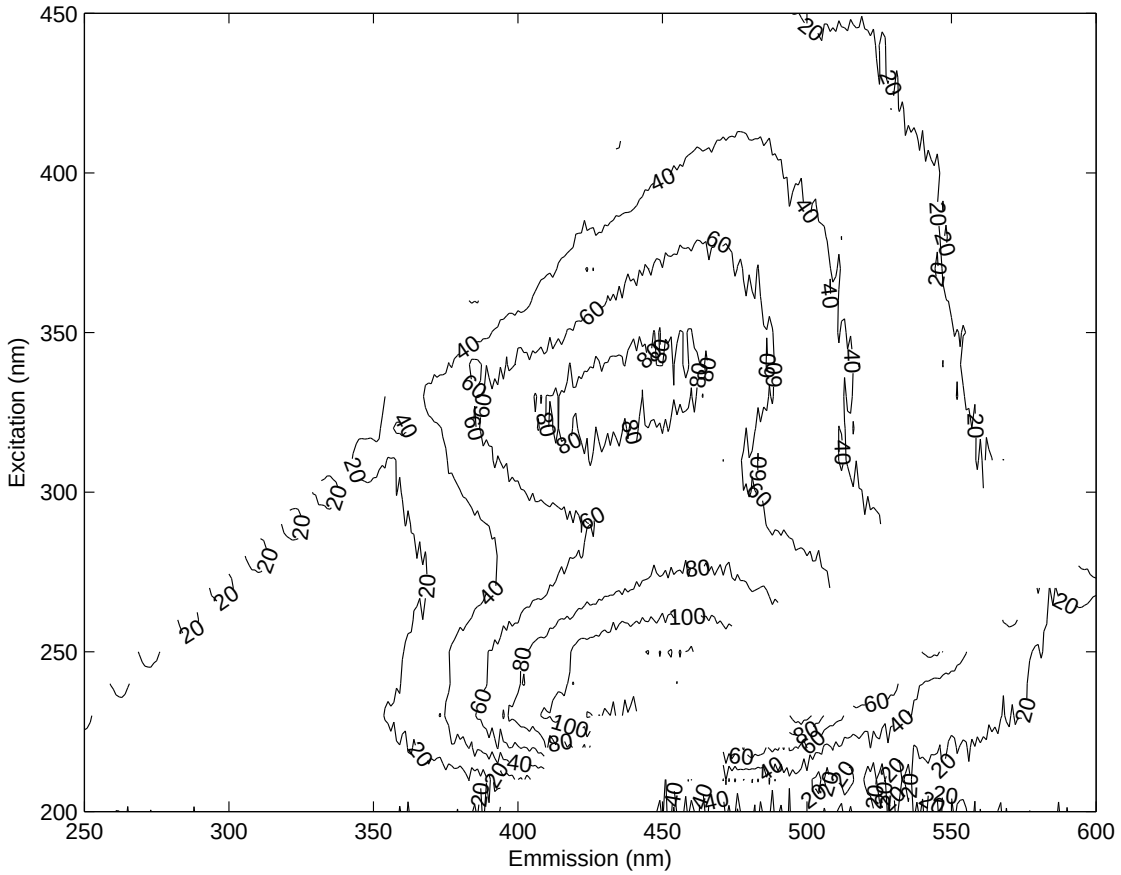

Figure 1.7: FEEM of Nordic River DOM in synthetic seawater, displayed as a contour plot. It is seen here that there are emission maxima at approximately 400 - 500 nm corresponding to two excitation maxima at approximately 275 nm and 325 nm.

Figure 1.7 is of Nordic River DOM dissolved in artificial seawater. The key features in Figure 1.7 are the Ex/Em wavelength pairs at approximately 275 - 325 nm / 425 nm and 275 - 325 nm / 460 nm. For allochthonous carbon within DOM, fulvic-like and humic-like fractions are the predominant fluorescent components, due to their high abundance of aromatic structural groups, and can be detected by Ex/Em wavelengths of 300 - 350 nm / 400 - 450 nm and 250 - 390 nm / 460-520 nm respectively (McKnight et al., 2001; Stedmon and Markager, 2005). For autochthonous carbon, the fluorescent groups consist of fractions incorporating the amino acids tryptophan and tyrosine due to their aromaticity. FEEMs of pure tryptophan and tyrosine dissolved in synthetic seawater are illustrated in Figure 1.8. The intensity values, labelled along the contour lines in Figures 1.7 and 1.8 are related to the abundance of each fluorophore as well as its fluorescence efficiency.

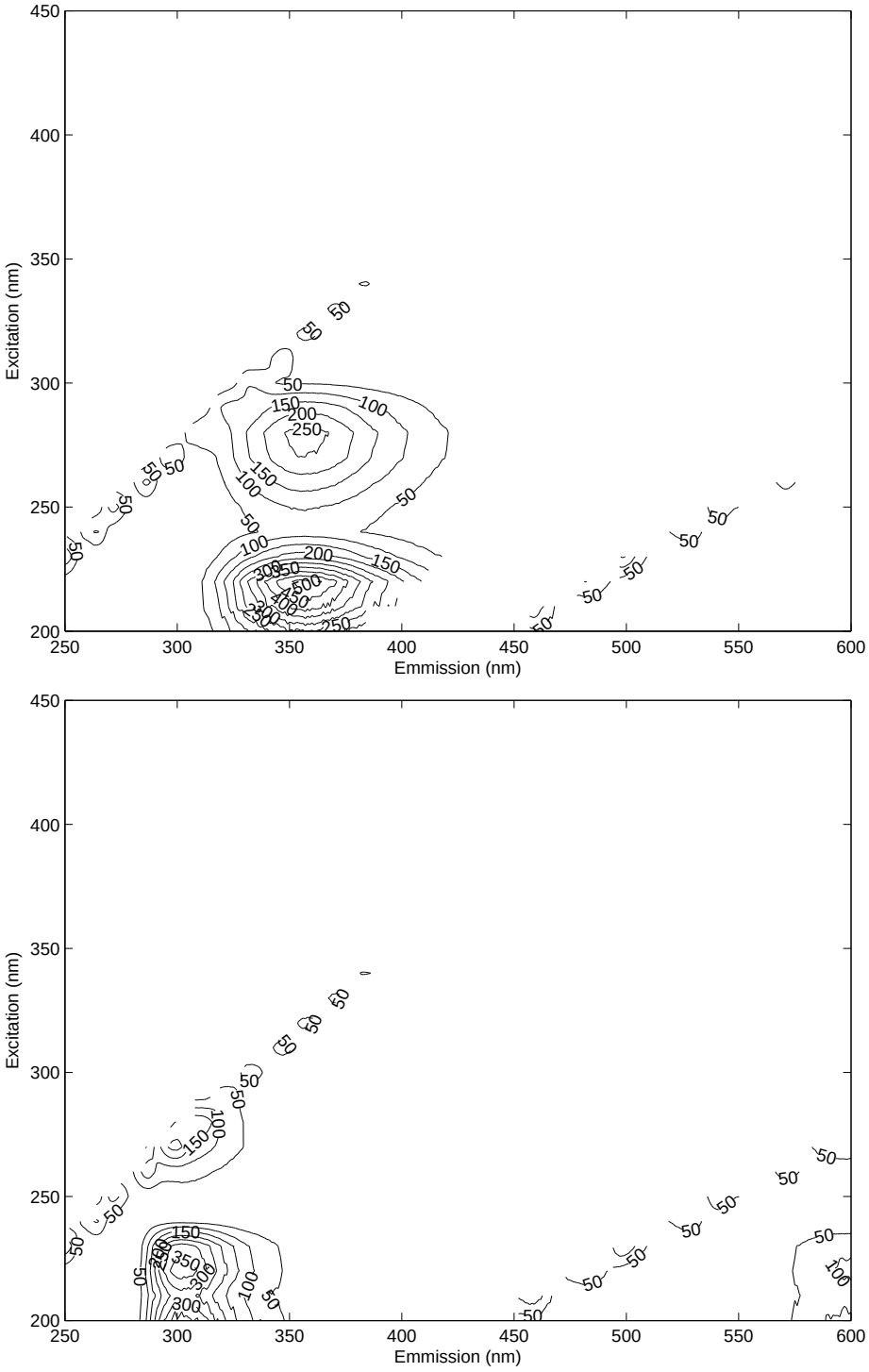

Figure 1.8: FEEMs of standard tryptophan (top) and tyrosine (bottom) solutions in synthetic seawater. It is seen here that tryptophan has an emission maximum at 350 nm while the emission maximum of tyrosine is 300 nm. Both emission wavelengths correspond to two excitation maxima at 225 nm and 275 nm.

Tryptophan-like and tyrosine-like Ex/Em peaks are in the ranges of 225 - 275 nm / 350 nm and 225 - 275 nm / 300 nm respectively (Baker, 2001; Stedmon and Markager, 2005). Phenylalanine also contains an aromatic ring in its molecular structure, but cannot be easily identified by fluorescence due to its low quantum yield. Phenylalanine is relatively nonpolar and so does not exhibit a strong dipole-moment when excited with high energy, which equates to a small extinction coefficient resulting in low absorption as identified by Beer's Law. Lower absorption results in lower emission that may not be detectable during the excitation-emission scans. However, the Em/Ex wavelength pairs for phenylalanine are 280 nm / 240 nm (Du et al., 1998). Although only a small fraction of total DOM is fluorescent, fluorescence spectroscopy provides insight into the qualitative differences between organic fractions in DOM.

1.2.3 Parallel Factor Analysis

To quantify in relative terms, the humic-, fulvic-, tryptophan-, and tyrosine-like fractions observed by fluorescence, spectral deconvolution via PARAFAC is used. PARAFAC is a 3-dimensional algorithm that defines a minimum number of independent fluorescent components, their fluorescent spectra, as well as their abundance in each water sample analyzed (Stedmon et al., 2003). It is accomplished through converting a series of large multi-variate data sets into a simple linear calculation that includes the number of components, the component spectra, and the abundance of each component as three separate variables. This mathematical approach has been successful in identifying separate fluorescent fractions in both freshwater (Stedmon et al., 2003), estuaries, and seawater (Stedmon and Markager, 2005; Hall and Kenny, 2007; Nadella et al., 2009).

When using PARAFAC, it is important to set the model to extract a number of fluorescent components that is considered mathematically reasonable in describing the data. Since this tri-linear model is calculated simultaneously for all fluorescent

components, a higher number of components results in a better fit of data with little undefined residual data, typically attributed to spectroscopic noise. Consequently, higher amounts of residual data is modelled and true components are separated and defined as multiple, correlating components. Recently, Stedmon and Markager (2005) resolved 8 components that described the fluorescent data of 1276 freshwater samples using PARAFAC analysis. With a very large data set as reported in Stedmon and Markager (2005), 8 components was considered spectrally reasonable in defining groups of fluorophores with similar fluorescing characteristics, as seen in Figure 1.9.

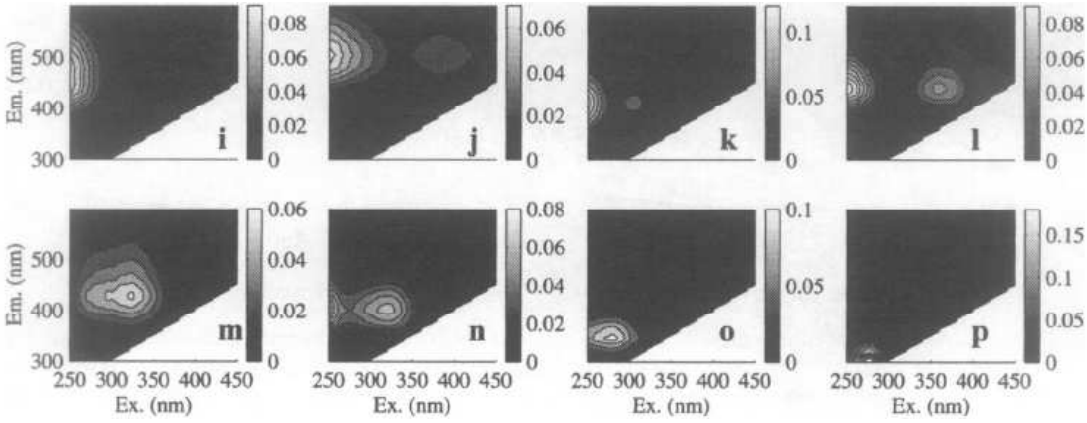

Figure 1.9: Spectra of 8 components defined by PARAFAC (Stedmon and Markager, 2005).

Stedmon and Markager (2005) found that higher than 8 components resulted in the modelling of instrument noise and the separation of components into co-varying components. Similarly, Hall and Kenny (2007) reported using PARAFAC to resolve 5 components from FEEMs of 2 estuarine and 1 freshwater sample. Differences between marine and freshwater humic acid was observed and both tryptophan-like and tyrosine-like components were resolved. However, their 5^{th} component had no conclusive identification and was classified as mathematical noise (Hall and Kenny, 2007). This study aims for a more simple classification scheme by resolving 4 fluorescent components in a data set of 72 coastal marine and estuarine samples. It is expected that 4 components would be mathematically reasonable, resulting in

little residual data, as well as spectroscopically reasonable in identifying humic-, fulvic-, tryptophan-, and tyrosine-like fluorescent fractions. This scheme should result in the simplest model that describes the data statistically well.

1.3 Reduced Sulfur

Sulfur is classified as a Group B soft ligand with a broad span of oxidation states (± 2, 4, 6). These characteristics result in a strong affinity for coordination with soft Group B metals, such as copper, due to their high polarizability. Another characteristic of sulfur is its ability to form catenated sulfide ions (S_n^{2-}), which serve as chelating ligands for soft metals resulting in (meta)stable metal-sulfide clusters. However the molecular structure of these metal-sulfide clusters are not well understood (Bianchini and Bowles, 2002), which makes quantifying reduced sulfur with respect to metal toxicity difficult. Dehnen et al. (1996) has demonstrated the stability of (meta)stable copper-sulfide clusters through molecular modeling techniques, as seen in Figure 1.10.

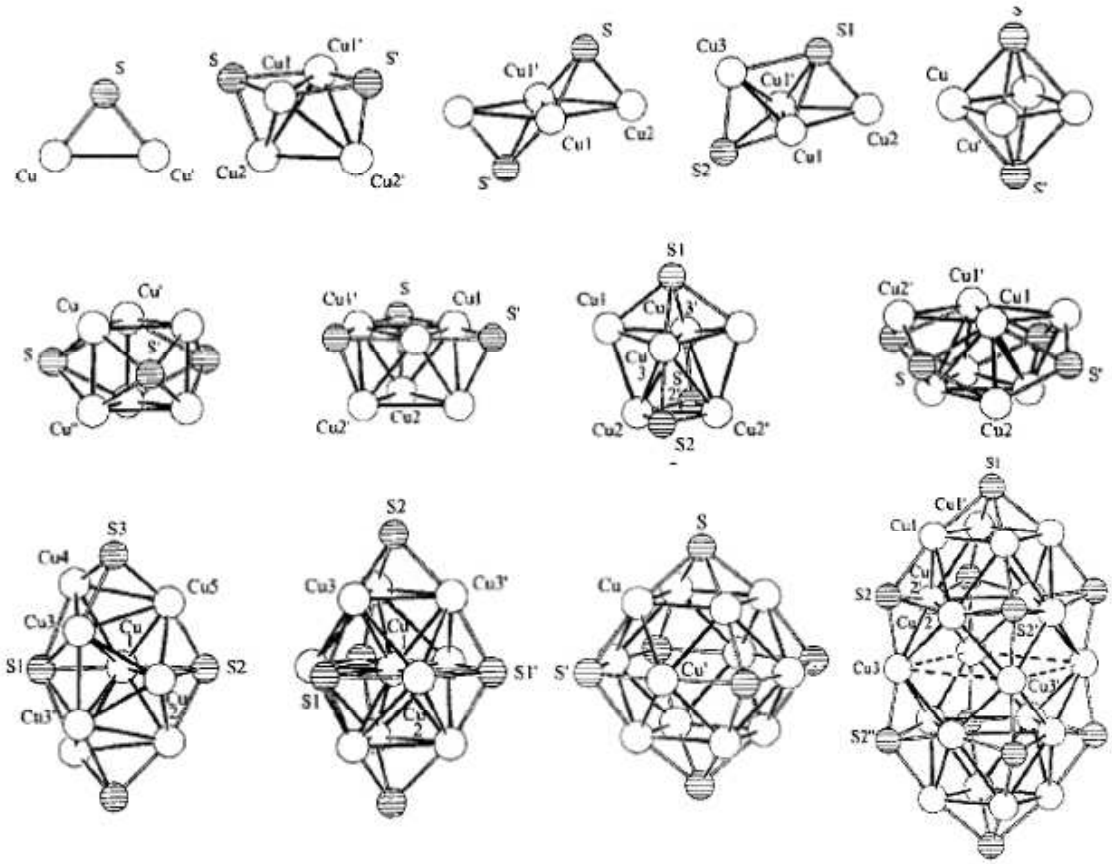

Figure 1.10: Proposed model structures of copper-sulfide clusters as $Cu_{2n}S_n$ (Dehnen et al., 1996).

The models illustrated in Figure 1.10 are representative theoretical structures and isomers of copper-sulfide clusters, calculated as an attempt to explain observations in aquatic systems (Dehnen et al., 1996). Recent research has focused on complexation between reduced sulfur and copper in oxic waters due to its strong coordination capabilities with copper and potential importance to copper bioavailability (Bowles et al., 2002; Bianchini and Bowles, 2002; Smith et al., 2002). Reduced sulfur includes free sulfide anions (S^{2-}, HS^-), metal-sulfides (Figure 1.10) and pyrite complexes, polysulfides (Na_2S_4), thiosulfates ($Na_2S_2O_8$), sulfites (Na_2SO_3), and thiols (R-SH) (Bowles et al., 2003). This group of sulfur species were once thought to be of little importance in oxygenated aquatic systems, due to spontaneous oxidation. However research has shown that reduced sulfur is

kinetically stabilized when bound to metals such as Cu(I,II) and Ag(I), in both freshwater (Rozan et al., 2000; Bowles et al., 2003) and seawater (Luther and Tsamakis, 1989). Research by Kramer et al. (2007) proposed that reduced sulfur in natural freshwater systems form complexes with metals, particularly copper due to its relative abundance, either intermixed within natural organic matter, or as colloid clusters surrounded by NOM through electrostatic attraction (Figure 1.11).

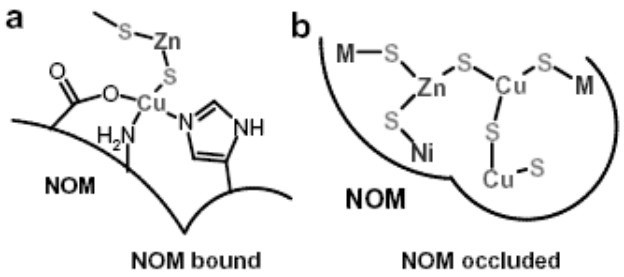

Figure 1.11: Proposed model structures of metal sulfide clusters in freshwater, either interconnected with natural organic matter (left) or bound externally through electrostatic attraction (right) (Kramer et al., 2007).

From Figure 1.11, two possible metal sulfide clusters were proposed: 1) metal sulfide clusters interconnected with NOM through multi-metal, multi-ligand association, and 2) metal sulfide colloid complexes within nano-pores of NOM, associated by electrostatic bonds (Kramer et al., 2007). In addition, Smith et al. (2004) suggested reduced sulfur may contribute strong binding sites in natural waters for metals within groups 11 and 12 ($\log K$>11 for Ag(I)). Strong binding sites refer to metal ion complexation with binding constants ($\log K$) of 12 - 14 and concentrations between 1 and 40 nM·dm^{-3} (Town and Filella, 2000). Research by Al-Farawati and van den Berg (1999) found that in seawater, sulfide had a higher binding affinity to free copper than other free metals such as aluminium, lead, and silver at environmentally relevant concentrations, with over 99% of the reduced sulfur complexed as $Cu(HS)^+$. However, in the presence of organic ligands, $Cu(HS)^+$ complexation dropped to about 28%, and copper-organic matter complexation was at 71%. Since the molecular structure of these complexes are

not fully understood, it is possible that observations made by Al-Farawati and van den Berg (1999) may be attributed to structures illustrated in Figure 1.11. However, it was reported that over 99% of the copper in solution was complexed with either reduced sulfur or organic matter (Al-Farawati and van den Berg, 1999). High complexation of copper with reduced sulfur alone or in combination with organic matter would markedly affect its bioavailability in natural waters. It is important to determine its implications as a protective ligand and/or predictive measure in coastal marine and estuarine environments.

Reduced sulfur has not been used as a predictive measure for quantifying copper bioavailability because current analytical methods for measuring reduced sulfur are difficult, time consuming, and the results are generally inconsistent (Bianchini and Bowles, 2002). Furthermore, the methods that do exist are not capable of identifying the nature of all reduced sulfur species. A method known as methylene blue sulfide (MBS) determination is commonly used for hydrogen sulfide and metal sulfide determination (Cline, 1969; Tang and Santschi, 2000). However, it was found to estimate less than 25% of metal sulfide clusters with soft Group B metals such as Ag_2S, CoS, CuS, HgS, MnS, and PbS due to incomplete oxidation of sulfides (Bowles et al., 2002). Cathodic stripping voltammetry (CSV) has been used to identify metastable metal-sulfide clusters such as CuS, however resultant peaks may be indiscernible from free sulfide and thiols (Al-Farawati and van den Berg, 1999). In addition, results from conventional CSV may be unstable due to precipitation with the mercury in the voltammetric cell (Al-Farawati and van den Berg, 1999). Furthermore, CSV instrumentation is not typically available for use because of high costs.

A method for reduced sulfur determination suggested by Bowles et al. (2003) known as CRS is an acceptable method because Cr(II) successfully releases reduced sulfur in forms of pyritic sulfur, elemental sulfur, and polysulfides (Canfield et al.,

1986), otherwise undetected by MBS (Bowles et al., 2002). This method can measure reduced sulfur, at nanomolar scale provided trace analytical techniques for clean labware are strictly followed. With good analytical practices, CRS results in approximately 94 - 109% recovery with 3.9 - 25% precision (Bowles et al., 2003). In addition, extensive studies show there is no interference by sulfate ions in CRS determination (Bowles et al., 2003; Canfield et al., 1986, and references therein). Sulfate interference would result in over-estimation of CRS, which is unfavourable, especially in marine waters where sulfate concentrations are high compared to sulfide (Bowles et al., 2003). However, this method is very time consuming such that only four samples can be analyzed per day, and does not account for some metal sulfides, such as Ag(I)S. In addition, CRS does not measure organic sulfides, such as thiols, which are also believed to play a major role in copper speciation (Bowles et al., 2003). In terms of quantifying inorganic sulfide species, CRS can be applied with acceptable recovery and good reproducibility.

Studies on reduced sulfur and/or CRS determination in freshwater have reported CRS concentrations up to 600 nM in freshwater rivers (Rozan et al., 2000). Luther and Tsamakis (1989), Al-Farawati and van den Berg (1999), Bianchini and Bowles (2002) and references therein reported an overall concentration of <0.001 to 162 nM of reduced sulfur in marine and coastal waters by means of voltammetry, HPLC, GC, and various spectroscopic methods such as UV/Vis. However, no published results were found on CRS determination in coastal marine or estuaries. Smith et al. (2002) concluded that in freshwater, reduced sulfur contributes strong binding sites for metal ions such as Cu^{2+}. If evidence suggests that reduced sulfur binds strongly with copper in estuarine environments and if toxicologically-relevant concentrations are found, then it may be beneficial to develop more reliable methods for quick reduced sulfur determination.

1.4 Ambient Water Quality Criteria for Copper

Metals in freshwater has been studied for about thirty years in terms of speciation and bioavailability, physiological effects on aquatic organisms, and toxicity, resulting in development of regulatory guidelines (Paquin et al., 2002, and references therein). In terms of copper regulations in freshwater, the U.S. EPA (2007) currently bases its water quality criteria (WQC) on the knowledge that copper bioavailability and toxicity is a function of water chemistry such as concentrations of DOC, inorganic ligands, and competing cations for binding sites on the aquatic organisms (McGeer et al., 2000; DiToro et al., 2001; Santore et al., 2001; Paquin et al., 2002). At a molecular level, bioavailable copper is measured based on the concentrations and binding affinities of free copper ions to organic and inorganic abiotic ligands (Allen and Hansen, 1996). Furthermore, if copper concentrations exceed available abiotic ligand binding sites or if the binding affinities of abiotic ligands to copper are relatively low, then copper has the capacity to bind with biotic ligands.

Biotic ligand is the generalized term for sites on aquatic organisms where metals can bind, such as the transport proteins within fish gills (Figure 1.12) (Paquin et al., 2002). If the accumulation of copper reaches a critical concentration at the biotic ligand, toxic effects occur (Paquin et al., 2002). This critical value may be written in terms of acute lethal accumulation at the biotic ligand that kills 50% of the test organisms (LA_{50}). With the addition of organic or inorganic abiotic ligands, the concentration of bioavailable copper decreases via complexation and so the concentration of free copper that will kill 50% of the species, acute LC_{50}, is higher than the LA_{50}. The endpoint of toxicity is commonly lethality, however acute concentrations that disrupt growth, development, or fecundity of 50% of the test organisms (EC_{50}) can be measured as well.

Toxicity criteria concentrations for metals, such as LC_{50}, LA_{50}, and EC_{50}, were

commonly reported as total dissolved metal concentrations, however reports argue the necessity to report toxicity data based on bioavailable metal species, which is key in quantifying the toxic effects at the biotic ligand (Allen and Hansen, 1996; Eriksen et al., 2001). Research done by Pagenkopf et al. (1974) and Allen (1993), among others, have suggested that in freshwater, copper toxicity was dependent on free copper(II) ion concentrations. In marine water, similar findings have been published by Sunda and Gillespie (1979), in which it was suggested that the total bioavailable copper in marine water at pH 8.1 is equal to $10^{1.8} \times \mathrm{Cu}_{free}$. This equation approximates the concentration of hydroxy copper species in addition to free copper(II), which would be present at that pH. These hydroxy copper species are also considered bioavailable (De Schamphelaere and Janssen, 2002). However, when calculating bioavailable copper based on equilibrium modelling, numerous approximations based on theoretical models are applied, resulting in approximated free copper values.

The Canadian Environmental Quality Guidelines (CEQG) for copper is currently based on total copper concentrations that are considered 'safe' copper levels in both fresh and marine water. The Canadian freshwater copper criteria range from 2 to 4 μg Cu·L^{-1} (0.03 - 0.06 μM), depending on water hardness, and the saltwater criteria state a limit of 3 μg Cu·L^{-1} (0.05 μM) (CCME, 2007). The U.S. EPA has established that regulations of bioavailable metals are variable with respect to site-specificity for both fresh and marine waters (U.S. EPA, 2007). The research involved in determining the freshwater copper criteria has advanced into the development of a computer model that describes copper toxicity based on site-specific water chemistry characteristics and the binding capacity of copper to biotic ligands, known as the BLM (Santore et al., 2001; DiToro et al., 2001; Paquin et al., 2002). A basic schematic displaying the protective and competitive effects of ligands and cations with respect to metal toxicity at the site of toxic action (generic biotic ligand) is illustrated in Figure 1.12.

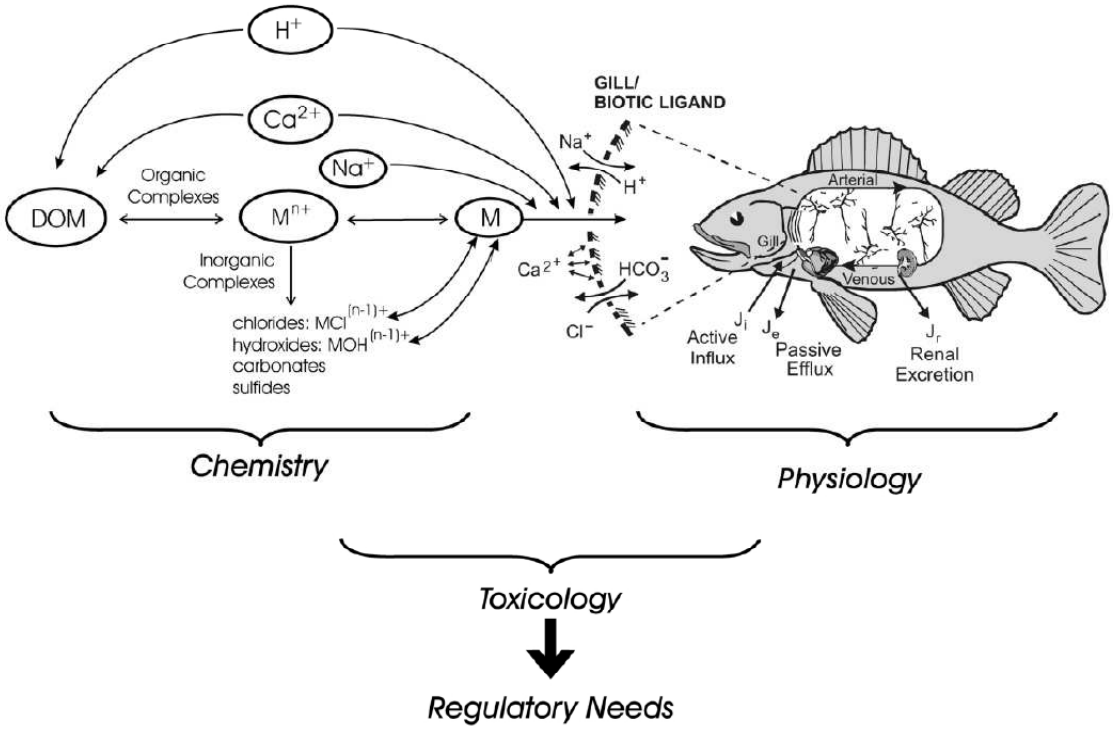

Figure 1.12: Schematic of chemical, physiological, and toxicological effects on the biotic ligand in natural waters. This schematic was the basis for the computerized chemical equilibrium BLM, which quantifies metal toxicity given specific water chemistry parameters. (Paquin et al., 2002)

The framework for the BLM (Figure 1.12) is a complex chemical equilibrium model designed for aqueous systems that calculates simultaneous metal-ligand concentrations and relates the calculated concentration of metal-biotic ligand to the predetermined LA_{50} for that specific metal and test freshwater species. From Figure 1.12, a metal (M) is capable of binding to the biotic ligand, which could initiate a toxic effect. However, this metal may compete with other cations in the water for the same binding sites on the biotic ligand, such as Na^+ at the Na^+/H^+ channel. Furthermore, this metal may form complexes with various organic and inorganic anions, such as DOM, decreasing its bioavailability, as illustrated on the left-most portion of Figure 1.12. Combining the concentration of the metal, complexation with anions, and competition for the biotic ligand with cations, the overall free metal concentration that is available to bind to the biotic ligand can be calculated.

The idea for a BLM originally stemmed from work done by Pagenkopf (1983). The BLM unifies numerical models applicable to natural aquatic systems such as chemical equilibria in soils and solutions (CHESS) (Santore and Driscoll, 1995) and the Windermere humic aqueous model (WHAM), which calculates chemical and electrostatic interactions in the aquatic environment (Tipping, 1994). Using these models, calculated output from the BLM include acute toxicity for a variety of freshwater organisms in addition to concentrations of bioavailable species of several metals such as copper, lead, cadmium, and silver. These calculated output values are determined by user-selected metal and test organisms in addition to water chemistry input parameters including temperature, pH, DOC, Ca^{2+}, Mg^{2+}, Na^{+}, K^{+}, Cl^{-}, SO_4^{2-}, and alkalinity. It is currently available for freshwater criteria, adapted by the U.S. Environmental Protection Agency (U.S. EPA, 2007).

Industrial and municipal growth along the coasts of North America result in higher anthropogenic output in estuaries and coastal marine waters, possibly increasing metal concentrations to unsafe levels. For industries along the coasts that release metal-containing effluent, an efficient numerical method for predicting metal bioavailability based on their water chemistry measurements would be beneficial and cost-effective. A predictive computerized method for coastal waters, similar to the freshwater BLM, would be quick, allowing for fast responses to improving wastewater treatment methods if necessary.

Research on predicting copper toxicity in coastal marine and estuarine water has recently come into focus (Arnold, 2005). Prior to site-specific calculations of copper toxicity in marine and estuarine waters (such as with the BLM for freshwater), a criteria for safe levels of copper was calculated based on available reported toxicity data in marine water (U.S. EPA, 1995a). In terms of copper toxicity in marine and estuarine waters, it is ideal to protect the most sensitive

species, which is determined by plotting all the available dissolved copper toxicity data with respect to each tested species, showing the probability distribution of genus mean acute values (GMAV), as seen in Figure 1.13. These data indicate that *Mytilus* is an especially sensitive genus, and therefore is an ideal test species for establishing copper water quality criteria. Indeed, *Mytilus* sp. was used as the standard for the final acute value (FAV) at the 95% limit (Arnold, 2005).

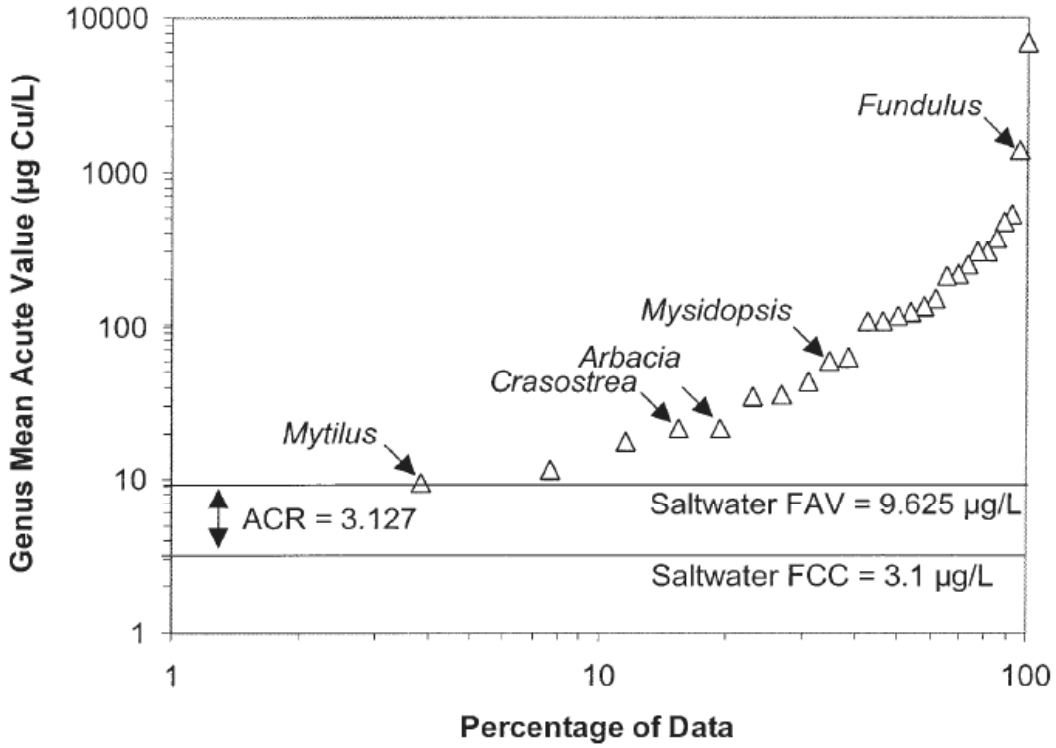

Figure 1.13: Plot of genus mean acute values of available seawater organisms to copper toxicity. The aim is to select a final acute value (FAV) that would protect 90% of genus' population. However for the case of copper criteria, the U.S. EPA lowered it to 9.625 μg Cu·L^{-1} to protect the *Mytilus* species because of its high commercial importance (Arnold, 2005).

In Figure 1.13, the FAV refers to the copper concentration that will kill approximately 50% of the *Mytilus* population. A final acute criterion (FAC) is calculated from the FAV (FAV/2), yielding a value of 4.3 μg Cu·L^{-1} (0.068 μM), which describes the approximate 'safe' level that protects 95% of the *Mytilus* population from lethality (U.S. EPA, 2007). Final chronic criterion (FCC) of 3.1

μg Cu·L^{-1} (0.049 μM) for dissolved copper in marine water is approximated by dividing the FAC by an experimentally-determined acute-to-chronic ratio (ACR) (U.S. EPA, 1995a; Arnold, 2005). Applications of these criterion values to natural marine and estuarine systems involves a water effect ratio (WER) calculation. The WER is the quotient of measured LC_{50} for the natural water in question and the LC_{50} performed in laboratory reference waters, which is meant to 'correct' the FAC making it applicable for that particular site (Paquin et al., 2002, and references therein). This simple approach allows for approximations of site-specific safe levels of copper without the necessity of understanding the effects of water chemistry (Wood et al., 1997). This WQC was implemented into the most recent documents issued by the U.S. EPA (2007).

A marine-specific BLM is under development that will incorporate abiotic and biotic ligands pertaining to saltwater characteristics in order to assess site-specific marine water copper criteria. However, in the meantime there exists a simple model to approximate EC_{50} in marine water based on the strong linear relationship between DOC and EC_{50} as proposed by Arnold et al. (2006). This relationship is shown in Figure 1.14.

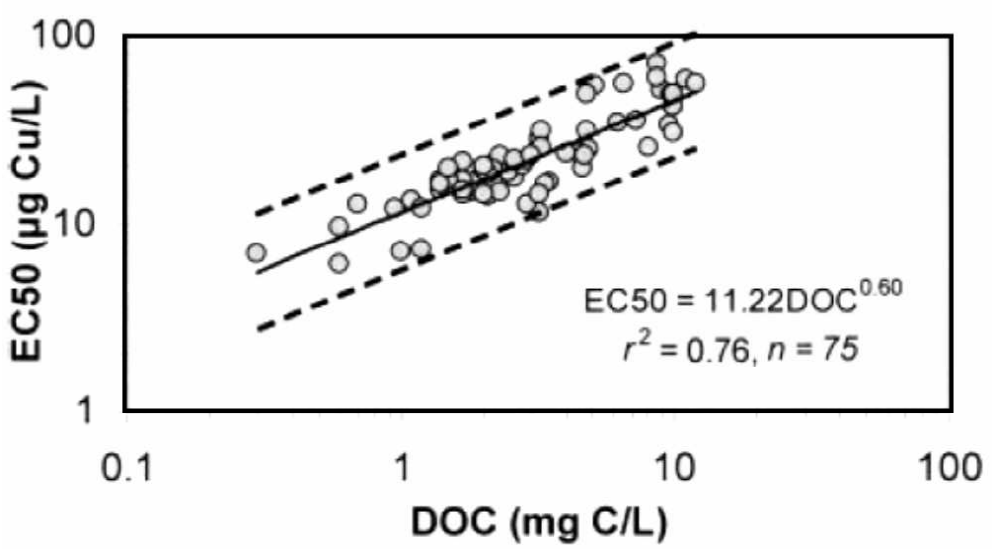

Figure 1.14: Plot of dissolved copper EC_{50} with respect to DOC concentrations in marine water (Arnold et al., 2006). Toxicity tests were performed on the embryos of *Mytilus* sp. in natural water samples collected along coastal North America.

The solid line is a linear regression of the plotted points, with the equation EC_{50}=11.22 $DOC^{0.6}$ (r^2=0.76, p<0.0001). The dotted lines represent a factor of 2 from the line, which is the generally accepted predictability limits for toxicity modeling (Santore et al., 2001; DiToro et al., 2001; Paquin et al., 2002).

1.5 Research Objectives and Approach

A primary research objective of this thesis was to determine whether DOM quality and CRS are appropriate input parameters in the development of a marine-specific BLM. In order to meet these objectives, coastal marine and estuarine water samples were characterized through measurements of DOC, DOM quality, and CRS. Following characterization, these measureables were tested for protective and/or predictive relationships with copper EC_{50}. In terms of identifying potential input parameters, predictive relationships with copper EC_{50} is key. Would DOM quality contribute a better approximation of copper toxicity than DOC concentrations? Furthermore, does CRS need to be a measureable input in the BLM as well?

Currently, the available HydroQual BLM software Version 2.2.3 (Santore, 2007) includes an input for CRS, but it is currently deactivated. The answers to these questions will have implications on copper regulation in coastal marine and estuarine environments. The approach taken to achieve these objectives are outlined in the following list:

1. Develop a sampling strategy to obtain a set of coastal marine and estuarine water samples along the east, west, and south coasts of North America that vary in salinity and input sources (i.e. allochthonous, autochthonous, and wastewater material).
2. Measure the quantity and quality of DOM in the water samples through DOC and fluorescence analysis.
3. Determine the quantity of reduced sulfur via CRS in the water samples.
4. Analyze data for extreme DOC, fluorescent, and CRS signatures, i.e. high CRS/low DOC, by factorial analysis to identify a good sample subset for toxicity analysis.
5. Run static 48-hr acute EC_{50} assays on the sample subset using embryos of *Mytilus galloprovincialis*. DOC, CRS, and fluorophore concentrations will be re-measured to account for any natural changes to the samples. Absorbance measurements at 340 nm will be performed, along with total copper measurements by inductively-coupled plasma with optical emission spectroscopy (ICP-OES).
6. Analyze the data for possible correlations between the water chemistry measurements (DOC, CRS, fluorescence) and total copper EC_{50}.

The testable hypotheses for this thesis is outlined in the following list:

1. Fluorescence measurements in combination with PARAFAC would identify a reasonable set of operationally-defined DOM fractions that best describe DOM quality and their relative concentrations in each coastal marine and estuarine water sample.
2. Fluorescence measurements of DOM quality would contribute an improved approximation of copper EC_{50} from DOC, particularly the allochthonous fluorescent components, such as humic and fulvic material.

3. Optically-defined allochthonous carbon, through SAC_{340} measurements, would be more protective than autochthonous with respect to copper toxicity.

4. Reduced sulfur, through CRS measurements, would be protective of copper toxicity and a necessary input parameter for a marine-specific BLM.

In the following chapters, the steps taken to achieve the objectives of this thesis will be addressed in detail. Chapter 2 includes experimental details common to all experimental and computational methods applied in this thesis. Chapters 3 and 4 are intended for submission as journal publications. External contributions to these chapters was limited to collection of the marine and estuarine samples, assistance with developing the partial factorial design, and free copper calculations. In Chapter 3, measurements of DOC, fluorescence, and CRS are addressed in detail as a means to characterize source variability. Chapter 4 discusses the factorial analysis and selection of a sample subset along with toxicity measurements. The toxicity results obtained here were pooled with a subset of data published by Arnold (2005) and Arnold et al. (2006). Chapter 5 contains a summary and conclusions of the research and experimental findings of this thesis.

Chapter 2

Methods

2.1 Reagent and Material Preparation

2.1.1 Synthetic Seawater

Synthetic seawater was prepared by dissolving commercial-grade sea salt mixtures (Kent Marine, Atlanta, GA, USA) in millipore grade water (MilliQ water) (18.2MΩ) and adjusted to 30‰ salinity using a PINPOINT® Salinity Monitor (American Marine Inc., Ridgefield, CT). It was prepared in 20 L batches and replenished every week. This synthetic sea salt was recommended for use in marine copper toxicity tests by Arnold et al. (2007). All chemical characterization measurements described in Sections 2.3 and 2.4 were performed on this synthetic seawater for comparisons. All marine standard solutions and dilutions were prepared using this synthetic seawater as the solvent. The reference toxicity tests were performed using this synthetic seawater.

2.1.2 Tyrosine and Tryptophan Solutions

A 5×10^{-4} M stock solution of reagent-grade L-tryptophan (>98% pure, Sigma-Aldrich, St. Louis, MO) and a 5×10^{-3} M stock solution of reagent-grade L-tyrosine

(>98% pure, Sigma-Aldrich, St. Louis, MO) were prepared using synthetic seawater (Section 2.1.1. These stock solutions were used to prepare diluted solutions of 2.5×10^{-7} M pure tryptophan and 5×10^{-7} M pure tyrosine. A mixture solution containing both tryptophan and tyrosine at concentrations of 2.5×10^{-7} M and 5×10^{-7} M respectively was prepared as well. These diluted pure and mixture solutions were used to calibrate PARAFAC during spectral analysis.

2.1.3 ZnHg Amalgam for the Jones Reductor

The amalgamated zinc in the Jones Reductor column (Jones, 1888) was prepared by mixing 150 g 20 mesh Zn (99.8% pure, Sigma-Aldrich, St. Louis, MO), 150 mL MilliQ water, 3.0 g mercuric chloride (99.5% pure, Alfa Aesar, Ward Hill, MA), and 1 mL 16 N HNO_3. The supernatant was discarded and the amalgam was rinsed thoroughly with MilliQ water. All of the amalgam was spooned into a glass column, plugged at the bottom with glass wool to hold the amalgam within the column. The column was filled with deoxygenated MilliQ water and plugged at both ends to store the amalgam in a wet and reducing environment.

2.1.4 Chromium(II)

A 1 M solution of Cr(III) was prepared by dissolving crystalline $CrCl_3{\cdot}6H_2O$ (98% pure, Sigma-Aldrich, St. Louis, MO) in 50% v/v HCl (prepared from 12 N HCl). Under Ar, the Cr(III) was reduced by a Jones Reductor (see Section 2.1.3. The resulting Cr(II) solution was collected in an Erlenmeyer flask at the base of the reductor and sealed with a septum and Parafilm to prevent exposure to the atmosphere. The airspace in the flask was purged with Ar when aliquots of the Cr(II) solution were removed. Removal of Cr(II) aliquots was done with a clean, dry syringe and long-nose needle inserted through the septum. This solution is stable in reduced form for about two weeks.

2.1.5 Mixed Diamine Reagent (Parts A and B)

The mixed diamine reagent (MDR) was prepared in two parts (A and B) (Andreae et al., 1991) with increased acidity (Bowles et al., 2003). Part A consisted of dissolved N,N-dimethyl-p-phenylenediamine (98% pure, Aldrich, St. Louis, MO) in 50% v/v HCl and stored in a Nalgene bottle at 4°C. Part B consisted of dissolved $FeCl_3 \cdot 6H_2O$ (99.0% pure, Fluka, Switzerland) in 50% v/v HCl and stored in a Nalgene bottle at 4°C as well. Equivolumes of parts A and B were mixed immediately prior to use.

2.2 Sampling and Storage of Samples

A sampling strategy was devised prior to collection to ensure the sampling sites varied in salinity from brackish to marine and varied in natural and anthropogenic input sources such that both DOM quality and CRS concentrations should vary. These sources included wastewater, allochthonous sources (terrestrial degradation), autochthonous sources (autotroph activity, *in situ*), and a mixture of the three sources.

Ambient water samples were collected by Ray Arnold (Copper Development Association) and Scott Smith (Wilfrid Laurier University) from 71 marine and estuarine sites along the east, west, and south coasts of North America. Samples were collected in clean, 2 L opaque, high density polyethylene (HDPE) bottles. The bottles were rinsed three times with sampling water on-site before the actual sample was taken. The samples were collected near the water's surface and the bottles were capped while submerged to avoid air contact with the water during transport to the lab for analysis. One sample was collected at each site and sampling was done either near the shoreline or off a dock a few metres off shore.

The ambient water samples were shipped in coolers (approximately 24 hours)

at about 4℃. On arrival, pH, salinity and fluorescence was immediately measured, followed by DOC and CRS. Salinity was measured with a PINPOINT® Salinity Monitor and pH was measured with a Tananger dual pH meter (Scientific Systems Inc., USA) using an Orion double junction reference electrode and Ag/Ag-Cl pH electrode (Thermo Electron Corp., USA). Methodology for fluorescence, DOC, and CRS measurements can be found in Sections 2.3 and 2.4. To minimize oxidation of the reduced sulfur, the samples were stored under argon. The bottles were stored at 4℃. All precautions were made to ensure minimal contamination to the bottles and water samples during collection, transport, analyses, and storage.

2.3 Characterization of Organic Matter

2.3.1 Fluorescence Measurements

An aliquot from each of the 72 water samples (71 collected, plus synthetic seawater) was passed through a 0.45 μm pore size GMF GD/X membrane filter (25 mm diameter) (Whatman, Florham Park, NJ) and the filtrate was measured using a Varian Cary Eclipse Fluorescence Spectrophotometer (Varian, Mulgrave, Australia) in a 1 cm quartz cuvette. Fluorescence scans of emission wavelengths from 250 nm to 600 nm in 1 nm increments were measured for every 10 nm excitation wavelength between 200 nm and 450 nm. The excitation and emission monochromator slit widths were both set to 5 nm for all the measurements. The scan speed was at a rate of 400 nm·min^{-1} and the photomultiplier tube (PMT) was set to high detection (800 V).

The fluorescence data was processed in Matlab^{TM} (The MathWorks, Natick, MA) to produce 3-dimensional FEEMs, displayed as contour plots. Rayleigh scatterings were removed from the preprocessed data and replaced with not-a-number (NaN) values, which would otherwise cause mathematical interferences in subsequent spectral analyses. The Matlab scripts used to produce the contour plots are

found in Appendix A.1.

2.3.2 Spectral Analysis of Organic Matter

Fluorescence indices for every water sample was calculated to approximate DOM source, as proposed by McKnight et al. (2001) using Equation 2.1:

$$FI_{Ex370} = \frac{Em450}{Em500} \tag{2.1}$$

where *FI* is the fluorescence index, and *Em450* and *Em500* are the emission intensities at 370 nm excitation. These FI values were compared to qualitative observations of each site with respect to DOM source.

The 72 FEEMs were spectrally resolved using PARAFAC to elucidate four operationally-defined fluorescent fractions and observe their individual spectra. PARAFAC spectrally deconvolutes the three-way data set of excitation, emission, and intensity from the original FEEMs by mathematically breaking down these components into a linear equation incorporating the components spectra, their relative abundance, and quantum efficiencies (Stedmon et al., 2003) (Figure 2.1).

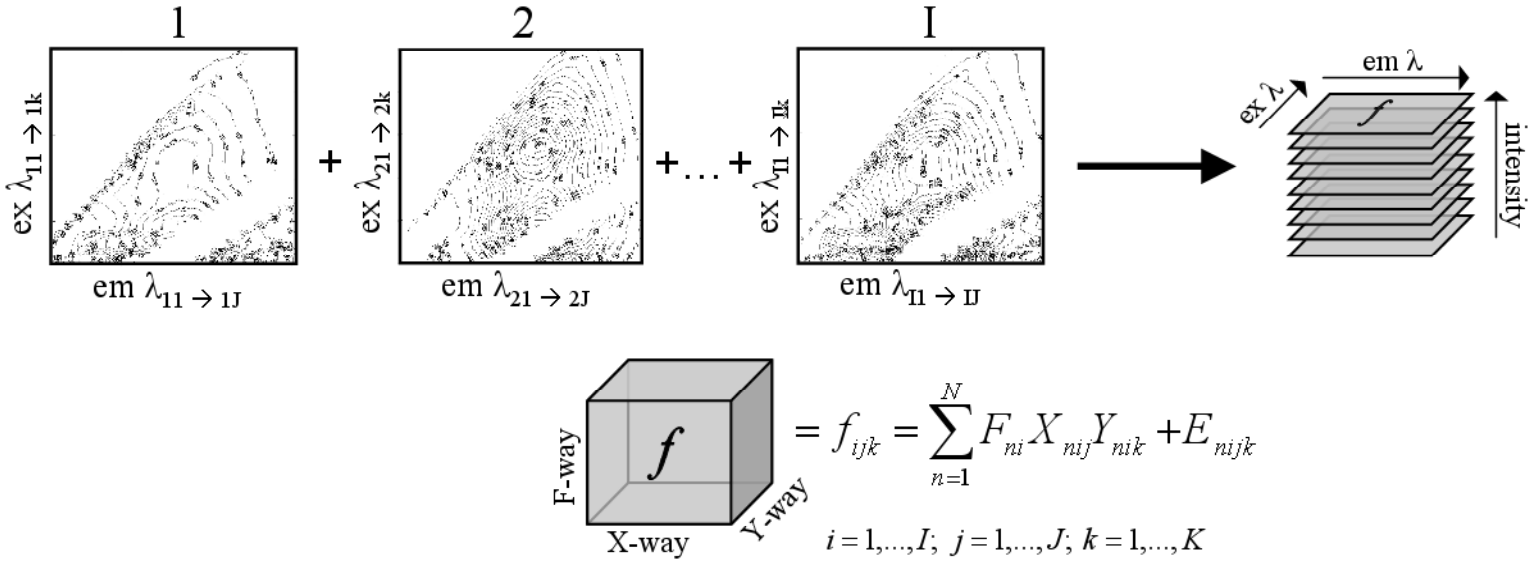

Figure 2.1: Graphical representation of the three-way PARAFAC model (Adapted from Nahorniak and Booksh (2003) and Stedmon et al. (2003)).

where f_{ijk} is the FEEM of the ith water sample with j emission wavelength, and k excitation wavelength, F_{xi} is the fluorophore abundance value of the nth fluorophore component defined by PARAFAC in sample i, X_{nij} is the emission wavelength (j) of component x in sample i, Y_{nik} is the excitation wavelength k of component x in sample i, and E_{nijk} is residual, or mathematical noise, not accounted for by PARAFAC (Stedmon et al., 2003). N defines the number of resolved fluorophore components and there are 4 components defined in this study. With this equation, the abundance value of each fluorophore component defined in PARAFAC can be calculated for every measured water sample based on the spectra of the components and the intensity of the Ex/Em peaks in the FEEM. These calculated abundance values are referred to here as 'concentrations', although it must be noted that they are not true concentrations. Rather, they are linearly proportional to their molar concentrations. If the molecular identity of the fluorophore and its quantum efficiency is known, then Equation 2.2 can then be applied (Guilbault, 1973):

$$F = kC \tag{2.2}$$

where F is the fluorophore abundance value described by PARAFAC, k is the linear proportionality constant incorporating the quantum efficiency of the fluorophore, and C is the molar concentration of the fluorophore. The components of DOM resolved by PARAFAC have no defined structure, however they do have similar structural characteristics to known compounds. Therefore, only approximations can be made on the relative concentrations of each component using Equation 2.2 provided that total fluorescent organic matter is used as an approximation for DOM as a whole (Stedmon and Markager, 2005). Concentrations (C, Equation 2.2) of the fluorophores quantified here were be approximated through the use of standard solutions of Suwanee River Fulvic Acid (SRFA) and pure tryptophan and tyrosine. Since the molecular identity of each fraction defined by PARAFAC is not known, the degree of uncertainty in the approximated concentrations cannot be

verified. Calculations to approximate the concentrations of each fluorophore can be found in Appendix C. The calculated concentration units are represented in equivalents of SRFA, pure tryptophan, and pure tyrosine appropriately. In this study, the fluorophore abundance values will be used, which limits these values to internal comparisons only. This approach provided insight into both the qualitative and quantitative differences within DOM in coastal marine and estuarine environments.

The PARAFAC algorithms used were from PLS_Toolbox version 4.1.1 in Matlab^{TM} (Eigenvector Research, Inc., WA). The fluorescence data of all 72 samples were inputted into PARAFAC for simultaneous analysis. In addition, fluorescence data from the tryptophan and tyrosine standards were added to the dataset after every 10 additions of ambient water fluorescence data to simultaneously calibrate the analysis. The Matlab scripts used to input the dataset and quantify the abundance of these four fractions is found in Appendix A.2. The mathematical output consisted of the individual spectra, $[X, Y]$, of four fluorescent components and the relative 'concentration', F, of each fraction in each water sample. Two spectra were of allochthonous material and labelled as fulvic-like and humic-like fractions based on their average molecular weights, at Ex/Em 354 nm / 460 nm and 467 nm / 548 nm respectively (Wu et al., 2003). Since the molecular weight of humic material is generally higher than fulvic material, it was assumed that the spectrum emitting higher fluorescence wavelengths was more humic-like. FEEMs of tryptophan and tyrosine standards were used to identify the remaining two spectra resolved by PARAFAC.

2.3.3 DOC Analysis

Quantitative measurements of organic matter in the ambient water samples was approximated through DOC analysis. DOC concentrations were measured with a Shimadzu TOC-5050A Total Carbon analyzer using an ASI-5000A autosampler (Mandel Scientific, Guelph, ON). Prior to measurements of the ambient water sam-

ples, solutions of total carbon (TC) as 5 mg C·L^{-1} and 10 mg C·L^{-1} potassium hydrogen phthalate ($C_6H_4(COOH)(COO^-K^+)$) dissolved in synthetic seawater were used as marine standards to verify the accuracy of the analyzer with marine samples. A 10 mL aliquot of each ambient water sample was passed through a 0.45 μm pore size GMF GD/X membrane filter (25 mm diameter), acidified with 16 N HNO_3, and sparged with N_2 for 15 minutes immediately prior to analysis in order to remove inorganic carbon as suggested by Dafner and Wangersky (2002a). Two vials of acidified MilliQ water were placed between every 10 ambient water samples in the autosampler to ensure any salt deposits were rinsed thoroughly from the analyzer syringes. The TC marine standard solutions were treated the same way as the ambient water samples prior to analyzing.

2.3.4 Specific Absorption Coefficient at 340 nm

Absorbance measurements at 340 nm were performed using a 1 cm quartz cuvette. An LS-1 tungsten halogen lamp light source was shone through the cuvette, the signal was detected by a USB2000 fiber optic spectrometer and the signal was visualized using the Ocean Optics Spectra Suite version 1.4.2 (Ocean Optics Inc., Dunedin, FL). References of synthetic seawater were used. SAC_{340} can be calculated using the following equation (Equation 2.3) (Schwartz et al., 2004):

$$SAC_{340} = 2,303 \times \frac{Abs_{340}}{DOC} \tag{2.3}$$

2.4 Quantification of Reduced Sulfur

The CRS method used here involves a redox reaction between Cr(II) and either the metal bound to sulfide, or the partially oxidized sulfide under acidic, anoxic conditions. Two representative chemical reactions involving oxidation of metal-sulfides (M-S) and sulfites are shown in Equations 2.4 and 2.5:

$$Cr^{2+}_{aq} + M - S_{aq} + 2H^{+}_{aq} \longrightarrow Cr^{3+}_{aq} + M^{+}_{aq} + H_2S_g \tag{2.4}$$

$$6Cr^{2+}_{aq} + SO^{2-}_{3aq} + 8H^{+}_{aq} \longrightarrow 6Cr^{3+}_{aq} + H_2S_g + 3H_2O_{aq} \tag{2.5}$$

Through purge-and-trap techniques, the reduced sulfur is protonated under acidic conditions to produce gaseous H_2S and transferred by N_2 (purged) to a NaOH solution where it is redissolved and deprotonated (trapped). MDR is then added to the basic solution to develop with S^{2-}, producing methylene blue coloured complex, which can be analyzed via colorimetric techniques.

2.4.1 Chromium(II) Reducible Sulfide

The CRS method was followed as outlined by Bowles et al. (2003). A simple schematic of the reaction apparatus is illustrated in Figure 2.2. The apparatus was made of borosilicate glass with ground glass joints, and Teflon tubing.

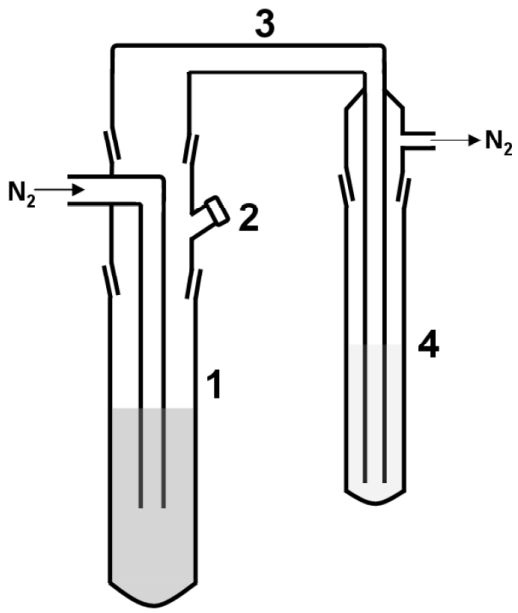

Figure 2.2: Simple schematic of the reaction apparatus used in the CRS measurements (Adapted from: Bowles et al. (2003)). 1. reaction tube (60 mL), 2. Teflon-lined silicon injection septum, 3. glass connecting piece, 4. trapping tube (40 mL). Six of these apparati were set up to run simultaneously - two were used as a reference and the rest were used to run two samples in duplicate. The high purity N_2 gas ran through individual pressure meters to ensure each apparatus was purged at 65 mL·min^{-1}. The glass joints produced air-tight seals and the trapping tubes were held in place with plastic clips.

A 30 mL aliquot of the ambient water was transferred into a clean, dry reaction tube (Figure 2.2). 15 mL of 0.05 M NaOH was dispensed into the trapping tube and attached to the reaction tube via the connecting piece, held in place with a plastic clip (Figure 2.2). High purity N_2 was allowed to flow through the system at 65 mL·min^{-1} for 5 minutes, monitored with an airflow pressure meter. The frosted glass joints sealed the apparatus, creating a closed system, but Teflon tape was used to seal any leaks as needed. 5 mL of 1 M Cr(II) followed by 5 mL of 50% v/v HCl were transferred into the reaction tube through the septum (Figure 2.2) and the system was again purged with N_2 at 65 mL·min^{-1} for 30 minutes. While purging, equivolumes of parts A and B of the MDR reagent (preparation described in Section 2.1.5) were dispensed into an opaque vial and stored in the dark until use. With the gas shut off, the 15 mL NaOH in the trapping tube was transferred into a clean dry borosilicate glass vial and rinsed with 5 mL deoxygenated MilliQ

water. 0.5 mL of the prepared MDR reagent was pipetted into the vial, the vial was immediately capped and shaken, and the solution was stored in the dark for 24 hours to allow the methylene blue coloured complex to develop. Six of these apparati were set up and run simultaneously. Two were used as a reference with deoxygenated MilliQ water and two samples were run in duplicate.

2.4.2 Colorimetric Analysis

The final coloured solution in the vials were analyzed colorimetrically with a 10 cm quartz cuvette. An LS-1 tungsten halogen lamp (Ocean Optics Inc., Dunedin, FL) light source was shone through the cuvette, the signal was detected by a USB2000 fiber optic spectrometer (Ocean Optics Inc., Dunedin, FL) and the signal was visualized using the Ocean Optics Spectra Suite version 1.4.2 (Ocean Optics Inc., Dunedin, FL). To avoid saturating the detector, the measurement time was set to 4 ms and averaged 100 measurements. One of the reference solutions was measured first to calibrate the instrument. A dark (light off) and light (light on) reference was subtracted from every intensity reading. This allowed for internal calculations of absorbance within the software. Subtraction of the reference absorbance was done on each sample to remove variation with the light source. Each reference followed by each sample was measured in triplicates of triplicates, with removal and replacement of the cuvette between each triplicate measure, at 670.11 nm and an average absorbance was calculated. Calculations as described by Beer's Law determined the concentration of sulfide, with an experimentally-determined extinction coefficient of $\epsilon = 4.0 \times 10^4 L \cdot mol^{-1} cm^{-1}$. A concentration factor of 2/3 was included to account for the concentration difference from the 30 mL in the reaction tube and 20 mL in the trapping tube.

2.5 Analysis and Comparisons between Fluorescent DOM and CRS

The data collected from fluorescence and CRS measurements were used to identify possible correlations between each measured quality index of humic-, fulvic, tryptophan-, and tyrosine-like fractions, as well as between FI and CRS. The quality index values for each fluorescent fraction was calculated using Equation 2.6:

$$qualityindex = \frac{F}{DOC} \tag{2.6}$$

where F represents the fluorophore concentration (Arb) and DOC is in mg C·L^{-1}. Using these 6 variables, a 6×6 Pearson correlation matrix was applied based on the correlation coefficient equation (Equation 2.7):

$$r = \frac{\Sigma(xy) - n\overline{xy}}{(n-1)s_x s_y} \tag{2.7}$$

where x and y are the values of variables 1 and 2, $\overline{x}$, $\overline{y}$, s_x, and s_y are the averages and standard deviations of variables 1 and 2, and n is the sample size (n=72). Correlation coefficients and probability of each variable combination were calculated in Matlab™. The data used in this analysis can be found in Appendix B.

2.6 Acute Copper EC_{50} Toxicity Assay

The methodology for running copper toxicity tests were obtained from the standard operating procedures at Pacific EcoRisk (Fairfield, CA). These procedures followed the guidelines in A.S.T.M. International (2004) for the 48-hour static acute toxicity tests starting with *Mytilus* sp. embryos.

2.6.1 Sample Selection

A subset of samples were selected from the 72 listed in Appendix B to measure copper toxicity, based on the measurements of DOC, fluorescence, and CRS. A 2^3 factorial design (Box et al., 1978) was implemented to initially divide the sample set into eight categories through simultaneous comparisons of three parameters: DOC, tryptophan, and CRS. From these categories, samples were selected that best represented extreme concentrations of these parameters.

2.6.2 Mussel Handling

Estuarine bivalve mussels (*Mytilus galloprovincialis*) were purchased from Proteus SeaFarms International Inc. (Ojai, CA, USA). Upon arrival, they were gently transferred into aerated synthetic seawater at 12℃ and allowed to acclimate for 1 - 2 days before use in tests. The synthetic seawater was replaced every 1 - 2 days. The mussels were not genetically verified and so are referred to here as *Mytilus* sp.

2.6.3 Test Solution Preparation

1 L of each sample, selected in the partial factorial, was upward adjusted to 30 ‰ ± 1 ‰ (as per U.S. EPA (1995b)) using commercial-grade sea salt, or downward adjusted with MilliQ water. Following salinity adjustment, the sample was filtered through Purabind 0.45 μm filters (Whatman, Florham Park, NJ). The filtrate was divided into seven aliquots, prepared in volumetric flasks: one was set as a reference sample and six were spiked with Cu(II), using $Cu(NO_3)_2$ stock, to produce concentrations that encompassed the predicted EC_{50} for *Mytilus* sp. This predicted EC_{50} was calculated based on the equation, $EC_{50} = 11.22DOC^{0.6}$ (Arnold et al., 2006). The reference and spiked filtrate aliquots were stored under Ar overnight at 4℃ to equilibrate, prior to the toxicity assay. Separate sub-aliquots of the reference solutions were used to re-measure pH, CRS, DOC, fluorescence, and SAC_{340}.

Aliquots of 10 mL were added to 20 mL glass scintillation vials (cleaned in 10% HNO_3, rinsed thoroughly with MilliQ and allowed to dry, then rinsed with synthetic seawater before use). Five replicates of each concentration and five replicates of the reference solution were prepared in this manner. Ten additional reference vials (10 mL each) were set up for test monitoring. Vials were stored at 18℃ in preparation for the addition of embryos.

2.6.4 Total Copper Analysis

Total dissolved copper was measured on 10 mL sub-aliquots of all the reference and copper-spiked filtrate aliquots prior to the toxicity assay. Standards of 1, 10, 50, and 100 $\mu g \cdot L^{-1}$ were prepared using synthetic seawater and the $Cu(NO_3)_2$ stock. These standards and the sample aliquots were transferred into 15 mL polypropylene centrifuge tubes (Corning Inc. Corning, NY, USA) and acidified with 16 N trace metal-analysis grade HNO_3. Total copper measurements were performed by inductively-coupled plasma with optical emission spectroscopy (Perkin Elmer Optima 3000DV ICP-OES, Toronto, ON., Canada) with multi-element standard parameters, set in axial mode. Measurements were taken at the copper spectral line of 324.752 nm.

2.6.5 Spawning

Mussels were inspected for cracked shells and disposed of if cracks were found. Large mussels were selected and cleaned by scraping off detritus and cutting off all byssal threads. Once cleaned, they were transferred into synthetic seawater at 4℃ for about 10 minutes or until the spawning bath was ready.

The spawning bath and several 250 mL beakers were filled with synthetic seawater and warmed to 20℃. Clean mussels were roughly placed into the bath (completely submerged) and monitored for spawning activity. Each spawning

mussel was individually removed from the bath by inserting a disposable plastic pipette into the bivalve opening, thoroughly rinsing with clean warm synthetic seawater, and then submerging in one of the 250 mL beakers to collect isolated gametes. Isolated gametes were inspected under a light microscope for egg quality (round, uniform in size), as seen in Figure 2.3, and sperm motility (active movements). About 2 to 3 good spawning males and females were used for each test.

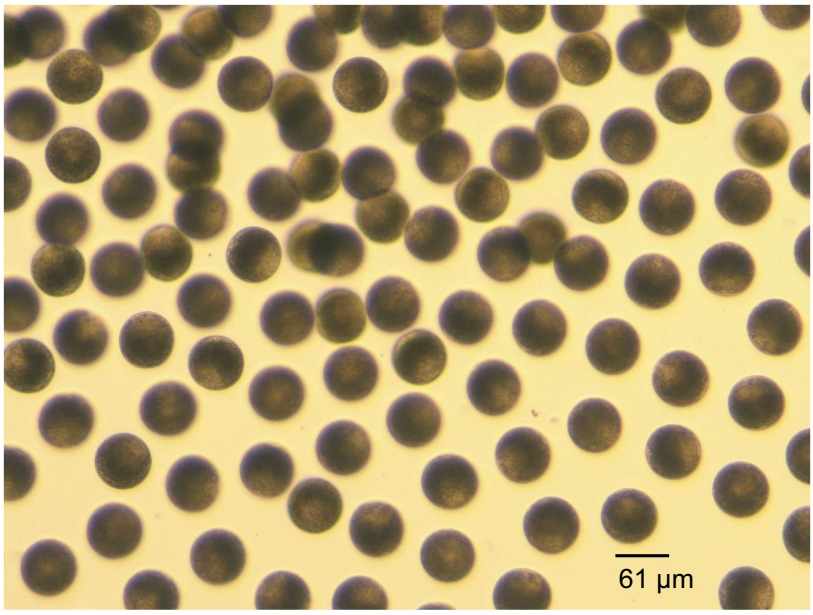

Figure 2.3: Good *Mytilus* sp. eggs. They can be either round or egg-shaped with small to no vacuoles present (lighter shade within egg). If there are a small number of abnormal eggs, it may still be used since abnormalities may produce good embryos.

The presence of >90% poor quality eggs (oblong shape, abnormal size, highly vacuolated), nonmotile sperm, and hermaphrodites rendered the gametes unusable and were discarded.

2.6.6 Gamete Fertilization and Embryo Production

Within 1 hour of spawning, an egg stock suspension was prepared by pipetting concentrated eggs from the bottom of the spawning beakers of good quality eggs

into 250 mL synthetic seawater. A 1 L egg suspension of about 1000 eggs·mL^{-1} was prepared by pouring a small aliquot of the stock into 1 L of synthetic seawater. The concentration was determined by viewing a 100 μL aliquot of the suspension under a microscope to ensure about 100 eggs were present. This was done in triplicate and an average was taken to obtain the exact egg concentration. The suspension was stirred continuously to keep eggs from settling while measuring the concentration. The egg stock was stored at 18℃ until the end of the test, then disposed of.

The egg suspension was divided into four 100 mL beakers. A small amount of concentrated, motile sperm was obtained from the spawning beakers. 0.025, 0.05, 0.1, and 0.2 mL of the concentrated sperm was pipetted into one of the 100 mL beakers, gently stirred immediately with a glass stir rod, and stored at 18℃ for 2 hours, gently stirred every 20 minutes. After this time, the embryos were quantified and examined for fertilization. Solutions with the lowest volume of sperm stock added and highest (up to 95%) amount of normal embryo development were selected for the test. Embryos were left to develop (if necessary) to the 4-cell stage prior to test inoculation. The suspension concentration was double checked prior to inoculation (number of eggs·mL^{-1} = number of embryos·mL^{-1}). An image of the 4-cell embryonic stage is in Figure 2.4.

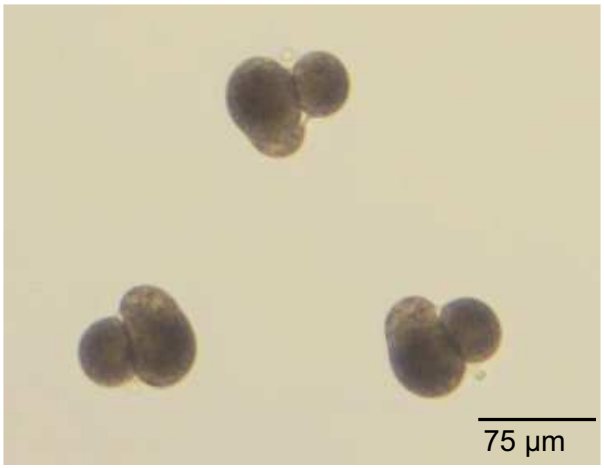

Figure 2.4: *Mytilus* sp. embryos in the 4-cell stage. Once they are in this stage of development, they can be injected into the reference and test solutions to initiate the toxicity assay. If >10% are seen in the 8-cell stage, they cannot be used.

2.6.7 Test Inoculation

An aliquot of the embryo suspension (mixing continuously) containing about 100 embryos was pipetted into each glass scintillation vial containing 10 mL test, reference, and monitoring solutions (see Section 2.6.3) to initiate the toxicity assay. The inoculated vials were capped with unlined polyethylene caps and placed in a temperature chamber at 18℃ ± 0.1℃ for 48 hours.

2.6.8 Test Termination and Water Chemistry Measurements

After 48 hours, the developmental progress was observed from a monitoring vial to ensure >90% were in the normal D-shaped prodissoconch shell development stage, illustrated in Figure 2.5, otherwise the vials were left until complete development to this stage. Tests that required more than 54 hours for development were discarded.

Figure 2.5: Normal embryo development of *Mytilus* sp. after 48 hours of fertilization. Normal development is observed as D-shaped calcified shell formation as well as good, consistent, brown flesh formation.

The test acceptability was >90% normal development or >30% survival in the control treatment. 1 - 2 mL of 5% v/v gluteraldehyde was pipetted into each vial to terminate the test. The end point was abnormal shell development as a measure of adverse effects. All 'normal', 'abnormal', and 'dead' embryos were counted under a dissecting microscope at 50× magnification. The percentage of larvae that did not survive or develop normally was calculated for each replicate. Strict guidelines were followed to ensure identification of abnormal development was consistent between all toxicity tests.

2.6.9 Test Enumeration

After fixation, the larvae were observed in the vial under a dissecting microscop. A grid was drawn on the base of the vial to aid in counting. All larvae from all test vials were observed separately. The number of normal (Figure 2.5), abnormal (abnormally-shaped shell, poor quality flesh colour), and dead (empty shell, no brown flesh) larvae were counted. Images of typical abnormal and dead larvae are

found in Figure 2.6. Unfertilized eggs were not counted.

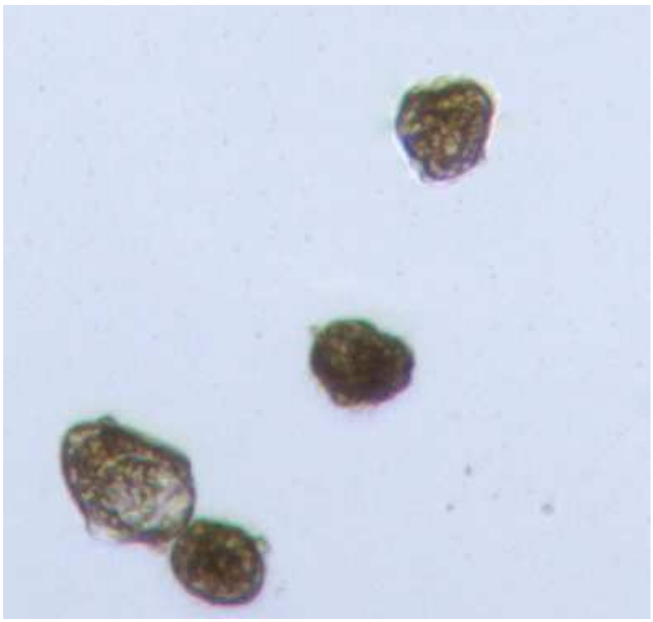

Figure 2.6: One dead D-shell (left-most) and three abnormal larvae.

2.6.10 Toxicity Analysis

The 50% shell development inhibitory concentration (EC_{50}) was estimated with 95% confidence intervals for each sample by probit analysis using the Statistical Analysis System software (SAS Institute Inc., Cary, NC, USA). The toxicity data obtained here was pooled with data from Arnold (2005) and Arnold et al. (2006) in which their sampling sites were the same as ones among the 72 analyzed in this study. To statistically justify pooling the data together, a t-test was performed on the intensive values, $EC_{50} \cdot DOC^{-1}$, of the two data sets to show that with 95% confidence there is no significant difference between the data, other than what can be described as random variation. The full statistical analysis can be found in Appendix E.

2.6.11 Data Pooling

To assign fluorescence values to the sample set obtained from Arnold (2005) and Arnold et al. (2006), the assumption was made that the fluorescent fractions (Arb.) per mg of DOC ('quality index') remains constant. So the measured fluorescence values for the same sites in this study were normalized to DOC and multiplied by the DOC concentrations reported in Arnold (2005); Arnold et al. (2006). Furthermore, the new re-measured fluorophore concentrations were adjusted to account for instrumentation drift by using a correction factor that was determined by comparing fluorescence measurements obtained in Chapter 3 and in Chapter 4. This factor was applied to all the new fluorescent data. This adjustment was performed to ensure pooling of fluorophore concentrations in the two data sets was valid. This assumption allowed for separate comparisons of total copper EC_{50} as a function of DOC, fluorescence humic-, fulvic-, tryptophan-, and tyrosine-like fractions using both data sets, and analyzed for linear responses.

Chapter 3

Chemical Characterization of DOM and CRS in Coastal Marine and Estuaries

3.1 Introduction

Metal toxicity in aquatic environments is influenced by the chemical characteristics of the water in which the metal is found, such as pH and concentrations of inorganic and organic ligands. Furthermore, these chemical characteristics potentially vary over time and by location. This suggests that metal toxicity has both spatial and temporal dependence. In particular, bioavailability of metals in coastal marine and estuarine waters are influenced by input from surrounding coastal environments. With over 53% of the US population living along the coast (NOAA, 2004), it is important to research the nature of these inputs and quantify the variability of water quality with respect to metal toxicity. In the development of a marine-specific biotic ligand model (BLM), these measurements would be used as input parameters for a computerized chemistry-based BLM, similar to existing freshwater BLMs. Freshwater BLMs, such as the HydroQual© BLM, is a numerical approach to predicting metal toxicity through complex chemical

equilibrium modelling (DiToro et al., 2001; Santore et al., 2001; Paquin et al., 2002). The focus of this chapter is on characterization of two potential parameters with respect to spatial variability, for a marine-specific BLM: dissolved organic matter (DOM) and chromium(II) reducible sulfide (CRS).

DOM is operationally defined here as organic matter passed through a 0.45 μm membrane filter. The molecular nature, or quality of organic matter, is influenced by input source. Its concentration as a whole is commonly approximated by quantifying dissolved organic carbon (DOC) in mg C·L^{-1}. Typical DOC concentrations in the open ocean range from about 0.7 mg C·L^{-1} to 0.9 mg C·L^{-1}, coastal marine waters are around 2 mg C·L^{-1}, and estuaries have been reported with concentrations that can reach up to approximately 10 mg C·L^{-1} (Dafner and Wangersky, 2002b, and references therein).

DOM can be characterized, by input source, through several spectroscopic techniques. DOM can be initially categorized by two broad end-member classes: allochthonous carbon and autochthonous carbon (McKnight et al., 2001). However, there is considerable variability within the nature of these two end-members themselves. Allochthonous and autochthonous carbon can be approximated by their specific absorption coefficients at 340 nm (SAC_{340}), defined by Equation 3.1:

$$SAC_{340} = 2,303\frac{Abs_{340}}{DOC} \tag{3.1}$$

which is a calculated measure of organic matter based on molecular size and structure. In freshwater, it was shown that optically-darker allochthonous material is more protective of copper, cadmium and lead toxicity (as acute LT_{50} for rainbow trout, based on comparisons of SAC_{340} (Schwartz et al., 2004). Further characterization can be done through fluorescence spectroscopy, which is a highly selective and sensitive spectroscopic technique that can differentiate fluorescent molecules (fluorophores) in a heterogeneous system based on their different

fluorescent properties. A fluorescence excitation-emission matrix (FEEM) is the result of compiling data from simultaneous scanning of excitation and emission wavelengths over the fluorescence spectrum. When observed as a contour plot, FEEMs provide qualitative information on the molecular structures of fluorophores based on their peak positions and intensity.

McKnight et al. (2001) suggested a method for inferring DOM source based on fluorescence index (FI), calculated by the ratio of emission intensities at 450 nm and 500 nm, at 370 nm excitation. Fluorescence indices of approximately 1.4 and 1.9 indicate terrestrial-sourced and microbially-derived DOM respectively (McKnight et al., 2001). Based on FEEM analysis, allochthonous carbon can be detected in the Ex/Em ranges of 300 - 350 nm / 400 - 450 nm and 250 - 390 nm / 460 - 520 nm, suggesting the presence of terrestrially-derived fulvic and humic material respectively (Smith and Kramer, 1999; McKnight et al., 2001; Wu et al., 2003; Stedmon and Markager, 2005). Autochthonous carbon can be detected by the Ex/Em peaks of 225 - 275 nm / 350 nm and 225 - 275 nm / 300 nm identifying microbially-derived tryptophan-like and tyrosine-like fractions respectively (Baker, 2001; Stedmon and Markager, 2005). Recently, Winter et al. (2007) identified humic-, fulvic-, tryptophan-, and tyrosine-like fractions in freshwater through fluorescence. In seawater, fluorescence spectroscopy has been a useful technique for DOM characterization as well (Mopper and Schultz, 1993; Coble, 1996; Hall and Kenny, 2007).

To quantify in relative terms, the humic-, fulvic-, tryptophan-, and tyrosine-like fractions observed by fluorescence, parallel factor analysis (PARAFAC) is used here. Through spectral deconvolution of a stack of FEEMs, PARAFAC quantifies a minimum number of fluorescent components to describe each FEEM. Stedmon and Markager (2005) resolved 8 components by PARAFAC that described the fluorescent data of 1,276 samples. This chapter aims for a more simple classifi-

cation scheme by resolving 4 operationally-defined fractions of humic-, fulvic-, tryptophan-, and tyrosine-like material in a sample set of 72 coastal marine and estuarine waters. This classification scheme is designed to describe a minimum number of components that will best describe DOM, with the possibility of usefullness in improving metal toxicity predictions for regulatory purposes.

Reduced sulfur in aquatic systems were once thought to be of little importance in oxygenated systems. However research has shown that they are (meta)stabilized when bound to Class B metals, such as Cu(I,II) and Ag(I), in both freshwater (Rozan et al., 2000; Bowles et al., 2003) and seawater (Luther and Tsamakis, 1989). Studies on reduced sulfur and/or CRS determination in freshwater have reported CRS concentrations up to 600 nM in freshwater rivers (Rozan et al., 2000). Bianchini and Bowles (2002) and references therein reported an overall concentration of <0.001 to 162 nM in open ocean and coastal marine waters, however no published results were found on CRS determination in coastal marine or estuarine waters. Smith et al. (2002) reported that in freshwater, reduced sulfur contributes strong binding sites for metal ions such as Cu^{2+}. These findings may have implications in quantifying metal bioavailability in coastal marine and estuarine environments.

In this chapter, characterization of fluorescent DOM and CRS are reported in 69 unconcentrated samples of coastal marine and estuarine ambient waters, collected along the east, west, and south coasts of North America. In addition, 3 reference waters were used in this study, 2 of which were collected from Granite Canyon Marine Laboratories and 1 was lab-created synthetic seawater, for a total of 72 water samples. This chapter will focus on changes in DOC concentrations with salinity and the concept of DOM quality will be addressed, with both qualitative and quantitative measures of fluorescent humic-, fulvic-, tryptophan-, and tyrosine-like fractions. The varying concentrations of these four fractions will be investigated

with respect to different source inputs and compared to FI-defined input source. Following discussions on DOM, this chapter will focus on the span of CRS concentrations on unfiltered samples of the same marine and estuarine environments. The change in CRS with respect to DOC will be evaluated, with freshwater data shown for comparison.

3.2 Experimental Section

3.2.1 Reagent and Material Preparation

Synthetic Seawater

Synthetic seawater was prepared by dissolving commercial-grade sea salt mixtures (Kent Marine, Atlanta, GA, USA) in millipore grade water (MilliQ water) (18.2MΩ, MilliQ) and adjusted to 30‰ salinity using a PINPOINT® Salinity Monitor (American Marine Inc., Ridgefield, CT). All chemical characterization measurements described in Sections 3.2.3 and 3.2.4 were performed on this synthetic seawater for comparisons. All marine standard solutions and dilutions were prepared using this synthetic seawater as the solvent.

Tyrosine and Tryptophan Solutions

A 5×10^{-4} M stock solution of reagent-grade L-tryptophan (>98% pure, Sigma-Aldrich, St. Louis, MO) and a 5×10^{-3} M stock solution of reagent-grade L-tyrosine (>98% pure, Sigma-Aldrich, St. Louis, MO) were prepared using synthetic seawater as described above. These stock solutions were used to prepare diluted solutions of 2.5×10^{-7} M pure tryptophan and 5×10^{-7} M pure tyrosine. A mixture solution containing both tryptophan and tyrosine at concentrations of 2.5×10^{-7} M and 5×10^{-7} M respectively was prepared as well.

Chromium(II)

A 1 M solution of Cr(III) was prepared by dissolving crystalline $CrCl_3 \cdot 6H_2O$ (98% pure, Sigma-Aldrich, St. Louis, MO) in 50% v/v HCl (prepared from 12 N HCl). Under Ar, the Cr(III) was reduced by a Jones Reductor (Jones, 1888). The resulting Cr(II) solution was collected in an Erlenmeyer flask at the base of the reductor and sealed with a septum and Parafilm to prevent exposure to the atmosphere. This solution is stable in reduced form for about two weeks.

Mixed Diamine Reagent (Parts A and B)

The Mixed Diamine Reagent (MDR) was prepared in two parts (A and B) (Andreae et al., 1991) with increased acidity (Bowles et al., 2003). Part A consisted of dissolved N,N-dimethyl-p-phenylenediamine (98% pure, Aldrich, St. Louis, MO) in 50% v/v HCl and stored in a Nalgene bottle at 4°C. Part B consisted of dissolved $FeCl_3 \cdot 6H_2O$ (99.0% pure, Fluka, Switzerland) in 50% v/v HCl and stored in a Nalgene bottle at 4°C as well. Equivolumes of parts A and B were mixed immediately prior to use.

3.2.2 Sampling and Storage of Samples

A sampling strategy was devised prior to collection to ensure the sampling sites varied in salinity from brackish to marine and varied in natural and anthropogenic input sources such that both DOM quality and CRS concentrations should vary. These sources included wastewater, allochthonous sources (terrestrial degradation), autochthonous sources (autotroph activity, *in situ*), and a mixture of the three sources. Ambient water samples were collected from 71 marine and estuarine sites along the east, west, and south coasts of North America. Samples were collected in clean, 2L opaque, high density polyethylene (HDPE) bottles. The bottles were rinsed three times with sampling water on-site before the actual sample was taken. The samples were collected near the water's surface and

the bottles were capped while submerged to avoid air contact with the water during transport to the lab for analysis. One sample was collected at each site and sampling was done either near the shoreline or off a dock a few metres off shore.

The ambient water samples were shipped in coolers (approximately 24 hours) at about 4℃. On arrival, pH, salinity and fluorescence was immediately measured, followed by CRS and DOC. To minimize oxidation of the reduced sulfur, the samples were stored under argon. The bottles were stored at 4℃. All precautions were made to ensure minimal contamination to the bottles and water samples during collection, transport, analyses, and storage.

3.2.3 Characterization of Organic Matter

DOC Analysis

DOC concentrations were measured with a Shimadzu TOC-5050A Total Carbon Analyzer using an ASI-5000A Autosampler (Mandel Scientific, Guelph, ON). Prior to measurements of the water samples, total carbon standards, as 5 mg $C{\cdot}L^{-1}$ and 10 mg $C{\cdot}L^{-1}$ potassium hydrogen phthalate ($C_6H_4(COOH)(COO^-K^+)$) dissolved in synthetic seawater, were used as marine standards to verify the accuracy of the analyzer with marine water. An aliquot of each water sample was passed through a 0.45 μm pore size GMF GD/X membrane filter (25 mm diameter) (Whatman, Florham Park, NJ), acidified with 16 N HNO_3 and sparged with N_2 for 15 minutes immediately prior to analysis in order to remove inorganic carbon as suggested by Dafner and Wangersky (2002a). Acidified MilliQ was used to flush the analyzer after every 10 water sample measurements to ensure any salt deposits were rinsed thoroughly from the analyzer syringes. The total carbon marine standards were treated the same way as the ambient water samples prior to analyzing.

Fluorescence Measurements

An aliquot of each water sample was passed through a 0.45 μm pore size GMF GD/X membrane filter and the filtrate was measured using a Varian Cary Eclipse Fluorescence Spectrophotometer (Varian, Mulgrave, Australia) in a 1 cm quartz cuvette. Fluorescence surface scans of emission wavelengths from 250 nm to 600 nm in 1 nm increments were measured for every 10 nm excitation wavelength between 200 nm and 450 nm. The excitation and emission monochromator slit widths were both set to 5 nm for all the measurements. The scan speed was at a rate of 400 nm/min and the photomultiplier tube (PMT) was set to high detection (800 V).

The fluorescent data was processed in Matlab^{TM} (MathWorks, Natick, MA) to produce 3-dimensional FEEMs. Rayleigh scatterings were removed from the preprocessed data and replaced with Not a Number (NaN) values, which would otherwise cause mathematical interferences in subsequent spectral analyses.

Spectral Analysis of Organic Matter

Fluorescence indices for every water sample was calculated to approximate DOM source, as proposed by McKnight et al. (2001) using Equation 3.2:

$$FI_{Ex370} = \frac{Em450}{Em500} \tag{3.2}$$

where *FI* is the fluorescent index, and *Em 450* and *Em 500* is the emission intensity at 370 nm excitation. These FI values were compared to qualitative observations for each site with respect to DOM source.

The 72 FEEMs were spectrally resolved using PARAFAC to elucidate four operationally-defined fluorescent fractions and observe their individual spectra. The PARAFAC algorithms used were from PLS_Toolbox version 4.1.1 in Matlab^{TM} (Eigenvector Research, Inc., WA). The two spectra of allochthonous material were

labelled as fulvic-like and humic-like based on their average molecular weights at Ex/Em 354 nm/460 nm and 467 nm/548 nm respectively (Wu et al., 2003). Since the molecular weight of humic material is generally higher than fulvic, it was assumed that the spectrum emitting higher fluorescence wavelengths was humic-like. FEEMs of tryptophan and tyrosine standards were used to identify the remaining two spectra resolved by PARAFAC. The abundance values calculated by PARAFAC are linearly proportional to the actual concentration of each component, such that $F = kC$, where C is the concentration in mg·L^{-1}, F is the fluorophore abundance value (arbitrary units), and k is the linear proportionality constant that incorporates the molecular identity and quantum efficiency of the fluorophore. Concentrations of these fluorophores can be approximated through the use of standard solutions of Suwanee River Fulvic Acid (SRFA) and pure tryptophan and tyrosine. The molecular identity of each fraction defined by PARAFAC is not known, so the degree of uncertainty in the approximated concentrations cannot be verified. Calculations to approximate the concentrations of each fluorescent component can be found in Appendix C. In this study, the fluorophore abundance values will be used and referred to herein as 'concentrations', which limits these values to internal comparisons only.

3.2.4 Chromium(II) Reducible Sulfide

The CRS method was followed as outlined by Bowles et al. (2003). Full details on background and methodology can be found in Chapter 2 Section 2.4. A 30 mL unfiltered aliquot of each ambient water sample was initially purged with high purity N_2 at a rate of 65 mL·min^{-1}, monitored with an airflow pressure meter. Equivolumes of acidic 1 M Cr(II) and 50% v/v HCl were added to the water sample under anoxic conditions and the acidic mixture was purged again for 30 minutes. Protonated sulfur (as H_2S) released from this mixture, was trapped in a 15 mL solution of 0.05 M NaOH. With the N_2 shut off, the NaOH containing S^{2-} was transferred into a dry borosilicate glass vial and

rinsed once with 5 mL degassed MilliQ. Equivolumes of parts A and B of the MDR reagent were mixed and pipetted into the vial, which was shaken, and stored in the dark for 24 hours for development of the methylene blue coloured complex. Each water sample was measured in duplicate. Degassed MilliQ was used as a reference and analyzed concurrently with each set of samples by CRS.

The final coloured solution in the vials were analyzed colorimetrically with a 10 cm quartz cuvette. An LS-1 tungsten halogen lamp light source and a USB2000 fiber optic spectrometer was used (Ocean Optics Inc., Dunedin, FL). Calculations as described by Beer's Law determined the concentration of sulfide, with an experimentally-determined extinction coefficient $\epsilon = 4.0 \times 10^4 L \cdot mol^{-1} cm^{-1}$. A concentration factor of 2/3 was included to account for the concentration difference from the 30 mL in the reaction tube and 20 mL in the trapping tube.

3.2.5 Analysis and Comparisons between Fluorescent DOM and CRS

The data collected from fluorescence and CRS measurements were used to identify possible correlations between each measured quality index of humic-, fulvic, tryptophan-, and tyrosine-like fractions, as well as between FI and CRS. The quality index values for each fluorescent fraction was calculated using Equation 3.3:

$$QualityIndex = \frac{F}{DOC} \tag{3.3}$$

where F represents the fluorophore concentration (Arb) and DOC is in mg C·L^{-1}. Using these 6 variables, a 6×6 Pearson correlation matrix was implemented based on the correlation coefficient equation (Equation 3.4):

$$r = \frac{\Sigma(xy) - n\overline{xy}}{(n-1)s_x s_y} \tag{3.4}$$

where x and y are the values of variables 1 and 2, $\overline{x}$, $\overline{y}$, s_x, and s_y are the averages and standard deviations of variables 1 and 2, and n is the sample size. Correlation coefficients and probability of each variable combination were calculated in Matlab™.

3.3 Results and Discussion

3.3.1 Sampling

The 69 ambient water samples represented coastal marine and estuarine waters across the coasts of North America varying in both salinity and source inputs ranging from allochthonous, autochthonous, and wastewater sources. A map of the 69 sample sites plus the 3 reference sites is shown in Figure 3.1. Salinity of the water samples ranged from 1.9‰ to 38.3‰ with a pH range of 7.19 to 8.40.

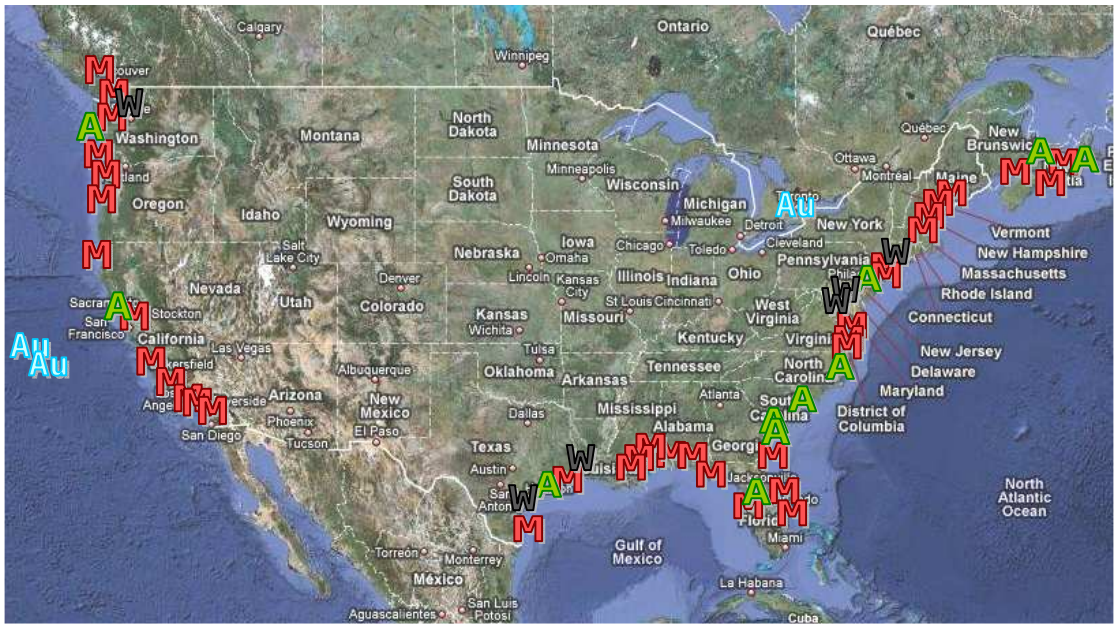

Figure 3.1: Aerial view of North America displaying each of the 72 sample site locations (Adapted from: http://www.maps.google.ca.). Sites are pinpointed based on primary source, such that A=allochthonous, Au=autochthonous, W=wastewater, and M=mixed source

The samples were divided based on primary input, indicating the main source of DOM, including allochthonous (A), autochthonous (Au), wastewater (W), and a mixture of the three (M). Upon observations of the physical location of each water site, the majority of the samples were labelled as mixtures typically due to high anthropogenic activity near the coast alongside terrestrial areas such as small forrests. Observations were considered unbiased, based only on images of the surrounding environments. Out of the 72 samples pinpointed in Figure 3.1, 3 were listed as Au, 8 as W, 11 as A, and the rest (50) as M. 2 of the 3 reference water sites labelled as autochthonous-source were from Granite Canyon Marine Laboratory (Monterey County, CA), where samples were collected off the coast of the Pacific Ocean, outside of San Francisco Bay. Water from this source has been used as reference waters in marine toxicity tests (Arnold, 2005). The third reference sample was lab-created synthetic seawater. Some other noted sample sites here that have been researched in the past in relation to toxicity include San Francisco Bay (Martin et al., 1984; Long et al., 1990; Hoenicke et al., 2003; Arnold, 2005), Chesapeake Bay (Lenwood et al., 1998; Hall et al., 2004), and Galveston Bay (Tang et al., 2002). A list of these sites and their primary input sources can be found in Table 3.3.1.

Table 3.1: Description of sampling sites. The categories under 'Primary Input' are: W = Wastewater effluent from nearby treatment plants; Au = Autochthonous or pristine environment primarily consisting of marine organism degradation; A = Allochthonous (terrestrial degradation) material from forrests and marshes along the water line with very little to no anthropogenic activity nearby; M = Mixture of both autochthonous and allochthonous sources from urban or industrial sites including, boat docks, public beaches, paths/roadways near the water line, neighbourhood developments, parks, and small terrestrial sites.

ID	Location	Waterway	Latitude (N)	Longitude (W)	Date	Time	Primary Input
GCML-1	Monterey, CA	Granite Canyon Marine Lab (used as reference)			070507		Au
GCML-2	Monterey, CA	Granite Canyon Marine Lab (used as reference)			070507		Au
SFBay-1	San Francisco, CA				070507		W
SFBay-2	San Francisco, CA				070507		W
RA-1	Sewaren, NJ	Arthur Kill	40 32 43.12	74 15 13.90	071207	920	W
RA-2	Belmar, NJ	Shark River	40 10 45.72	74 02 02.82	071207	1015	M
RA-3	Gilford Park, NJ	Barnegat Bay	39 56 58.85	74 06 49.45	071207	1112	M
RA-4	Fairfield, MD	Baltimore Harbor / Chesapeake Bay	39 12 31.70	76 31 57.39	072507	1220	W
RA-5	Morgantown, MD	Potomac River	38 21 52.58	76 58 59.07	072507	1350	W
RA-6	Norfolk, VA	Elizabeth River / Chesapeake Bay	36 50 26.46	76 18 08.91	072507	1736	M
RA-7	Delaware City, DE	Delaware Bay	39 34 43.99	75 35 11.77	072607	936	A
RA-8	Portland, ME	Casco Bay	43 38 34.05	70 15 06.08	081307	717	M
RA-9	Portsmouth, NH	Piscataqua River	43 04 45.07	70 45 27.82	081307	836	M
RA-10	Boston, MA	Dorchester Bay / Boston Harbor	42 19 36.97	71 02 49.36	081307	836	M
RA-11	Narragansett, RI	Narragansett Bay	41 42 59.60	71 21 29.88	081307	1220	M
RA-13	S. Padre Island, TX	Laguna Madre	26 04 09.79	97 09 38.50	083107	925	M
RA-14	Corpus Christi, TX	Corpus Christi Bay	27 47 59.29	97 23 27.25	083107	1340	W
RA-15	Point Comfort, TX	Lavaca Bay	28 39 57.15	96 34 32.49	083107	1530	A
RA-16	Clear Lake, TX	Galveston Bay	29 33 49.47	95 00 50.76	090107	705	M
RA-17	Clear Lake, TX	Galveston Bay	29 45 40.84	95 04 57.24		1010	W
RA-18	Crown Island, CA	San Diego Bay	32 37 50.71	117 07 43.12	091607	1750	M
RA-19	Coronado Cays, CA	San Diego Bay	32 37 50.71	117 08 00.62	091607	1830	M
RA-20	Bay Shores, CA	Newport Bay	33 36 47.03	117 54 39.81	09607	540	M
RA-21	Long Beach, CA	Long Beach Harbor	33 45 37.26	118 11 50.56	091607	700	M
RA-22	Oxnard, CA	Channel Islands Harbor	34 10 22.81	119 13 24.54	091607	1050	M
RA-23	Baywood Park, CA	Morro Bay	35 19 36.80	120 50 29.54	091607	1540	M
RA-24	Vallejo, CA	San Pablo Bay	38 05 45.52	122 15 29.11	091707	1130	M
RA-25	Inverness, CA	Tomales Bay	38 06 09.68	122 50 17.19	091707	1320	A
RA-26	Fields Landing, CA	Humbolt Bay	40 43 34.79	124 13 17.38	091807	925	M
RA-27	North Bend, OR	Coos Bay	43 24 22.98	124 13 14.89	091807	1552	M
RA-28	Newport, OR	Yaquina Bay	44 37 47.55	124 03 08.94	091907	1020	M

ID	Location	Waterway	Latitude (N)	Longitude (W)	Date	Time	Primary Input
RA-29	Astoria, OR	Columbia River	46 11 26.75	123 50 57.13	091907	1555	M
RA-30	Laidlow, WA	Fray's Harbor	46 51 43.66	124 04 19.92	092007	1040	A
RA-31	Olympia, WA	Budd Inlet	47 03 30.25	122 53 49.19	092007	1237	M
RA-32	Tacoma, WA	Puget Sound	47 15 43.69	122 26 23.40	092007	1320	W
RA-33	Seattle, WA	Puget Sound	47 36 13.50	122 20 21.50	092007	1430	M
RA-34	Halifax, NS	Armview Terr.	44 38 19.01	63 36 32.28	100507	1327	M
RA-35	Halifax, NS	Bedford Basin	44 40 33.39	63 36 55.33	100507	1400	M
RA-36	Halifax, NS	Bedford Basin	44 42 52.90	63 40 23.12	100507	1430	M
RA-37	Digby, NS	Annapolis Basin	44 37 29.96	65 45 16.29	100607	1310	M
RA-38	Pictou, NS	East River of Pictou	45 40 28.40	62 42 31.90	100707	1120	M
RA-39	Tatamagouche, NS	Tatamagouche Bay	45 42 13.55	63 16 46.35	100707	1309	A
RA-40	Slidell, LA	Lake Pontchartrain	30 13 06.59	89 47 26.51	101307	950	M
RA-41	Biloxi, MS	Back Bay	30 24 49.43	88 53 46.95	101307	1110	M
RA-42	Mobile, AL	Mobile Bay	30 41 14.12	88 00 49.29	101307	1300	M
RA-43	Pensacola, FL	Pensacola Bay	30 25 00.25	87 11 38.33	101307	1430	M
RA-44	Panama City, FL	St. Andrews Bay	30 11 11.32	85 44 11.36	101407	810	M
RA-45	Apollo Beach, FL	Tampa Bay	27 45 45.66	82 25 16.12	101407	1710	M
RA-46	Cockroach Bay, FL	Cockroach Bay / Tampa Bay	27 41 13.82	82 31 14.61	101407	1740	A
RA-47	Tampa, FL	Tampa Bay	27 39 11.99	82 40 32.21	101407	1813	M
RA-48	Tampa, FL	Tampa Bay	27 56 28.41	82 32 09.80	101507	1035	M
RA-49	Fort Pierce, FL	Indian River	27 27 05.66	80 19 20.48	101507	1450	M
RA-50	Titusville, FL	Indian River	28 37 13.06	80 48 29.17	101507	1620	M
RA-51	Jacksonville, FL	St. Johns River	30 19 13.07	81 40 16.48	101607	1025	M
RA-52	Brunswick, GA	St. Simons River	31 09 02.27	81 28 33.11	101607	1215	A
RA-53	Darien, GA	Altamaha River	31 20 13.25	81 26 55.54	101607	1250	A
RA-54	Pea Ridge, NC	Albemarle Sound	35 57 34.89	76 29 15.90	101707	750	M
RA-55	New Bern, NC	Neuse River	35 06 23.22	77 02 03.31	101707	1025	M
RA-56	Wilmington, NC	Cape Fear River	34 13 14.69	77 58 51.37	101707	1300	A
RA-57	Charleston, SC	Charleston Harbor	32 46 25.21	79 55 27.86	101807	740	A
RA-58	Vancouver, BC	Burrard Inlet	49 17 14.58	123 06 37.68	120907	0920	M
RA-59	Vancouver, BC	Burrard Inlet	48 18 00.35	123 07 17.74	120907	0930	M
RA-60	Vancouver, BC	Coal Harbour	49 17 41.98	123 07 57.68	120907	1248	M
RA-61	Vancouver, BC	English Bay	49 16 26.85	123 08 03.31	120907	1413	M
RA-62	Vancouver, BC	False Creek	49 16 20.30	123 06 13.76	120907	1525	M
SS-1	Port Hastings, NS	Canso Strait	45 39 19.04	61 24 19.82	041707		A
SS-2	Bedford, NS	Moir's Pond	44 42 51.80	63 40 35.71	042707		M
SS-3	Bedford, NS	Mill Cove	44 42 52.90	63 40 23.12	042707		M
SS-4	Halifax, NS	Bedford Basin	44 40 33.39	63 36 55.33	042707		M
SS-5	Halifax, NS	Bedford Basin	44 38 19.01	63 36 32.28	042707		M
SS-6	Halifax, NS	Halifax Harbour	44 37 29.05	63 33 49.60	042707		M

3.3.2 Characterization of Organic Matter

DOC Analysis

DOC concentrations were measured as an approximation of DOM in each of the 72 water samples. A plot of DOC with increasing salinity is illustrated in Figure 3.2. Points are grouped based on primary input of organic matter.

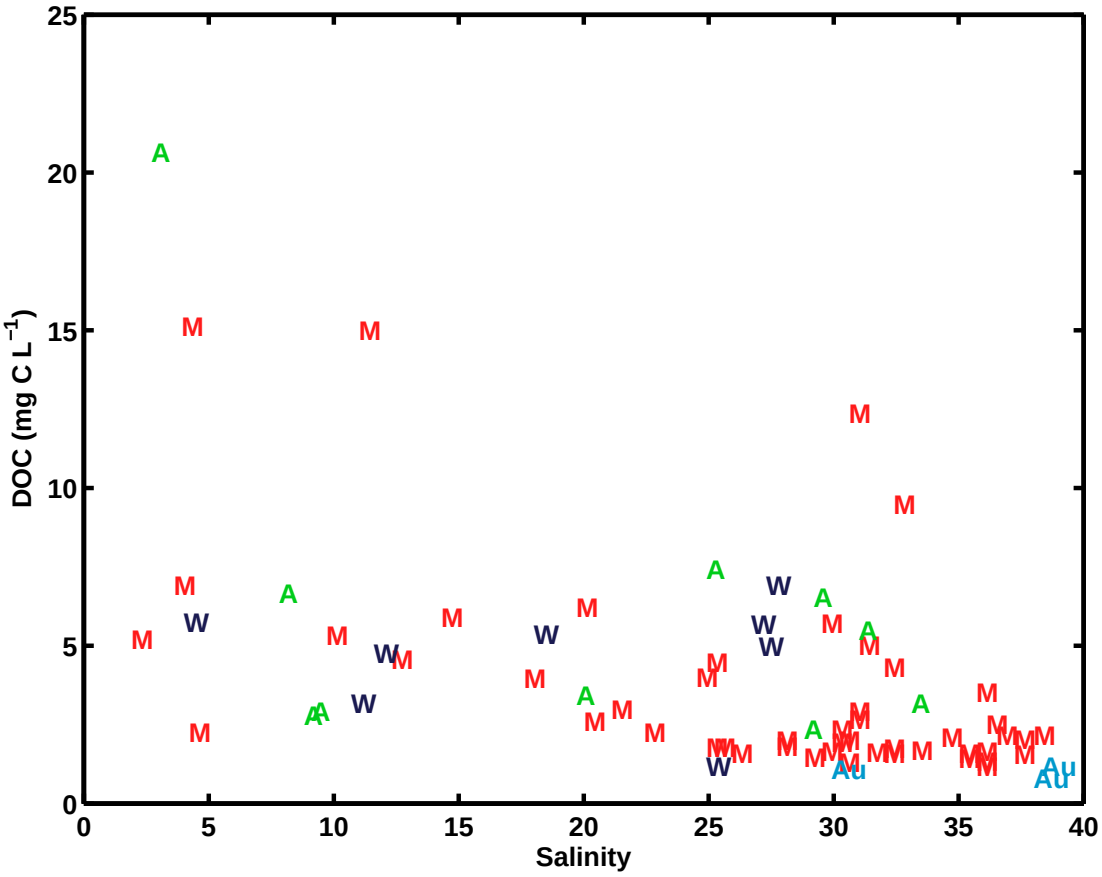

Figure 3.2: Plot of DOC with increasing salinity, separated based on primary organic matter input (A=allochthonous, Au=autochthonous, M=mixed source, and W=wastewater). There is no significant relationship between DOC and salinity.

DOC concentrations measured here spanned from 0.80 mg C·L^{-1} to 20.66 mg C·L^{-1}. Although there appeared to be a slight decrease in DOC with salinity, no statistically significant correlation between DOC and ionic strength was observed. The notion that DOC concentrations may drop significantly with higher salinity

can be attributed to the salting-out effect. This salting-out effect refers to the decrease in solubility of non-electrolytes with an increase in ionic strength (Xie et al., 1997; Millero, 2001). This effect has been observed using organic molecules in lab-created NaCl solutions (Xie et al., 1997) and of DOM in natural estuarine and marine coastal waters (Mantoura and Woodward, 1983). Furthermore, Mantoura and Woodward (1983) stated that estuarine samples collected near sewage or industrial effluent are expected to have abnormally high, yet localized, organic matter concentrations that do not contribute to the overall DOC found in marine water. A subset of water samples collected here that measured abnormally high DOC (> 5 mg C$\cdot$L^{-1}) are shown in Table 3.2. Observations of these sites are given in detail.

Table 3.2: List of water samples with abnormally high DOC concentrations.

ID	Location	Salinity (‰)	DOC (mg $C \cdot L^{-1}$)	Primary Input	Site Description
SFB-1	San Francisco, CA	26.7	5.7	Wastewater	Along shore of San Francisco Bay. Pooling and movement of water in this area decreases flow to the Pacific Ocean.
SFB-2	San Francisco, CA	27.0	5.0	Wastewater	Along shore of San Francisco Bay, near opening to Pacific Ocean.
RA-1	Sewaren, NJ	27.3	6.9	Wastewater	Off dock on Arthur Kill. Heavy industrial area, receiving effluents from several large treatment plants.
RA-2	Belmar, NJ	32.4	9.5	Mixed source	Shark River inlet, off a boat dock near opening of marshland outlet.
RA-14	Corpus Christi, TX	18.0	5.4	Wastewater	Off roadway in Corpus Christi Bay, near opening of Tule Lake Channel, containing effluents from several treatment plants along the river path.
RA-15	Point Comfort, TX	7.8	6.7	Allochthonous	Along shoreline between Matagorda Bay and Lavaca Bay near outflowing river through marsh-like forrest area.
RA-16	Seabrook, TX	9.7	5.3	Mixed source	Off boat dock in Galveston Bay, near opening of channel from Clear lake.
RA-17	La Porte, TX	4.0	5.8	Wastewater	Off shore of Ship Channel, downstream from several treatment plants.
RA-40	Slidell, LA	14.3	5.9	Mixed source	Off a boat dock in an enclosed inlet near Grand Lagoon, which empties into Lake Pontchartrain. Area is predominantly residential.
RA-41	Biloxi, MS	19.7	6.2	Mixed source	Off boat dock in Bay of Biloxi, near opening of a small stream, originating from a small treatment plant.
RA-45	Apollo Beach, FL	29.5	5.7	Mixed source	Off boat dock in highly residential area. Spaces of greenery along shoreline, contributed by Apollo Beach Golf Club. Water empties into Tampa Bay.
RA-46	Cockroach Bay, FL	31.0	5.5	Allochthonous	Along shoreline of marsh-like waters, originating from Cockroach Bay.
RA-48	Tampa, FL	31.0	5.020	Mixed source	Off a boat docking station in a residential / commercial area.
RA-50	Titusville, FL	30.6	12.4	Mixed source	Off boat dock within Yacht Basin, which opens into the Indian River. Parks and forrest areas along the river.
RA-51	Jacksonville, FL	3.9	15.1	Mixed source	Off boat dock on St. John's River at a point of river narrowing. Commercial area along the shoreline.
RA-52	Brunswick, GA	29.2	6.5	Allochthonous	Off dock along Marshes of Glynn. Marsh continues to the ocean.
RA-53	Darien, GA	2.7	20.7	Allochthonous	Off dock on Champneys River. Islands of forrest and field areas along the river right to the ocean.
RA-54	Pea Ridge, NC	3.6	6.9	Mixed source	Off dock in Albemarle Sound. Residential and forrest areas along shoreline.
RA-55	New Bern, NC	11.0	15.0	Mixed source	Off dock on Neuse River. Highly residential and commercial area along shoreline. Marsh/wetlands directly upstream.
RA-56	Wilmington, NC	24.9	7.4	Allochthonous	Small inlet pool directly off Brunswick River. Forrests and badland-type areas along shoreline and upstream. Small treatment plant located farther upstream.

Fluorescence Measurements

At a molecular level, the nature of organic matter has a significant aromatic character, identified through measurements of fluorescence spectroscopy to produce FEEMs for each of the 72 water samples. Using Matlab^{TM}, the FEEMs were visualized as contour plots to show the fluorescence intensity at each Ex/Em wavelength pair.

There was a clear qualitative indication of the presence of humic-, fulvic-, tryptophan-, and tyrosine-like fractions present in each sample based on their distinctive Ex/Em intensity signals, similar to what was seen by Wu et al. (2003) of humic and fulvic fractions, Baker (2001) of fulvic and tryptophan fractions, and Winter et al. (2007) of all four fractions in freshwater. Furthermore, it was evident from comparing the FEEMs between samples that the relative abundance of these fractions varied with site location. Figure 3.3 contains two representative FEEMs for illustration.

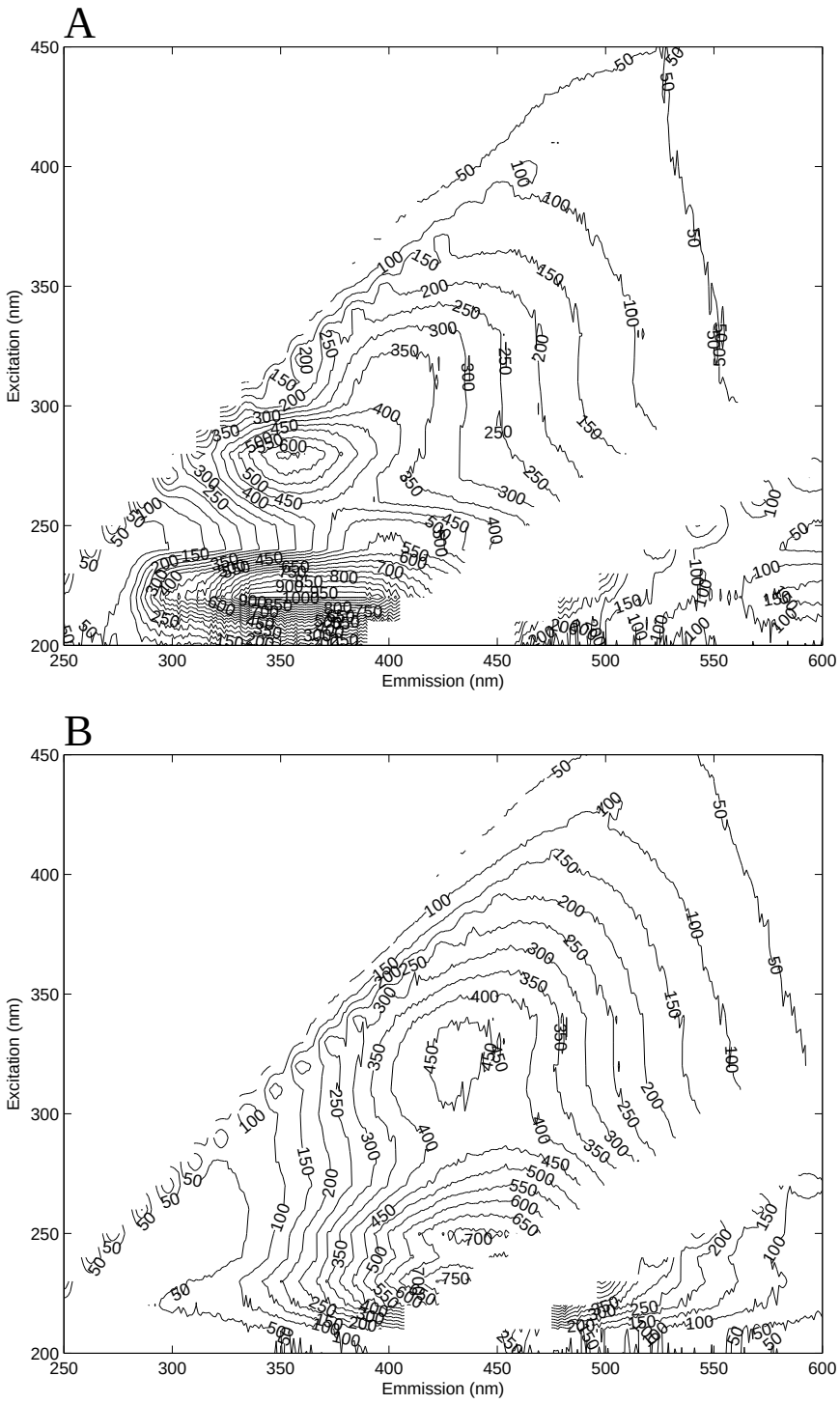

Figure 3.3: Fluorescence excitation-emission matrices of two ambient water samples. The Baltimore Harbour in Fairfield, MD (A) has higher tyrosine- and tryptophan-like fractions, seen by the high intensity peaks at 225 nm/350 nm and 275 nm/350 nm Ex/Em. Indian River in Fort Pierce, FL (B) has higher humic- and fulvic-like components, which is seen by the high intensity peaks at about 325 nm/420 nm and 350 nm/500 nm Ex/Em.

The Figure 3.3A sample is from Baltimore Harbor in Fairfield, MD, downstream from a large treatment plant (11.6 ‰ salinity) and the Figure 3.3B corresponding sample is from Indian River in Fort Pierce, FL off a boat dock near parks and marshes (32.0 ‰ salinity). These two FEEMs optically illustrate very different organic matter quality, with a difference in excitation peaks of about 100 nm and a difference in emission peaks of about 125 nm. There was strong evidence of wastewater effluent in Baltimore Harbor as indicated by the high intensity signals at 225 nm / 350 nm Ex/Em. These signals are unique to tryptophan-like fractions, which are good indicators of wastewater (Baker, 2001). Indian River displayed high intensity peaks at 325 nm / 420 nm and 350 nm / 500 nm Ex/Em, indicating the presence of fulvic-like and humic-like fractions from terrestrial runoff (Smith and Kramer, 1999; Wu et al., 2003). The intensity values, labelled along the contour lines in Figure 3.3 are related to the abundance of each fluorophore as well as its fluorescence efficiency, suggesting that fluorophore concentrations in each sample can only be compared between the same fluorophore. Concentrations cannot be compared between different fluorophores, contributing to differences in fluorescing efficiency. The intensity values of tryptophan-like material in Figure 3.3A are up to 900, suggesting a high abundance of tryptophan, whereas in Figure 3.3B intensity values of humic and fulvic material are up to 450. Despite the optical difference between these two samples, the DOC concentrations were very similar at 4.8 mg C·L^{-1} and 4.3 mg C·L^{-1} for Baltimore Harbor and Indian River respectively. Quantitative comparisons of fluorophores normalized to DOC will be discussed in Section 3.3.4.

Spectral Analysis of Organic Matter

The four most prevalent fluorescent fractions in all the FEEMs were defined by PARAFAC. The components that described the system were labelled as fulvic-like, humic-like, tryptophan-like, and tyrosine-like fractions as illustrated in Figure 3.4.

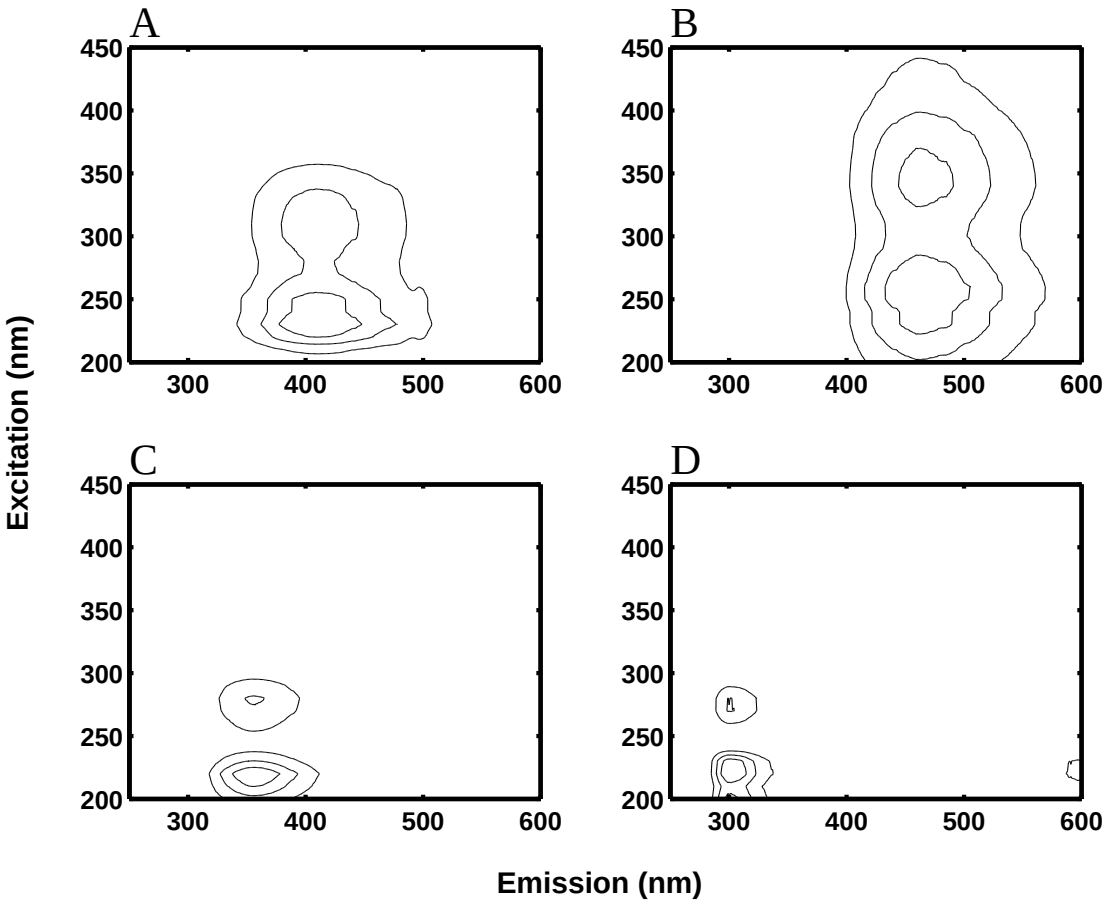

Figure 3.4: Spectra of the four main components that describe organic matter quality within the 72 water samples. The top two components represent fulvic-like (A) and humic-like (B) material. The bottom two components represent tryptophan-like (C) and tyrosine-like (D) material. This analysis described 97.843% of the fluorescent data as defined by Matlab^{TM}.

The concentrations obtained by PARAFAC were normalized to DOC, using Equation 3.3 (quality index values). The use of intensive values in this manner allowed for comparisons of fluorophore concentrations between samples, independent of DOC concentration. A broad span of fluorophore concentrations in the 72 water samples can be seen in Figure 3.5.

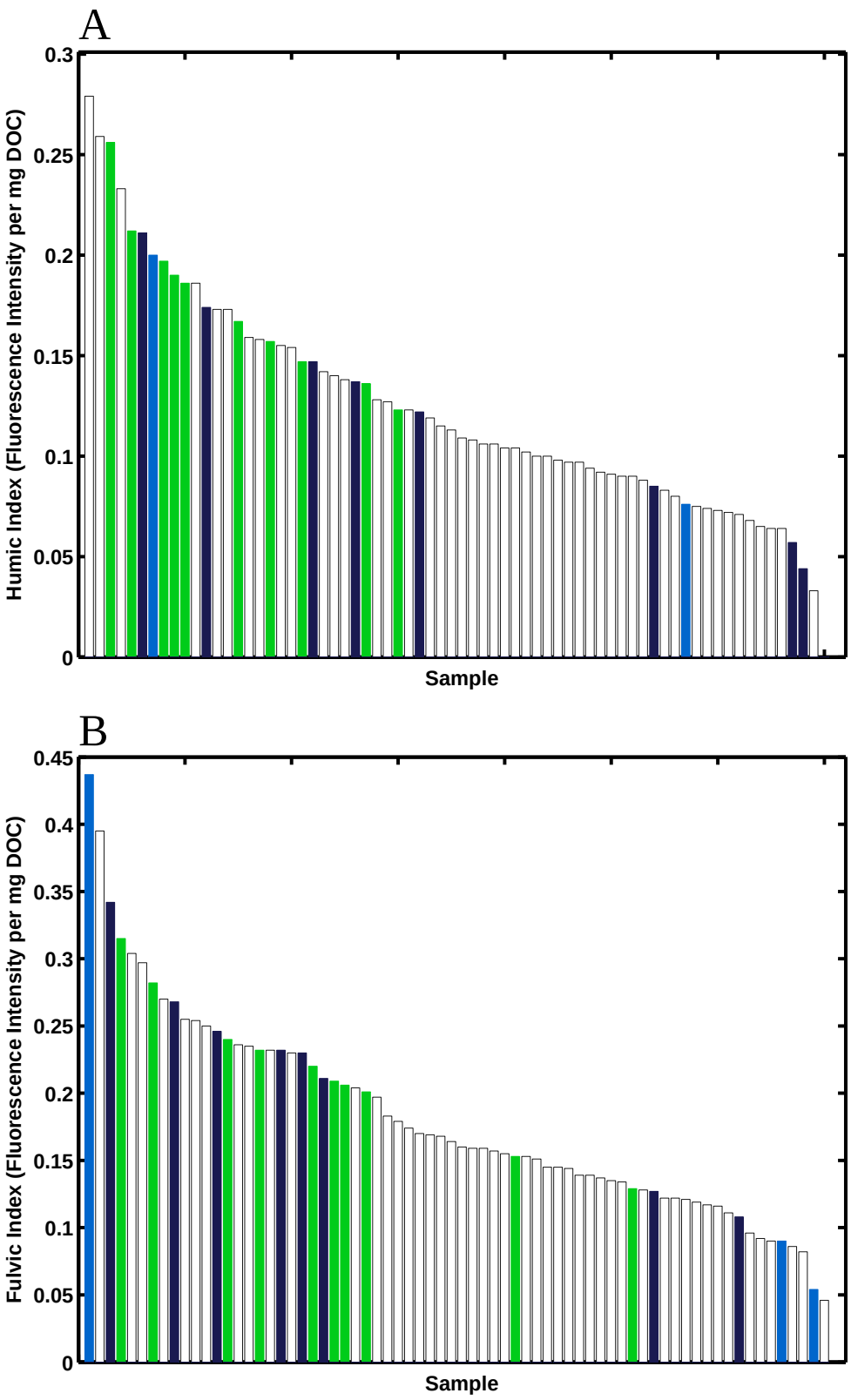
A
Humic Index (Fluorescence Intensity per mg DOC)
0.3
0.25
0.2
0.15
0.1
0.05
0
Sample
B
Fulvic Index (Fluorescence Intensity per mg DOC)
0.45
0.4
0.35
0.3
0.25
0.2
0.15
0.1
0.05
0
Sample

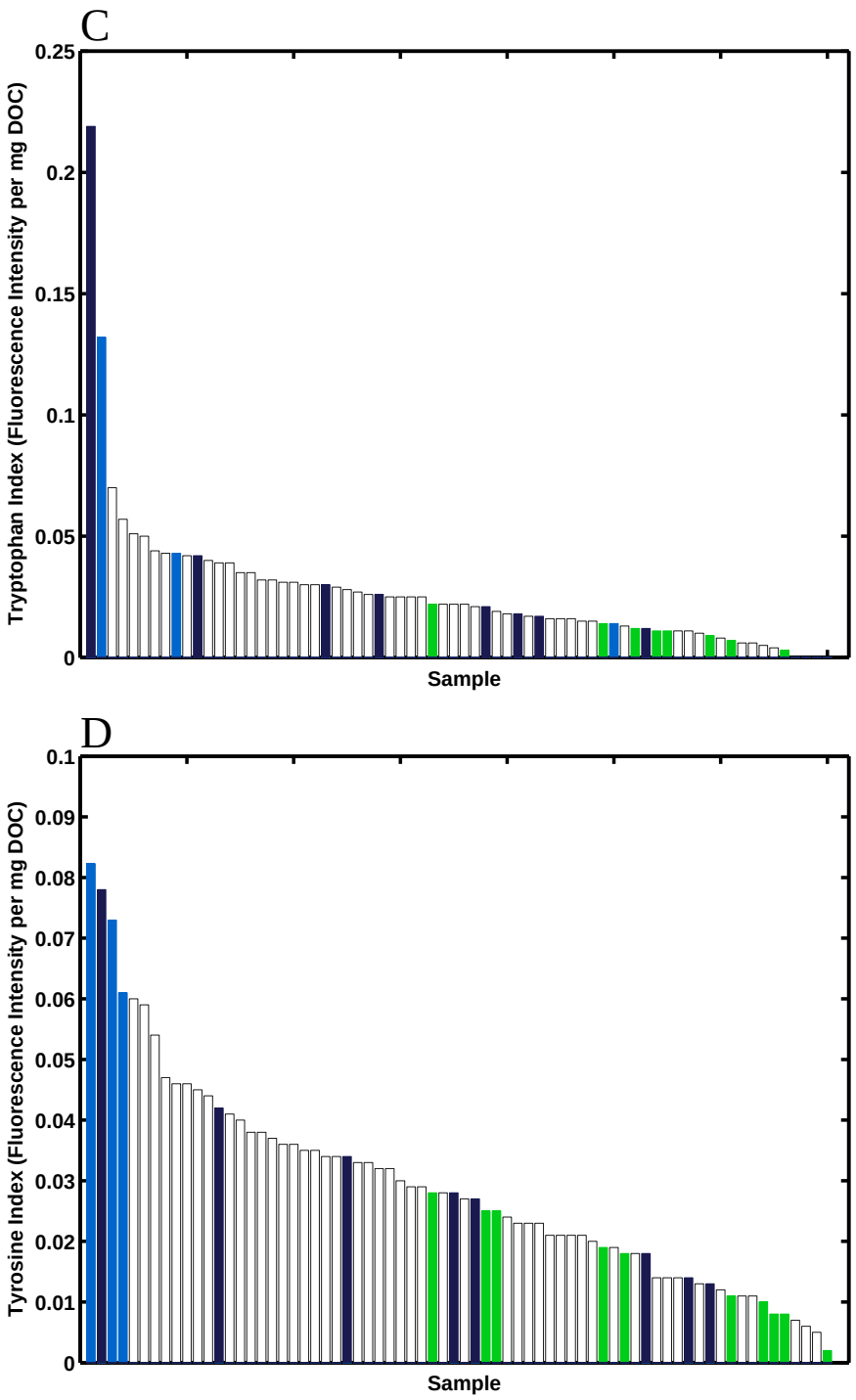

Figure 3.5: Quality index of A) humic-, B) fulvic-, C) tryptophan-, and D) tyrosine-like fractions (green = allochthonous, blue = autochthonous, white = mixed source, and gray = wastewater). The index values were arranged in decreasing order to identify the span of contributions from each fluorescent fraction for every mg of DOC.

The plots in Figure 3.5 display the large difference in fluorescent fractions, independent of DOC. It can be seen that the large dataset of water samples represented very different DOM quality based on input source. As expected, higher humic and fulvic material and lower tryptophan and tyrosine material were identified in allochthonous sources, as seen in green in Figure 3.5. Furthermore, blue autochthonous-sourced water showed high tyrosine content, indicative of microbial and algal activity in the open ocean. Wastewater-source water (gray bars in Figure 3.5) typically have high tryptophan and fulvic material (Baker, 2001), but this was not seen for every water sample, likely attributed to dilution of effluent if the sample collection was too far downstream from the source. No trends of quality index were expected from the mixed-source water samples. Overall, the water samples used here clearly show the large span and variation of each fluorescent component, suggesting that DOM quality has significant spatial dependence in estuarine and coastal marine environments.

3.3.3 Chromium(II) Reducible Sulfide

The concentrations of CRS spanned six orders of magnitude, ranging from 0.07 nM $\pm$ 0.01 nM to 7703 nM $\pm$ 98 nM. Figure 3.6 is a plot of CRS concentrations in decreasing order.

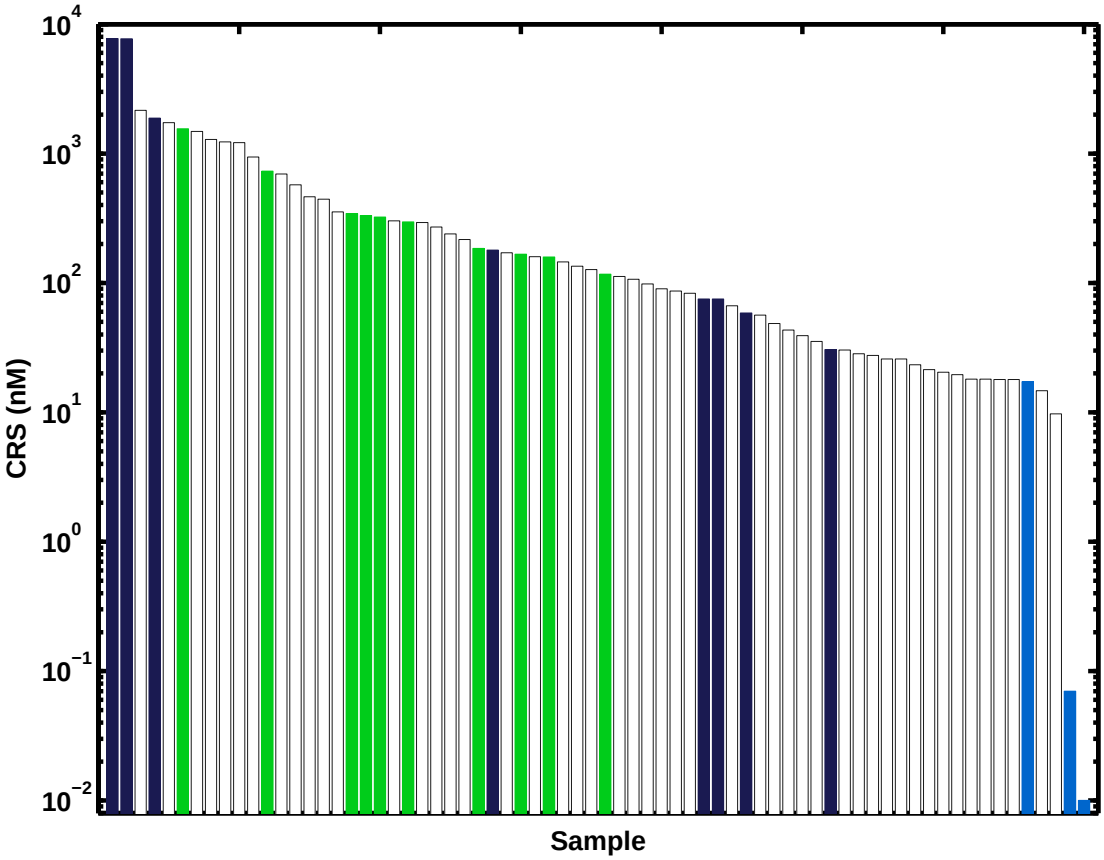

Figure 3.6: Log CRS concentrations in decreasing order. Colour schemes are as described in Figure 3.5. The lowest CRS concentrations were found in autochthonous-sourced sites, and the highest in wastewater.

The highest two samples, seen on the left side of the plot in Figure 3.6, were collected directly in San Francisco Bay in highly polluted water near wastewater effluent. The lowest two samples on the right side of the plot were from Granite Canyon Marine Laboratory. With the exclusion of the two (lowest) samples from Granite Canyon, CRS spanned four orders of magnitude in the coastal marine and estuarine water samples. Wastewater-source sites appeared to have the highest CRS concentrations, as seen in gray in Figure 3.6, however this trend was inconsistent. Furthermore, the majority of allochthonous-source sites (green) had relatively high CRS concentrations. Comparisons between DOC and CRS identified a strong correlation in allochthonous-source water, as shown in Figure 3.7.

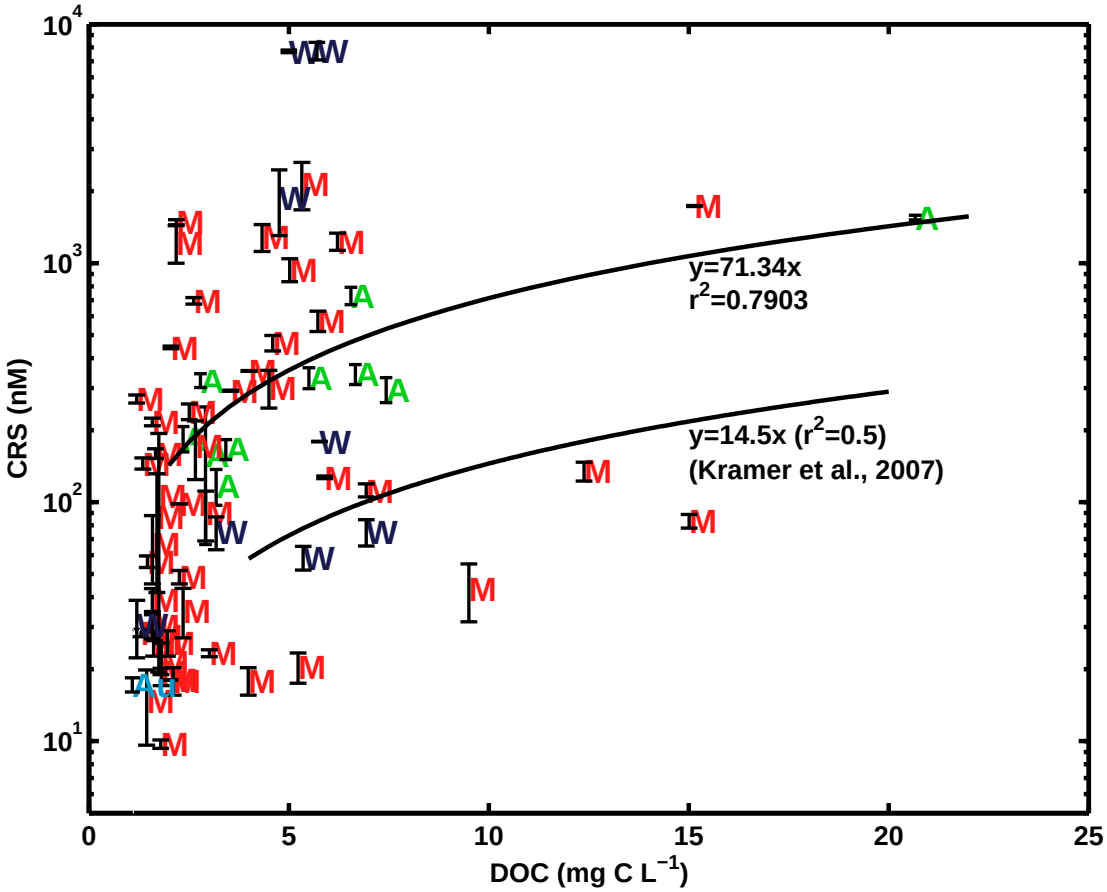

Figure 3.7: DOC compared to CRS for each of the 72 water samples. There was no significant correlation between these two measurements ($r^2 = 0.14, p = 0.001$) as a whole. However, a strong correlation was seen between DOC and CRS in allochthonous-source water samples ($r^2 = 0.79, p < 0.001$). A=allochthonous, Au=autochthonous, W=wastewater, M=mixed source.

Research done by Kramer et al. (2007) suggested a significant linear correlation between DOC and CRS ($r^2 \simeq 0.5$) in freshwater (lower solid line in Figure 3.7), and a stronger linear correlation between DOC and CRS from wastewater sources ($r^2 \simeq 0.55$). This correlation allowed for approximations of CRS for regulatory purposes. It was thought that if this correlation existed in marine water, it would have implications in marine toxicity analyses. However, a significant correlation was seen only in allochthonous-source waters, as shown in Figure 3.7 with a correlation coefficient of r^2=0.79, p<0.001. It should be noted that the CRS concentrations in the research by Kramer et al. (2007) spanned from 0 nM to

350 nM, whereas the concentrations in this study spanned 6 orders of magnitude. Further insight into estuaries and coastal marine water with primary allochthonous DOM input would be needed to draw conclusions on this observation. However, an overall correlation between estuarine and coastal marine DOC and CRS was not seen in this broad span of CRS concentrations.

3.3.4 Analysis and Comparisons between Fluorescent DOM and CRS

A Pearson correlation matrix allowed for direct comparisons between each quality index of humic-, fulvic-, tryptophan-, and tyrosine-like material, FI, and CRS, to identify possible correlations in a systematic fashion. Correlation coefficients and probability for each variable combination is presented in a 6×6 matrix in Table 3.3. A scatterplot matrix of the 6×6 dataset in Table 3.3 can be found in Appendix D. In addition, correlation coefficients were calculated for each input source of allochthonous, autochthonous, wastewater, and mixed samples separately, as four separate correlation matrices, which can also be found in Appendix D.

Table 3.3: Correlation matrix for fluorescent DOM and CRS. Values are correlation coefficients and probability, listed as r(p). HA=humic index, FI=fulvic index, Trp=tryptophan index, Tyr=tyrosine index, FI=fluorescent index, CRS=chromium(II) reducible sulfide.

	HA	FA	Trp	Tyr	FI	CRS
HA	1.0	0.47(<0.001)	0.27(0.03)	-0.34(0.004)	-0.19(>0.1)	0.33(0.005)
FA	0.47(<0.001)	1.0	0.33(0.005)	0.03(>0.1)	0.05(0.04)	0.43(0.002)
Trp	0.27(0.03)	0.03(>0.1)	1.0	0.72(<0.001)	0.26(0.03)	0.05(>0.1)
Tyr	-0.34(0.004)	0.03(>0.1)	0.72(<0.001)	1.0	0.44(0.001)	-0.36(0.002)
FI	-0.19(>0.1)	0.05(0.04)	0.26(0.03)	0.44(0.001)	1.0	-0.27(0.02)
CRS	0.33(0.005)	0.43(0.002)	0.05(>0.1)	-0.36(0.002)	-0.27(0.02)	1.0

Comparisons between the four fluorophores and FI examined the consistency of FI calculations in relation to input source, presented in Figure 3.8. Each point represents the qualitative observations of primary DOM source from Table 3.3.1.

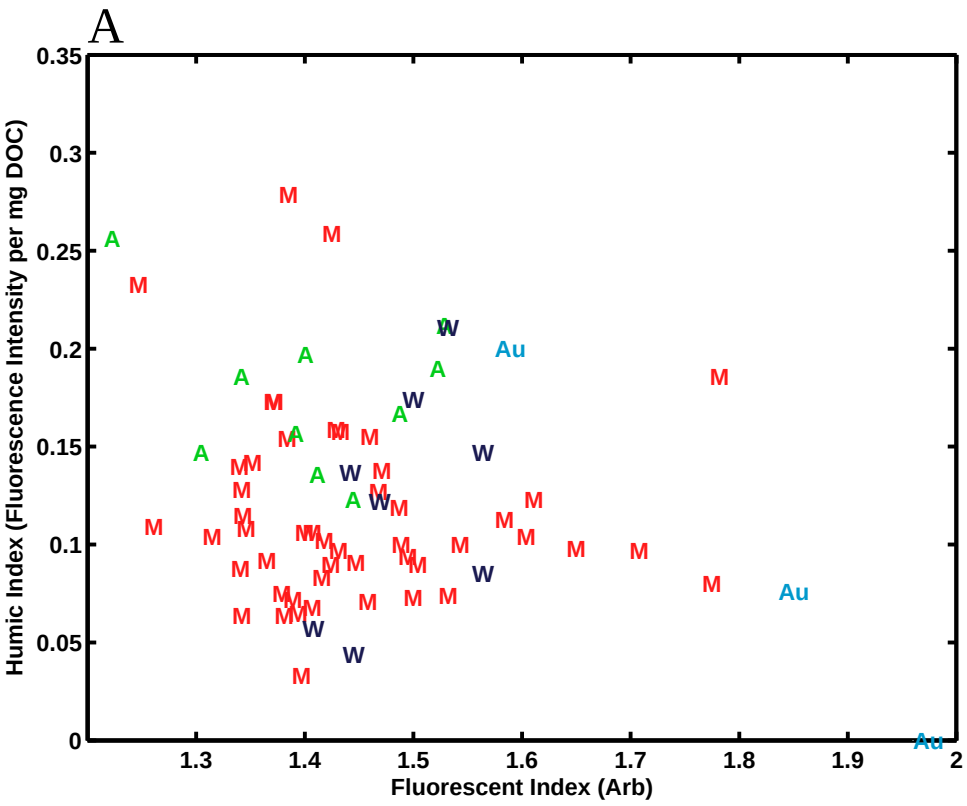
A
Humic Index (Fluorescence Intensity per mg DOC)
Fluorescent Index (Arb)
0
0.05
0.1
0.15
0.2
0.25
0.3
0.35
1.3
1.4
1.5
1.6
1.7
1.8
1.9
2
M
A
W
Au

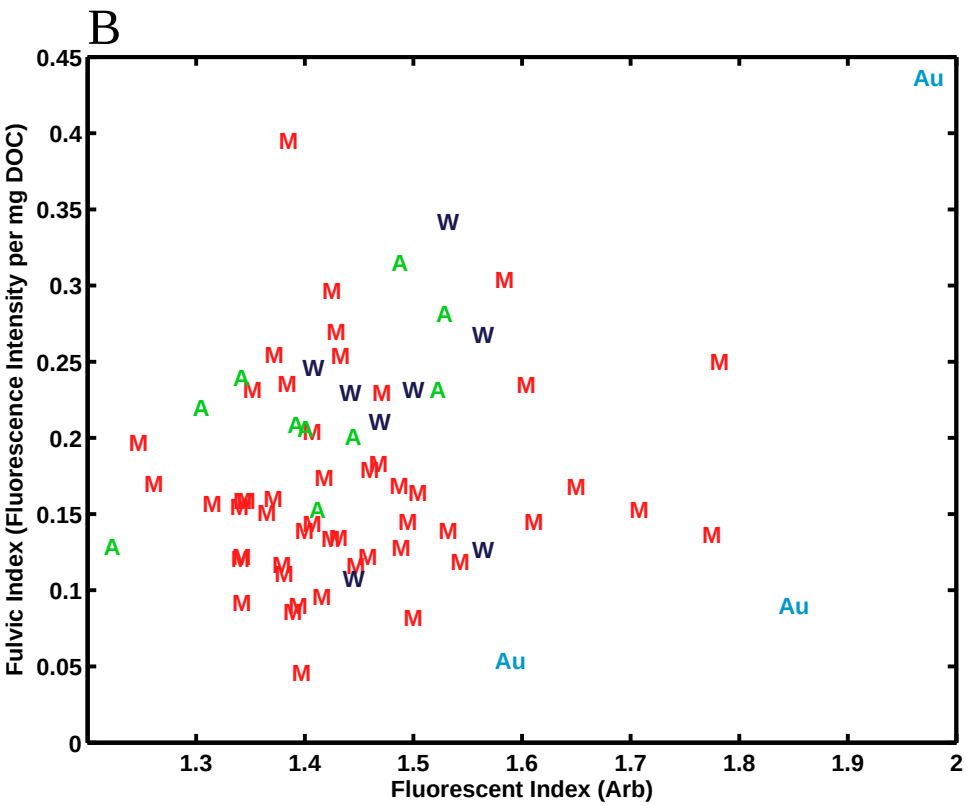
B
Fulvic Index (Fluorescence Intensity per mg DOC)
Fluorescent Index (Arb)
0
0.05
0.1
0.15
0.2
0.25
0.3
0.35
0.4
0.45
1.3
1.4
1.5
1.6
1.7
1.8
1.9
2
M
A
W
Au

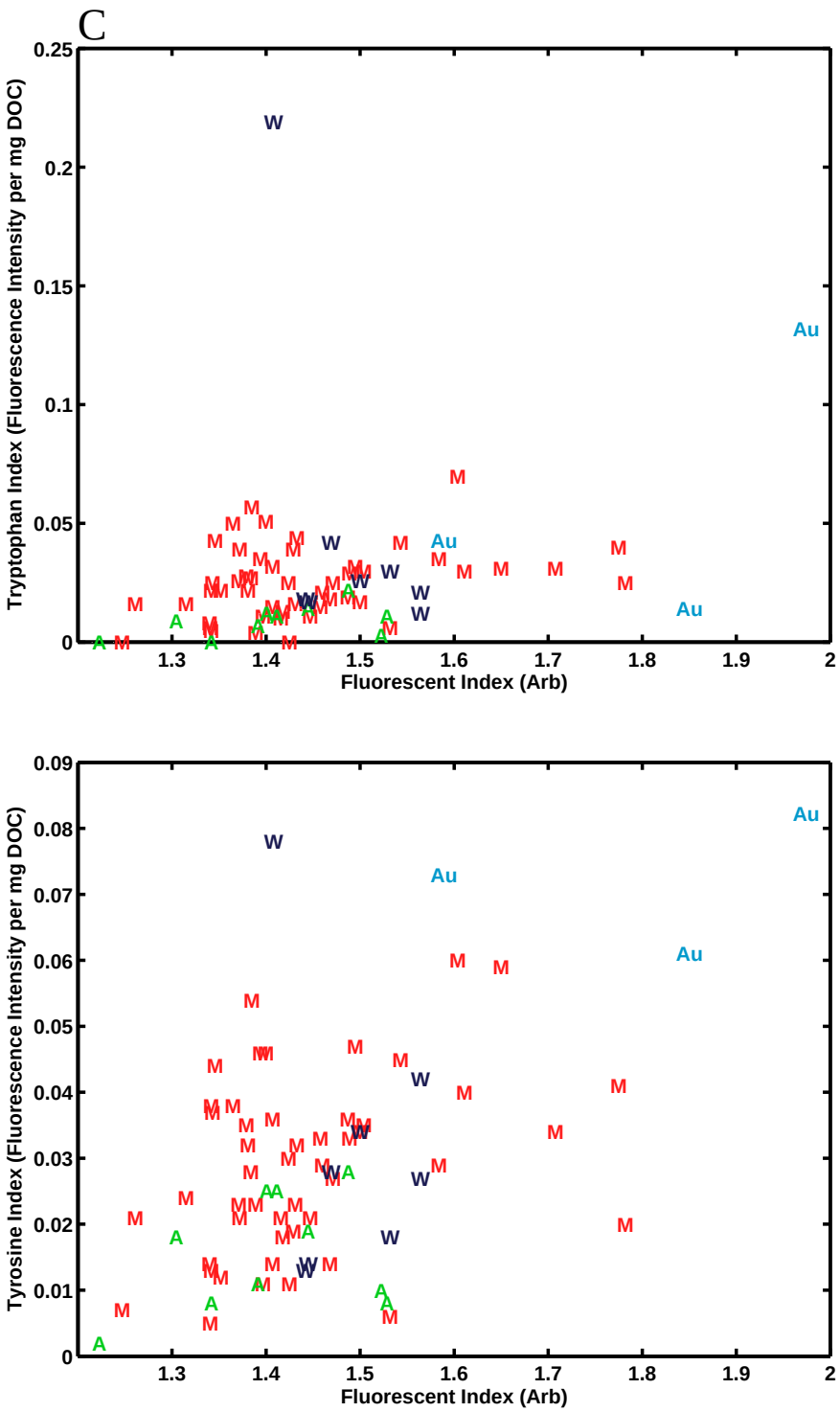

Figure 3.8: Plot of quality index values of A) humic-like, B) fulvic-like, C) tryptophan-like, and D) tyrosine-like fractions with increasing FI. Points are labelled based on input source: A=allochthonous, Au=autochthonous, W=wastewater, M=mixed source.

As seen in Figure 3.8, the majority of the qualitative observations coincided with the FI values for input source. FI values of ∼1.9 indicate autochthonous DOM whereas ∼1.4 indicate allochthonous DOM (McKnight et al., 2001). Figure 3.8A clearly shows allochthonous (Au) points on the higher end of the x-axis, allochthonous (A) on lower end, and wastewater in the middle, indicating a mixture of both allochthonous and autochthonous material. The same trend can be seen in Figures 3.8B-D. In addition, Au points are on the lower end of the y-axis in Figure 3.8A, indicating lower humic proportions in comparison to humic from other sources. However relatively higher tyrosine proportions of Au can be seen in Figure 3.8D, compared to other tyrosine sources. This comparison between FI (dependent of source) and fractions defined by PARAFAC (independent of source), confirms the validity of the qualitative observations of each water site.

Upon observations of Table 3.3, linear correlations were found between tryptophan and tyrosine index values followed by humic and fulvic index values with coefficients of 0.72 and 0.47 respectively. Figure 3.9 presents the plots of humic to fulvic, and tryptophan to tyrosine, showing these linear correlations. Statistically significant linear correlations between the two autochthonous and allochthonous fluorescent components can likely be attributed to originating from the same source, microbial and terrestrial respectively, independent of DOC concentration.

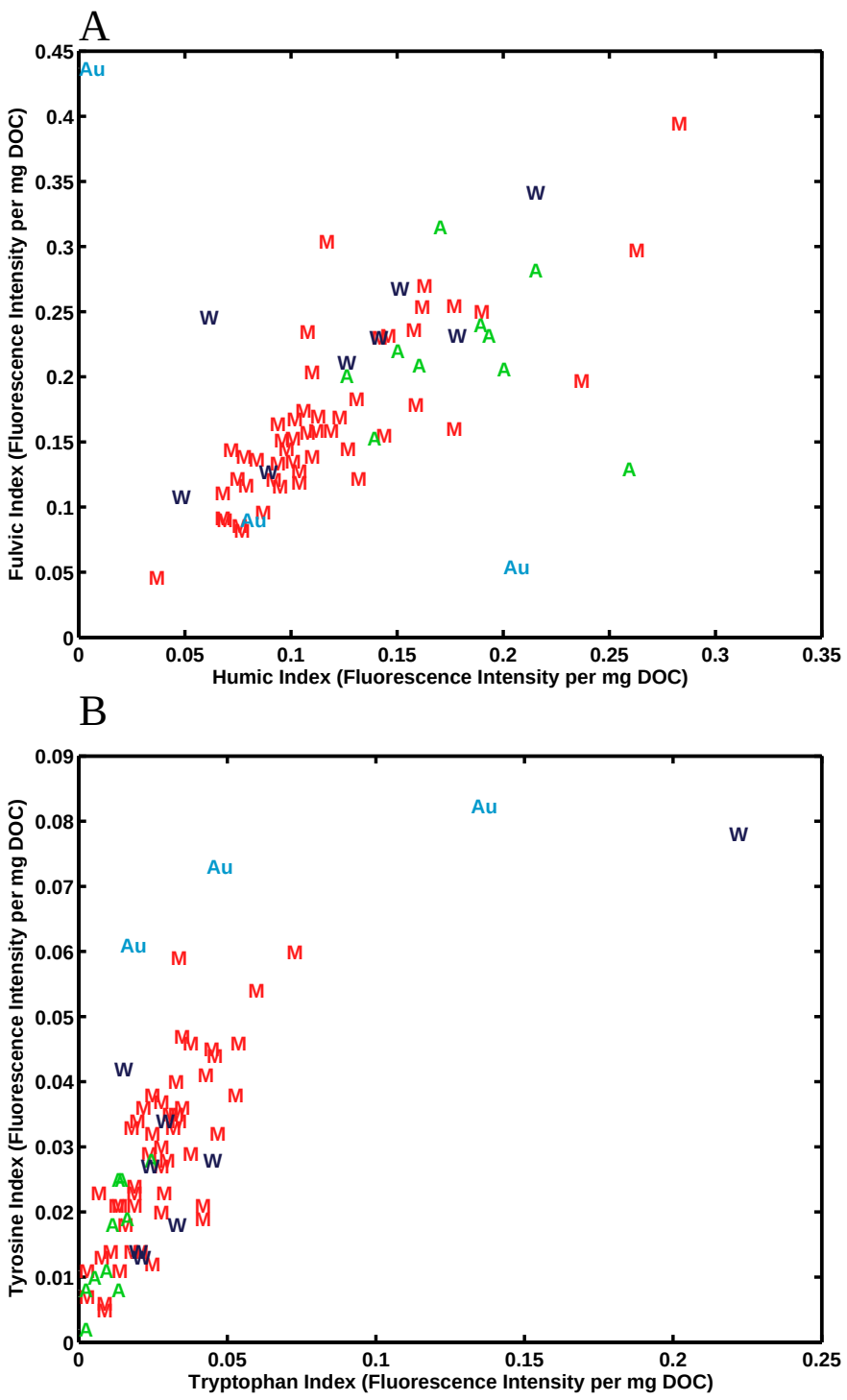

Figure 3.9: Comparisons of fluorescent A) humic index to fulvic index and B) tryptophan index to tyrosine index. A significant correlation between these components was calculated at 0.47, $p<0.001$ and 0.72, $p<0.001$ respectively. A=allochthonous, Au=autochthonous, W=wastewater, M=mixed source.

Based on Figure 3.9, it is interesting to note that the amount of fluorescent tryptophan and tyrosine in coastal marine and estuarine environments may be predicted based on the linear equation $Tyr = 0.4055Trp + 0.0182$ regardless of DOC concentrations. Furthermore, the equation $FA = 0.6507HA + 0.1014$ represents the linear combination of humic and fulvic material in these environments. However with a lower coefficient of 0.47, there is greater variability in this linear relationship. Separation of the input source points in Figure 3.9A identified the greatest correlation in the mixed source (r=0.81, p<0.001), followed by wastewater (r=0.77, p=0.02), with allochthonous source waters with the least significant correlation of r=0.10, p=0.1. However, in comparing allochthonous-source points in Figure 3.9B, the correlation was among the highest with r=0.82, p=0.003 in comparison to wastewater (r=0.87, p=0.005) and mixed-source (r=0.78, p<0.001). The number of autochthonous samples is insufficient in this study to draw conclusions on any correlations.

Comparisons between CRS and the four fluorophores of humic, fulvic, tryptophan, and tyrosine-like material is presented in Figure 3.10.

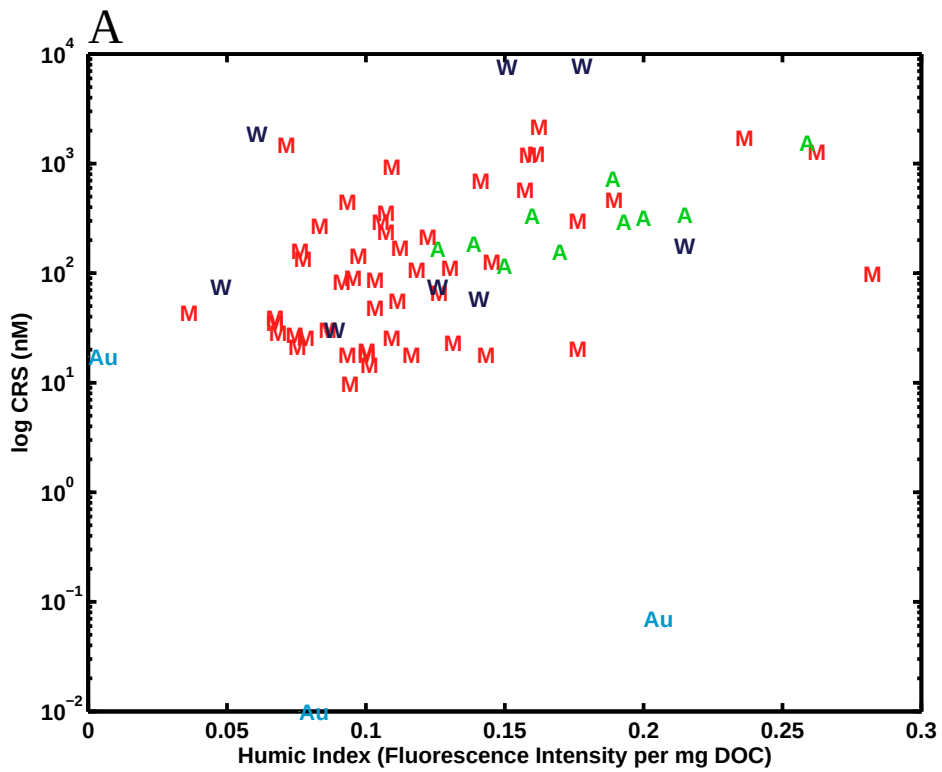
A
log CRS (nM)
Humic Index (Fluorescence Intensity per mg DOC)
B
log CRS (nM)
Fulvic Index (Fluorescence Intensity per mg DOC)

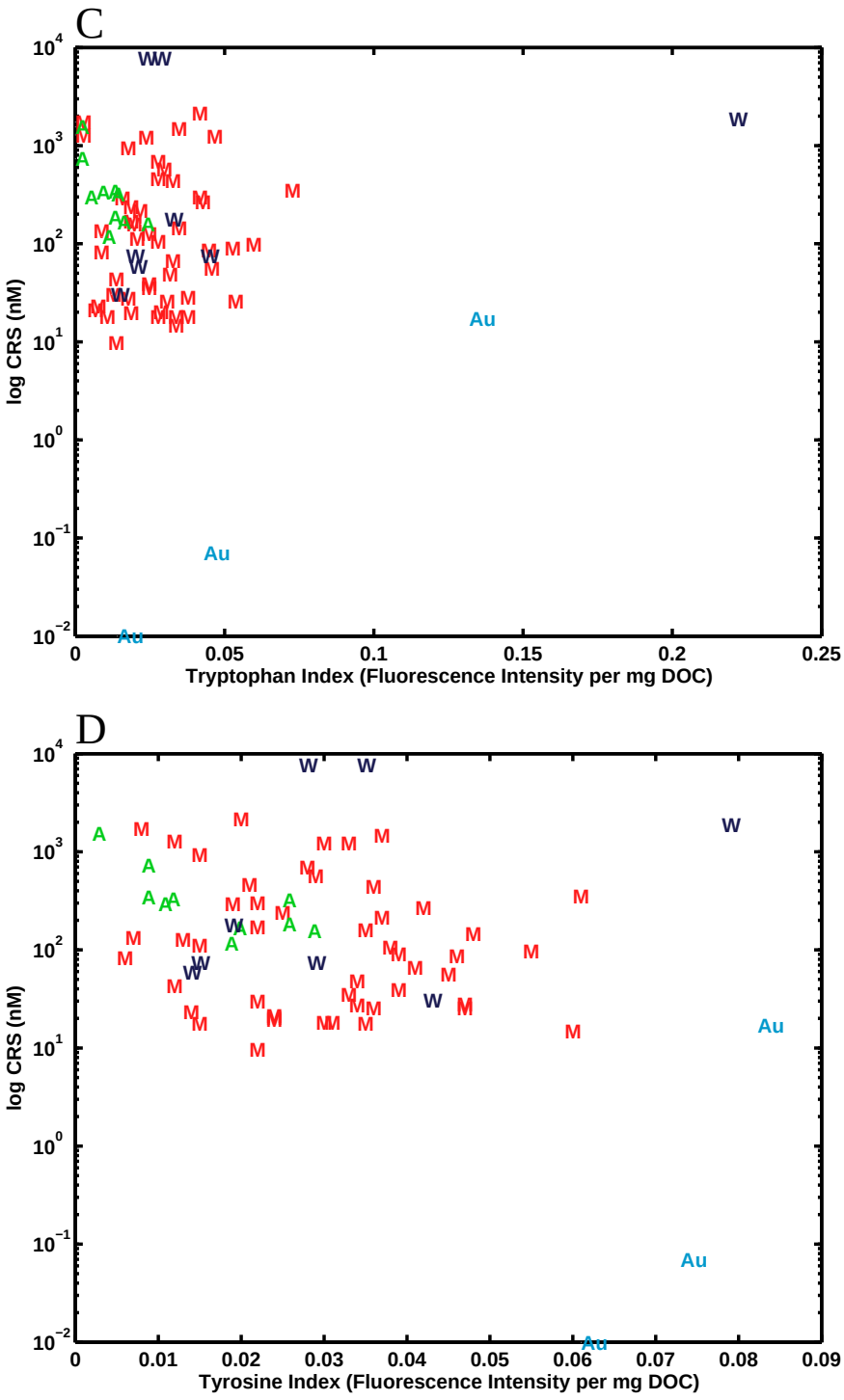

Figure 3.10: Comparisons of fluorescent A) humic index, B) fulvic index, C) tryptophan index, and D) tyrosine index to log CRS concentrations with correlation coefficients of 0.33, p=0.005, 0.43, p=0.002, 0.05, p>0.1, and -0.36, p=0.002 respectively. Correlation calculations were performed on a linear scale, however CRS was presented on a log scale due to the large span of concentrations. A=allochthonous, Au=allochthonous, W=wastewater, M=mixed source.

No significant correlation was identified in any of the fluorescent fractions to CRS from Figure 3.10. However, separation of the points by input source identified a strong correlation of the allochthonous (A) humic index (Figure 3.10A, r=0.83, p=0.003), followed by tyrosine index in Figure 3.10D (r=-0.76, p=0.01), tryptophan index in Figure 3.10C (r=-0.73, p=0.01), with fulvic index having the least correlation of r=-0.37, p>0.1 in Figure 3.10B. The wastewater (W) points did not show any significant correlation to CRS, the strongest correlation being between fulvic index and CRS (r=0.45) with a p-value greater than 0.1. Although the sample size of autochthonous (Au) samples is too small for acceptable identification of correlations between fluorophore indices and CRS (n=3), it was interesting to see the nearly perfect correlation between tryptophan Au and CRS in Figure 3.10C with r=1.0, p=0.01. Further insight into comparisons of tryptophan and CRS in the open ocean is needed to draw conclusions on this correlation.

3.4 Conclusions

Characterization of DOM and CRS were performed on 72 marine and estuarine samples. DOM in each sample was first characterized by quantifying DOC concentrations. Further characterization was performed by fluorescence spectroscopy which identified humic-like, fulvic-like, tryptophan-like, and tyrosine-like fractions. These four fractions were quantified via PARAFAC and compared internally to numerically identify differences in DOM quality with varying salinity and input sources.

CRS measurements were performed on unfiltered aliquots of the 72 ambient water samples. CRS concentrations spanned six orders of magnitude from 0.07 nM to 7703 nM. On comparing CRS to DOC, there was no significant correlation between the two measurements when comparing the sample set as a whole. However, a strong correlation was seen between DOC and CRS for the allochthonous

samples (r^2=0.79).

Evaluations on the linear relationships between the six variables of humic index, fulvic index, tryptophan index, tyrosine index, FI, and CRS using Pearson's correlation matrix identified a statistically significant linear correlation between tryptophan and tyrosine r=0.72, p<0.001 with allochthonous and wastewater contributing the strongest correlation of r=0.82, p=0.003 and 0.87, p=0.005 respectively. FI values calculating predominant allochthonous and autochthonous material based on fluorescence correlated with the qualitative observations identifying allochthonous and autochthonous water samples such that the majority of the allochthonous-labelled samples had low FI ($\sim$1.4) and the majority of autochthonous-labelled samples had high FI ($\sim$1.9), with wastewater-labelled samples in the middle. Although the quality indices did not have any statistically significant linear correlations with CRS, the humic index, contributed from allochthonous samples, displayed a strong linear correlation (r=0.83, p=0.003). The tyrosine and tryptophan indices, contributed from allochthonous samples as well, displayed significant inverse correlations with CRS of r=-0.76, p=0.01 and r=-0.73, p=0.01 respectively. Overall, coastal marine and estuarine waters show significant spacial variation in DOC concentrations, DOM quality, and CRS concentrations. Although many significant linear correlations were found between DOM and CRS quantity measurements, the observations made here open the door to in depth analyses of these correlations and possible causation may be identified.

Chapter 4

Protective Effects of DOM and CRS on Copper Toxicity in Coastal Marine and Estuaries

4.1 Introduction

Metal toxicity in aquatic environments is influenced by the chemical characteristics of the water. These chemical characteristics can vary over time and by location, which may alter the bioavailability of metals. With over 53% of the US population living along the coast (NOAA, 2004), the water chemistry of coastal marine and estuarine environments is impacted by increasing anthropogenic input. It is important to research the nature of these inputs and quantify the variability of water chemistry with respect to metal toxicity. Biotic ligand models (BLMs), such as the HydroQual© BLM, are widely used for predicting deleterious effects of metals in freshwater environments. These models are dependent on water chemistry and organism physiology, which makes up the framework for calculating the chemical equilibrium within a system (DiToro et al., 2001; Santore et al., 2001; Paquin et al., 2002). In the development of a marine-specific BLM, these water chemistry measurements would be used as input parameters for a software-based approach,

similar to existing freshwater BLMs. The focus of this chapter is on identifying the protective effects of dissolved organic matter (DOM) and chromium(II) reducible sulfide (CRS) that were originally characterized and quantified in Chapter 3.

Biotic ligand is the generalized term for sites on aquatic organisms where bioavailable metals, such as copper, can bind (Paquin et al., 2002, and references therein). When the copper accumulation at the biotic ligand reaches a critical concentration, toxic effects occur (Paquin et al., 2002). In the presence of organic or inorganic abiotic ligands, such as DOM and CRS, the concentration of bioavailable copper decreases via complexation. To determine the protective effects of these ligands, acute toxicity tests are performed in which the concentration of total copper that will affect 50% of the species is measured. The endpoint of acute toxicity is commonly lethality, namely LC_{50}, however acute concentrations that disrupt growth, development, or fecundity of 50% of the test organisms (EC_{50}) can be measured as well.

Toxicity criteria concentrations of metals, such as LC_{50} and EC_{50}, were commonly reported as total dissolved metal concentrations, however reports argue the necessity to report toxicity data based on bioavailable metal species, which is key in quantifying the toxic effects at the biotic ligand (Allen and Hansen, 1996; Eriksen et al., 2001). Research done by Pagenkopf et al. (1974) and Allen (1993), among others, have suggested that in freshwater, copper toxicity was dependent on free copper(II) ion concentrations. In marine water, both free copper(II) and copper-hydroxy species may be considered bioavailable (Sunda and Gillespie, 1979; De Schamphelaere and Janssen, 2002). However, when calculating bioavailable copper based on equilibrium modelling, numerous approximations based on theoretical models are applied, resulting in approximated free copper values.

The Canadian Environmental Quality Guidelines (CEQG) for copper is currently based on total copper concentrations that are considered 'safe' copper levels in both fresh and marine water. The Canadian freshwater copper criteria range from 2 to 4 μg Cu·L^{-1} (0.03 - 0.06 μM), depending on water hardness, and the saltwater criteria state a limit of 3 μg Cu·L^{-1} (0.05 μM) (CCME, 2007). The U.S. EPA has established that regulations of bioavailable metals are variable with respect to site-specificity for both fresh and marine waters (U.S. EPA, 2007).

Research on predicting copper toxicity in marine and estuarine water has recently come into focus (Arnold, 2005). Prior to site-specific calculations of copper toxicity in marine and estuarine waters (such as with the BLM for freshwater), a criteria for safe levels of copper was calculated based on available reported toxicity data in marine water (U.S. EPA, 1995a). In terms of copper toxicity in marine and estuarine waters, the most sensitive species should be protected. Arnold (2005) indicated that *Mytilus* is an especially sensitive genus, and therefore is an ideal test species for establishing copper water quality criteria. Current water quality guidelines for copper in coastal marine and estuarine systems are based on toxicity of *Mytilus*, with an acute criterion of 4.3 μg Cu·L^{-1} (0.068 μM), which describes the approximate 'safe' level that protects 95% of the *Mytilus* population from lethality (U.S. EPA, 2007). Further details on calculations of copper criteria in estuarine systems is found in Chapter 1 Section 1.4.

DOM has been found to be protective of metal toxicity (Morel, 1983) and is currently an input parameter in freshwater BLMs, measured as dissolved organic carbon (DOC). DOC is operationally defined as organic matter that passes through a 0.45 μm membrane filter. In coastal marine and estuarine systems, copper toxicity is found to be strongly influenced by DOC, independent of any other water chemistry measurements, within a factor of 2 (Arnold, 2005; Arnold et al., 2006). However, variation in DOM protectiveness has been found in

both freshwater (Schwartz et al., 2004) and marine water spiked with exogenous DOM (Nadella et al., 2009), so there is a possibility that measurements of DOM source material would improve toxicity predictions. Schwartz et al. (2004) reported specific absorption coefficients at 340 nm (SAC_{340}) of different DOM source material in freshwater as a characterization method of DOM that could be applied to distinguish the protective effects of DOM from different sources. High SAC_{340} is indicative of allochthonous carbon originating from terrestrial runoff where low SAC_{340} is indicative of autochthonous carbon, which originates directly from the water column (McKnight et al., 2001). Toxicity studies reported that optically-dark allochthonous carbon significantly decreased bioavailability of copper, lead, and cadmium, relative to autochthonous carbon in freshwater (Schwartz et al., 2004).

Characterization of DOM by fluorescence spectroscopy can differentiate fluorescent molecules (fluorophores) in a heterogeneous system based on different fluorescent properties. A fluorescence excitation-emission matrix (FEEM) is the result of compiling measured fluorescence data from simultaneous scanning of excitation and emission wavelengths. Based on FEEM analysis, allochthonous carbon can be detected in the Ex/Em ranges of 300-350 nm / 400-450 nm and 250 - 390 nm / 460-520 nm, suggesting the presence of terrestrially-derived fulvic and humic material respectively (Smith and Kramer, 1999; McKnight et al., 2001; Wu et al., 2003; Stedmon and Markager, 2005). Autochthonous carbon can be detected by the Ex/Em peaks within of 225 - 275 nm / 350 nm and 225 - 275 nm / 300 nm identifying microbially-derived tryptophan-like and tyrosine-like fractions respectively (Baker, 2001; Stedmon and Markager, 2005). Recently, Winter et al. (2007) identified humic-, fulvic-, tryptophan-, and tyrosine-like fractions in freshwater through fluorescence. In seawater, fluorescence has been a useful technique for DOM characterization as well, through characterization of the open ocean (Mopper and Schultz, 1993; Coble, 1996) and estuaries (Hall and Kenny, 2007). Mopper and Schultz (1993) identified a higher abundance of proteinaceous

material near the surface of marine water as compared to a higher abundance of humic-like material farther down (300 m to 4001 m) in samples collected from the Atlantic and Pacific Oceans, based on the fluorescence Ex/Em wavelengths of approximately 270 nm / 320 nm and 310 nm / 430 nm and respectively.

To quantify in relative terms, the humic-, fulvic-, tryptophan-, and tyrosine-like fractions observed by fluorescence, parallel factor analysis (PARAFAC) is used here. Through spectral deconvolution of a stack of FEEMs, PARAFAC quantifies a minimum number of fluorescent components to describe each FEEM in a set of related samples. Stedmon and Markager (2005) resolved 8 components by PARAFAC that described the fluorescent data of 1,276 samples. In Chapter 3, a simple classification scheme was implemented, resolving 4 operationally-defined fractions of humic-, fulvic-, tryptophan-, and tyrosine-like material. Here, these four components will be analyzed for correlations with copper toxicity and contributions of fluorescence measurements will be addressed in terms of improving metal toxicity predictions for regulatory purposes.

The presence of reduced sulfur in marine environments has been reported at concentrations of $<0.001 - 162$ nM in marine and coastal waters by means of voltammetry, HPLC, GC, and various spectroscopic methods such as UV/Vis (Luther and Tsamakis, 1989; Al-Farawati and van den Berg, 1999; Bianchini and Bowles, 2002, and references therein). Reduced sulfur is known to bind strongly to copper in aquatic systems, primarily via (meta)stable complexation (Rozan et al., 2000). Furthermore, it may bind to copper, as Cu(I) and Cu(II), in the presence of other competing metal ions and in the presence of other ligands such as DOM (Al-Farawati and van den Berg, 1999). Very little is known of reduced sulfur in coastal marine and estuarine systems in terms of its protective effects on copper toxicity. A method known as CRS can accurately measure reduced sulfur with approximately 95% recovery, as HS^-, metal sulfides, pyrite, polysulfides, S^0, thio-

sulfates, and sulfites, in nM (Bowles et al., 2003). In Chapter 3, CRS was measured on 72 unfiltered coastal marine and estuarine samples. Here, CRS will be analyzed for correlations with copper toxicity in 10 of the 72 samples measured in Chapter 3, in relation to protective effects and as a potentially predictive measure of toxicity.

The objectives of this study were to (I) measure acute copper EC_{50} in coastal marine and estuarine waters, (II) identify the relationships between total copper EC_{50} values and concentrations of humic-, fulvic-, tryptophan-, and tyrosine-like fractions, SAC_{340}, and CRS, and (III) evaluate whether organic matter quality and CRS concentrations should be included as input parameters in a marine-specific BLM. The samples used in this study were a subset of the 72 samples analyzed in Chapter 3. The subset was statistically selected to represent the extreme concentrations of each measured parameter for correlation analysis.

4.2 Experimental Section

4.2.1 Reagent Preparation

Synthetic Seawater

Synthetic seawater was prepared by dissolving commercial-grade sea salt (Kent Marine, Atlanta, GA, USA) in MilliQ water (18.2MΩ) and adjusted to 30 ‰ ± 1 ‰ salinity using a PINPOINT® Salinity Monitor (American Marine Inc., Ridgefield, CT). This synthetic sea salt was recommended for use in marine copper toxicity tests by Arnold et al. (2007). All marine standard solutions and dilutions were prepared using this synthetic seawater. The reference toxicity tests were performed using this synthetic seawater.

Copper Nitrate solution

A 10^{-4} M solution of reagent grade $Cu(NO_3)_2$ (>99.99%, Aldrich, USA) was prepared using synthetic seawater as described above. This stock solution was used to prepare diluted copper solutions with the ambient water samples for toxicity testing. When not in use, this $Cu(NO_3)_2$ stock was stored in a covered bottle at 4℃.

4.2.2 Sample Selection

A subset of samples were selected from the 72 listed in Chapter 3 to measure copper toxicity, based on the measurements of DOC, fluorescence, and CRS. A 2^3 factorial design (Box et al., 1978) was implemented to initially divide the sample set into eight categories through simultaneous comparisons of the main effects of three parameters: DOC, tryptophan, and CRS. From these categories, samples were selected that best represented extreme concentrations of these parameters. Nine samples were selected for toxicity analysis, and are listed in Table 4.1.

4.2.3 Toxicity Measurements

Preparation of Samples

Collection and storage of the ambient water samples used here are described in Chapter 2 Section 2.2. 1 L of each sample was adjusted to a salinity of 30 ‰ ± 1 ‰ (as per U.S. EPA (1995b)) using either commercial-grade sea salt, or MilliQ water, measured with a PINPOINT® Salinity Monitor (American Marine Inc., Ridgefield, CT). Following salinity adjustment, the sample was filtered through Purabind 0.45 μm filters (Whatman, Florham Park, NJ). The filtrate was divided into seven aliquots: one was set as a reference sample and six were spiked with Cu(II), using $Cu(NO_3)_2$ stock, to produce concentrations that encompassed the predicted EC_{50} for *Mytilus* sp. This predicted EC_{50} was calculated based on the

equation, $EC_{50} = 11.22DOC^{0.6}$ (Arnold et al., 2006). The aliquots spiked with Cu(II) were left to equilibrate overnight prior to the toxicity assay. Sub-aliquots, separated from the reference filtrate solutions, were used to measure pH, CRS, DOC, fluorescence, and SAC_{340}.

Water Chemistry

Water chemistry measurements, namely pH, DOC, fluorescence, and CRS were made shortly after salinity adjustments and filtration as suggested by Arnold et al. (2006). Background theory and detailed procedures on these water chemistry measurements are described in Chapter 2 Section 2.2 for pH, Section 2.3 for DOC and fluorescence, and Section 2.4 for CRS. pH of the reference filtrate was measured with a Tananger dual pH meter (Scientific Systems Inc., USA) using an Orion double junction reference electrode and Ag/Ag-Cl pH electrode (Thermo Electron Corp., USA). DOC was measured with a Shimadzu TOC-5050A Total Carbon Analyzer using an ASI-5000A Autosampler (Mandel Scientific, Guelph, ON) on a 10 mL sub-aliquot of the reference filtrate. Pretreatment for DOC measurements was acidification with 16 N trace metal-analysis grade HNO_3 followed by sparging with N_2 for 15 minutes.

Fluorescence of the reference filtrate was measured using a Varian Cary Eclipse Fluorescence Spectrophotometer (Varian, Mulgrave, Australia) in a 1 cm quartz cuvette. Fluorescence scans of emission wavelengths from 250 nm to 600 nm in 10 nm increments were measured for every 1 nm excitation wavelength between 200 nm and 450 nm. The excitation and emission monochromator slit widths were both set to 5 nm for all the measurements. The scan speed was at a rate of 400 $nm \cdot min^{-1}$ and the photomultiplier tube was set to high detection (800 V). Rayleigh light scattering was replaced with not-a-number (NaN) to avoid interference in subsequent spectral analyses.

Spectral resolution via parallel factor analysis (PARAFAC) was performed on the fluorescence data simultaneously to identify the spectra and quantification of four components within each water sample. This analysis described over 98% of the fluorescent data. Two of the components were loosely labelled as humic-like and fulvic-like based on the assumption that higher molecular weight humic material fluoresces at higher wavelengths (Wu et al., 2003). The other two components were labelled as tryptophan-like and tyrosine-like based on similar Em/Ex wavelength pairs of pure tryptophan and tyrosine standards. Full details on the identification of these fluorescent components can be found in Section 3.3.2. The PARAFAC algorithms used were from PLS_Toolbox Version 4.1.1 in Matlab^{TM} (Eigenvector Research Inc., WA, USA). The Matlab scripts used to remove the Rayleigh light scattering and analyze the data via PARAFAC can be found in Appendix A. The contribution of each component to total fluorescence, identified by PARAFAC, are linearly proportional to their actual concentration, where the unknown proportionality constant includes the fluorescence quantum efficiency, which is dependent on the molecular identity of that fraction. These values are referred to here as fluorophore 'concentrations' (arbitrary units, Arb.) and are restricted to internal comparisons only.

CRS was measured on a 30 mL sub-aliquot of the reference filtrate based on the method outlined by Bowles et al. (2003). Pretreatment for CRS measurements included sparging with high purity N_2, acidification with 50% v/v HCl, and addition of 1 M Cr(II), all under anoxic conditions. Through purge-and-trap techniques, reduced sulfur was collected in a vial of 0.05 M NaOH. Addition of a methylene diamine reagent and storage in the dark overnight resulted in development of a methylene blue coloured complex. Absorbance of the blue complex was measured colorimetrically. Calculations as described by Beer's Law determined the concentration of sulfide, with an experimentally-determined extinction coefficient $\epsilon = 4.0 \times 10^4 L \cdot mol^{-1} cm^{-1}$.

Absorbance measurements at 340 nm with a 1 cm quartz cuvette were performed on the reference filtrate using a LS-1 tungsten halogen lamp light source, USB2000 fiber optic spectrometer as a detector, and Ocean Optics Spectra Suite Version 1.4.2 (Ocean Optics Inc., Dunedin, FL). References of synthetic seawater were used. SAC_{340} was calculated based on the equation $SAC_{340} = 2303 \times Abs_{340}/DOC$ (Schwartz et al., 2004).

Total dissolved copper was measured on sub-aliquots of the sample filtrates, including the reference aliquots and ones spiked with $Cu(NO_3)_2$ prior to the toxicity assays. Standards of 1, 10, 50, and 100 $\mu g \cdot L^{-1}$ were prepared using synthetic seawater and the $Cu(NO_3)_2$ stock. These standards and the sample aliquots were transferred into 15 mL polypropylene centrifuge tubes (Corning Inc. Corning, NY, USA) and acidified with 16 N trace metal-analysis grade HNO_3. Total copper measurements were performed by inductively-coupled plasma with optical emission spectroscopy (Perkin Elmer Optima 3000DV ICP-OES, Toronto, ON., Canada) with multi-element standard parameters and set in axial mode. Optical emission measurements were taken at the copper spectral line of 324.752 nm.

Toxicity Assay

All toxicity tests on the nine selected samples and synthetic seawater were conducted using embryos collected from adult estuarine bivalve mussels *Mytilus galloprovincialis* that were purchased from Proteus SeaFarms International, Inc. (Ojai, CA, USA). The mussels were not genetically verified and so are referred to here as *Mytilus* sp.

The toxicity tests were performed following the guidelines for the 48-hour static acute toxicity tests starting with *Mytilus* sp. embryos, from A.S.T.M. International (2004). Full details on the methodology of the toxicity assay can be found in Chapter 2 Section 2.6. The tests were conducted in 20 mL glass scintillation vials

with five replicates per concentration and 10 mL of the solution in each vial. 10 adult *Mytilus* sp. mussels were thoroughly scraped and cleaned of byssal threads and epibionts, then transferred into a seawater bath (30.0‰) at 4℃ for about 5 minutes. Followed by lightly dropping the mussels into a seawater bath maintained at 20℃ to induce spawning. Once a mussel began releasing gametes, it were quickly rinsed and transferred into a separate 250 mL beaker filled with seawater in order to collect pure gametes from each mussel. Embryos were examined for quality under a light microscope at 200× magnification. Good quality eggs were identified as dark and round, with little to no visible vacuoles. Sperm were checked for motility under a microscope at 200× magnification. Motile sperm were pooled together for use in the toxicity test. Good quality eggs were suspended in seawater (∼1000 eggs·mL^{-1}). A small aliquot of sperm was injected into the egg suspension and gently stirred to initiate fertilization. The suspension was examined periodically under a microscope to ensure 90-95% fertilization. Once the embryos reached the 4-cell stage, they were resuspended by constant stirring to generate a uniform solution. To initiate the tests, approximately 100 eggs were transferred into each scintillation vial and incubated for 48 hours in a temperature-controlled chamber maintained at 18℃ ± 1℃. After 48 hours, one of the controls was observed for >90% normal D-shaped prodissoconch shell development. Tests that required more than 54 hours for development were discarded. The test acceptability was >90% normal development or >30% survival in the control treatment. 1 - 2 mL of 5% v/v gluteraldehyde was pipetted into each vial to terminate the test. The end point was abnormal shell development as a measure of adverse effects. All 'normal', 'abnormal', and 'dead' embryos were counted under a dissecting microscope at 50× magnification The percentage of larvae that did not survive or develop normally was calculated for each replicate. Strict guidelines were followed to ensure identification of abnormal development was consistent between all toxicity tests.

Toxicity Analysis

The 50% shell development inhibitory concentration (EC_{50}) was estimated with 95% confidence intervals for each sample by Probit Analysis using the Statistical Analysis System software (SAS Institute Inc., Cary, NC, USA). Acute EC_{50} values were reported as total dissolved copper measured in solution. Free copper concentrations at the EC_{50} were calculated for each water sample based on water chemistry measurements of toxicity test solutions including salinity, pH, and DOC. These calculations were done by R. Santore (HydroQual, personal communication).

Data Pooling

Toxicity data obtained in this study was pooled with some of the toxicity data from Arnold (2005) and Arnold et al. (2006), as the sampling sites were some of the same as ones among the 72 analyzed in Chapter 3. To statistically justify pooling the data, a t-test was performed on the intensive values, $EC_{50} \cdot DOC$, of the two data sets to show that with 95% confidence there is no significant difference between the data, other than what can be described as random variation. The full statistical justification can be found in Appendix E.

To assign fluorescence values to the samples obtained from Arnold (2005) and Arnold et al. (2006), the assumption was made that the fluorescence values normalized to DOC (fluorescence (Arb.) per mg DOC, referred to here as 'quality index') remains constant over time. The quality index values were then multiplied by the DOC concentrations reported in Arnold (2005) and Arnold et al. (2006). Furthermore, the new fluorophore concentrations measured here were adjusted to account for instrumentation drift by using a correction factor that was determined by comparing fluorescence measurements obtained in this chapter and in Chapter 3 Section 3.3.2. This factor was applied to all the new fluorescent data. This adjustment allowed for separate analyses of total copper EC_{50} as a function of DOC, fluorescence

humic-, fulvic-, tryptophan-, and tyrosine-like fractions using both data sets.

4.3 Results and Discussion

4.3.1 Sample Selection

A subset of the 72 samples from Chapter 3 were selected for toxicity measurements based on the concentrations of DOC, CRS, and humic-, fulvic-, tryptophan-, and tyrosine-like fluorescent fractions. Samples representing extreme high and low concentrations of each parameter (and combinations within) would provide quantitative insight into their individual protective effects on copper toxicity in estuarine environments. Initial categorization of the 72 sites was based on main effects of DOC, tryptophan, and CRS using a 2^3 partial factorial design. Humic and fulvic material were strongly correlated to each other (Figure 4.1A) and also to DOC, so only one parameter (DOC) was used to represent DOC, humic, and fulvic concentrations. Similarly, tryptophan and tyrosine were strongly correlated (Figure 4.1B) and so were represented as one parameter, Tryptophan.

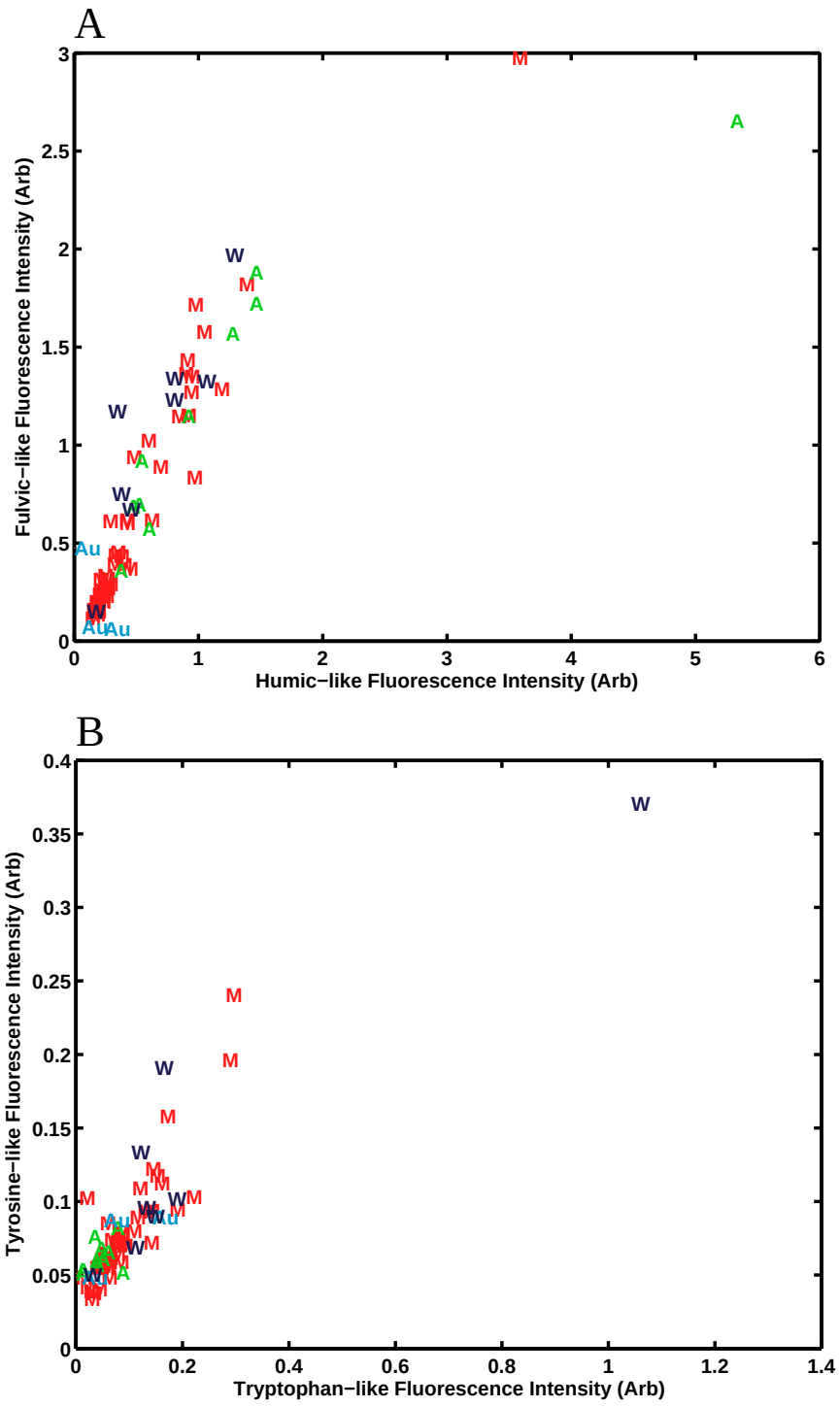

Figure 4.1: Comparison plots between A) fluorescent humic and fulvic material and B) fluorescent tryptophan and tyrosine material. The plotted points are separated by source material in each sample: A=allochthonous, Au=allochthonous, W=wastewater, M=mixed source (see Chapter 3, Table 3.3.1).

A *partial* factorial was implemented due to the nature of the water samples (i.e. not all of the conditions in a full factorial could be satisfied, which include every possible high and low combination of each parameter). From the partial factorial based on the three parameters of DOC, tryptophan, and CRS, a subset of samples were selected as shown in Table 4.1.

Table 4.1: Results from 2^3 partial factorial design with a focus on main effects of the three parameters, DOC, Trp, and CRS. Details on the locations of these sample sites can be found in Table 3.3.1.

	Extreme Signatures (+ = high, − = low)		
Water Sample	DOC	Trp	CRS
Artificial Seawater	Reference		
Arthur Kill	+	+	−
Chesapeake Bay	+	+	+
Potomac River	+	+	−
San Diego Bay	−	−	+
Tomales Bay	+	−	+
Puget Sound	−	−	−
Halifax Harbour	−	−	−
Albemarle Sound	+	+	+
Coal Harbour	+	−	−

High DOC, tryptophan, and CRS represented concentrations of approximately $\geq$3.0 mg C·L^{-1}, $\geq$0.1 (Arb.), and $\geq$100 nM whereas low DOC, tryptophan, and CRS were approximately <3.0 mg C·L^{-1}, <0.1 (Arb.), and <100 nM respectively. Outside of the parameter restriction in this partial factorial design, Arthur Kill and Albemarle Sound were selected because they both had DOC concentrations of 6.9 mg C·L^{-1} but their humic and fulvic fraction were very different (0.30 and 0.75 respectively for Arthur Kill; 0.85 and 1.29 respectively for Albemarle Sound). These selections allowed for separate comparisons of protective effects of humic and fulvic material, which will be discussed in detail in Section 4.3.3. Table 4.2 contains a list of sample sites from Arnold (2005) and Arnold et al. (2006) that were pooled with the data collected in this study. The same sites were sampled in

2007 and fluorescence was measured in Chapter 3, Section 3.3.2.

Table 4.2: List of sample sites, DOC concentrations, and measured EC_{50} obtained from Arnold (2005) and Arnold et al. (2006) that were pooled with the sample set used in this study.

Water Sample	DOC (mg C·L^{-1})	EC_{50} (μg Cu·L^{-1})
Granite Canyon [1]	0.8	6.3
Granite Canyon	1.2	10.9
Narragansett Bay	1.5	16.8
West Galveston Bay	3.3	24.8
Galveston Bay	8.7	71.0
Mugu Lagoon	1.9	17.4
Puget Sound	1.3	13.9
San Francisco Bay	5.7	34.8
San Francisco Bay	5.0	37.2

4.3.2 Sample Characterization in Exposure Media

Salinity adjustments were performed prior to filtering of the samples and are shown in Table 4.3. It was expected that some DOC might be lost during the storage period and/or the filtration, however this was not the case. The DOC concentrations showed no change outside the expected measurement variability (Table 4.3).

[1] Obtained from Granite Canyon Marine Laboratory and used as a reference.

Table 4.3: Measurements of pH, DOC, and salinity of the water samples in preparation for toxicity assays. Measurements are shown from both before and after salinity adjustments and filtration.

	pH		DOC (mg C·L^{-1})		Salinity (‰)	
Water Sample	Before	After	Before	After	Before	After
Artificial Seawater	n/a	8.17	n/a	1.1	n/a	30.6
Arthur Kill	7.40	7.78	6.9	6.9	27.3	29.9
Chesapeake Bay[2]	7.45	8.1	n/a	3.6	11.6	29.9
Potomac River	7.84	8.02	3.2	3.2	10.7	29.9
San Diego Bay	8.03	8.02	2.2	2.3	38.0	29.9
Tomales Bay	7.80	7.80	3.2	3.4	35.0	30.2
Puget Sound	7.62	7.52	1.6	1.9	29.5	29.5
Halifax Harbour	7.65	7.65	1.6	1.6	31.3	29.9
Albemarle Sound	7.58	7.58	6.9	6.9	3.6	30.2
Coal Harbour	7.80	7.44	3.0	3.3	19.7	30.2

As shown in Table 4.3, there was no apparent trend between the direction of salinity adjustment and change in DOC, suggesting that the variability may have been within the instrumental error. Additionally, the fluorescence results after salinity adjustments and filtration did not vary from the original measurements as seen in Table 4.4.

[2]Additional samples were taken from this site specifically for the toxicity assay and so DOC was not measured prior to salinity adjustments. Since the DOC measurement initially taken from this site was on a sample collected months earlier, comparisons to the salinity-adjusted sample used here would not be accurate.

Table 4.4: Fluorescent measurements of humic-(HA), fulvic-(FA), tryptophan-(Trp), and tyrosine-like (Tyr) fractions in solutions prepared for toxicity assays. Measurements are shown from both before and then after storage, salinity adjustments, and filtration.

	HA		FA		Trp		Tyr	
Water Sample	Before	After	Before	After	Before	After	Before	After
Artificial Seawater	n/a	0.00	n/a	0.48	n/a	0.14	n/a	0.09
Arthur Kill	0.30	0.33	0.75	0.78	0.12	0.11	0.10	0.09
Chesapeake Bay	n/a	0.34	n/a	0.83	n/a	0.17	n/a	0.18
Potomac River	0.39	0.30	0.67	1.10	0.13	0.10	0.09	0.09
San Diego Bay	0.15	0.14	0.31	0.20	0.07	0.06	0.08	0.07
Tomales Bay	0.47	0.43	0.70	0.83	0.03	0.01	0.06	0.08
Puget Sound	0.12	0.12	0.20	0.20	0.02	0.02	0.06	0.06
Halifax Harbour	0.12	0.04	0.19	0.74	0.04	0.08	0.06	0.06
Albemarle Sound	0.88	0.77	1.27	1.80	0.13	0.01	0.09	0.08
Coal Harbour	0.38	0.56	0.37	0.57	0.01	0.17	0.12	0.22

CRS measurements on the filtered samples returned concentrations that were much lower than what was originally measured on the unfiltered samples in Chapter 3. Section 3.3.3 (Table 4.5). This difference in concentration suggests that CRS may be predominantly present as particulate matter. To a lesser extent, CRS may have oxidized during storage, however precautions were made to ensure that exposure to the atmosphere was minimal by storing the samples under argon.

Table 4.5: Measurements of CRS concentrations (± standard deviation) in preparation of toxicity assays. Measurements are shown from both before and after storage, salinity adjustments, and filtration.

	CRS (nM) ± std dev.	
Water Sample	Before	After
Artificial Seawater	n/a	17.22±1.18
Arthur Kill	75.00±9.43	27.78±3.93
Chesapeake Bay	1880±575	44.17±0.00
Potomac River	75.00±11.78	25.56±0.78
San Diego Bay	1484±36.1	24.44±7.07
Tomales Bay	116.9±20.0	39.17±7.07
Puget Sound	27.50±1.18	30.00±2.36
Halifax Harbour	25.83±3.14	4.17±0.39
Albemarle Sound	112.2±7.1	28.33±5.50
Coal Harbour	23.33±0.78	23.33±1.18

4.3.3 Toxicity Assay

Comparisons of total copper EC_{50} and DOC concentrations resulted in a strong linear correlation (r^2=0.84) to the predictive equation line suggested by Arnold et al. (2006) from the pooled data sets of samples from Tables 4.1 and 4.2. The plot of total copper EC_{50} with increasing DOC concentration is shown in Figure 4.2.

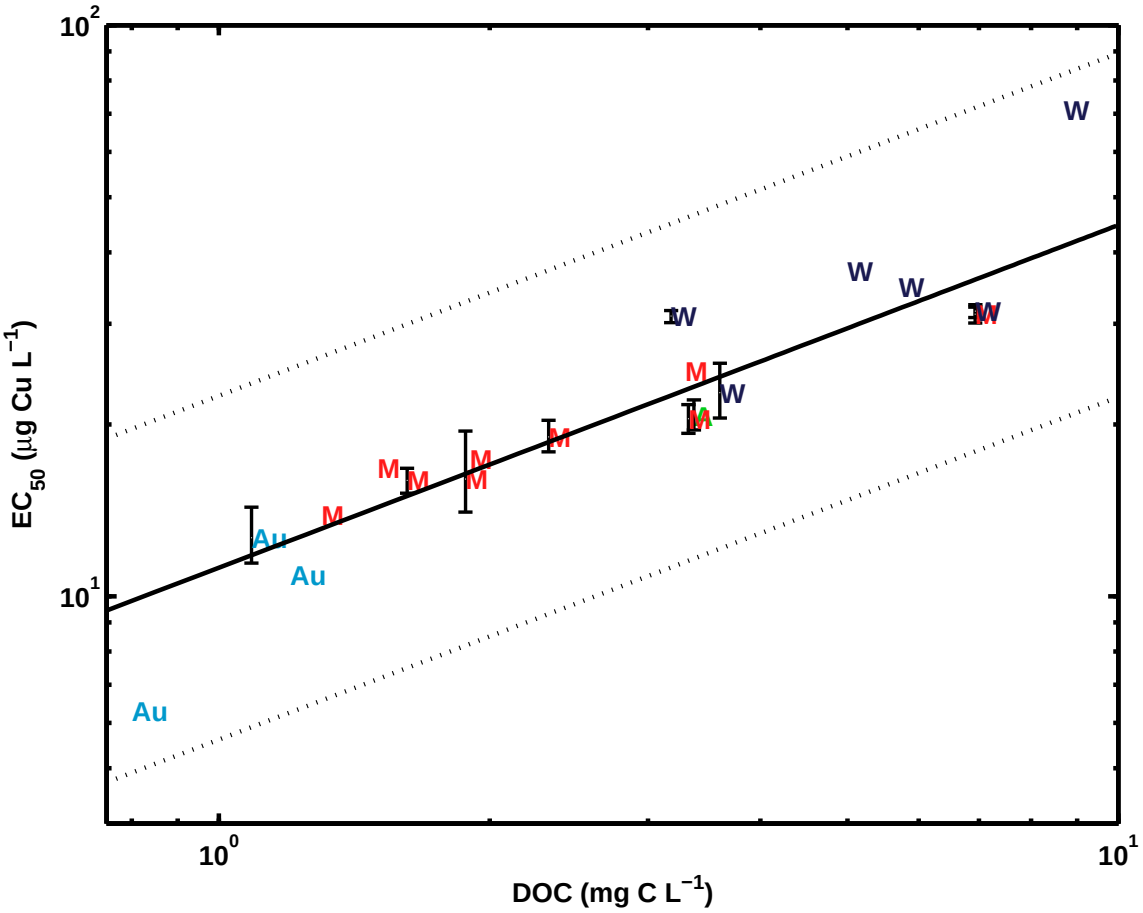

Figure 4.2: Plot of pooled results from this study, with 95% confidence intervals, and that of samples listed in Table 4.2 illustrating total dissolved copper EC_{50} as a function of DOC. The solid line is the predictive equation line suggested by Arnold et al. (2006), where the r^2 for the data points from the line is 0.84 (p=0.0001, n=19). The dotted lines represent a factor of 2 of the predictive equation. The plotted points are separated by source material in each sample: allochthonous (A), autochthonous (Au), mixed source (M), and wastewater (W).

Although the datasets were pooled, the data obtained in this study can be differentiated from those published by Arnold (2005) and Arnold et al. (2006) with the presence of error bars on the points measured here, in Figure 4.2. This same figure (4.2) can be found in Appendix E Figure E.1 with the points from both datasets distinguished with different markers. The solid line represents the predictive equation, $EC_{50} = 11.22DOC^{0.6}$ from Arnold et al. (2006) while the dotted lines represent a factor of 2 about the line. Linear regression through sum of squares was calculated to express the fit of the plotted points to the predictive

equation, resulting in a r^2 of 0.84 (p=0.0001, n=19). This strong linear correlation between DOC and EC_{50} suggests DOC as a major component in coastal marine and estuaries with protective effects on copper toxicity via complexation (Nadella et al., 2009) possibly independent of any other water chemistry parameters, within acceptable predictability limits of a factor of 2 (Arnold et al., 2006).

SAC_{340} has been suggested as a measure of DOM quality and showed good correlation with metal toxicity to rainbow trout in freshwater (Schwartz et al., 2004). In the coastal marine and estuarine samples measured here, only a weak correlation was seen between SAC_{340} and total copper EC_{50} (r^2=0.28, Figure 4.3).

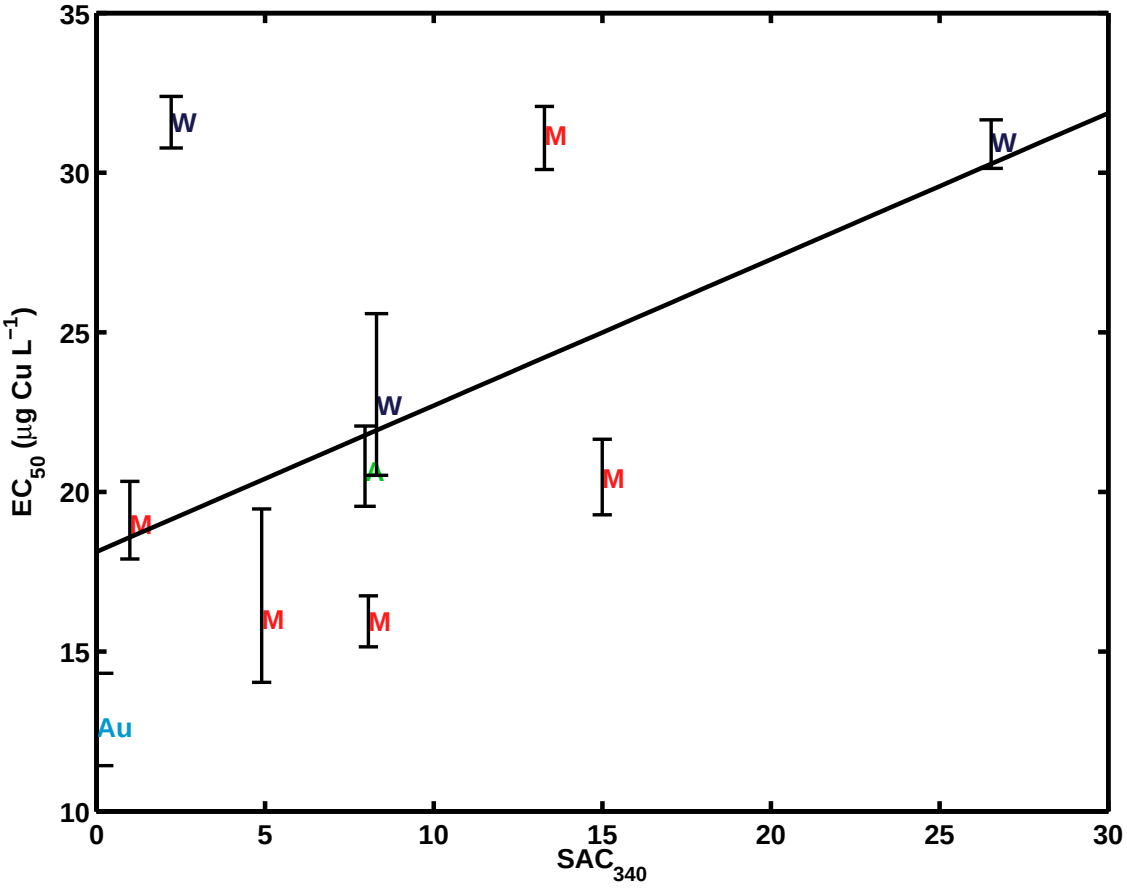

Figure 4.3: Plot of total copper EC_{50} with increasing SAC_{340} on the samples measured in this study. The solid line is the line of best fit ($y = 0.46x + 18.13$, $r^2 = 0.28$, n=10).

SAC_{340} is a measure of colour, which is an intensive property and might not correlate with EC_{50} (Figure 4.3), which depends on the amount of DOC (extensive property). Comparisons of absorbance at 340 nm to total copper EC_{50} displayed a relatively stronger linear correlation ($r^2 = 0.52$, n=10). A positive correlation was expected here because absorbance is proportional to DOC.

Based on the idea that allochthonous material should be more protective (Schwartz et al., 2004) due to its prevalent phenolic and carboxylic groups, and that allochthonous is primarily made up of humic and fulvic material, it was thought that DOC will show higher protectiveness when relative amounts of fluorescent humic- and fulvic-like material are high. Lorenzo et al. (2006) identified fulvic material as the prominent fraction of marine DOM in terms of protective effects on copper toxicity. Humic-like and fulvic-like fluorescent fractions compared to total copper EC_{50} identified a strong linear correlation ($r^2 = 0.84$, $p<0.0001$ and 0.88, $p<0.0001$ respectively) as shown in Figure 4.4 A and B. However, there was no significant relationship between the lower molecular weight autochthonous fractions and EC_{50} (Figure 4.4 C and D) with r^2 values of 0.40, $p=0.004$ and 0.21, $p=0.05$ respectively.

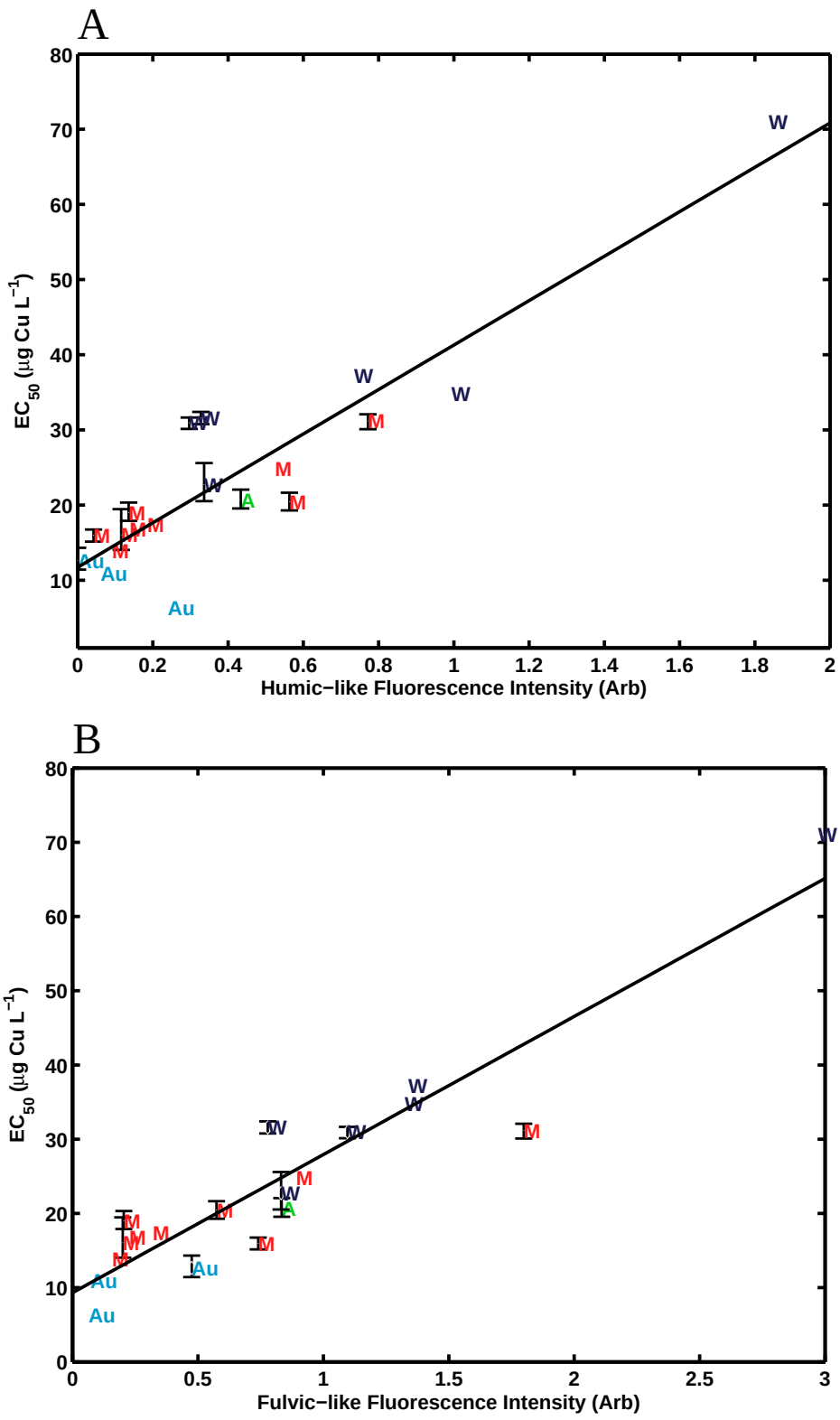
A
B
EC50 (µg Cu L−1)
Humic−like Fluorescence Intensity (Arb)
Fulvic−like Fluorescence Intensity (Arb)

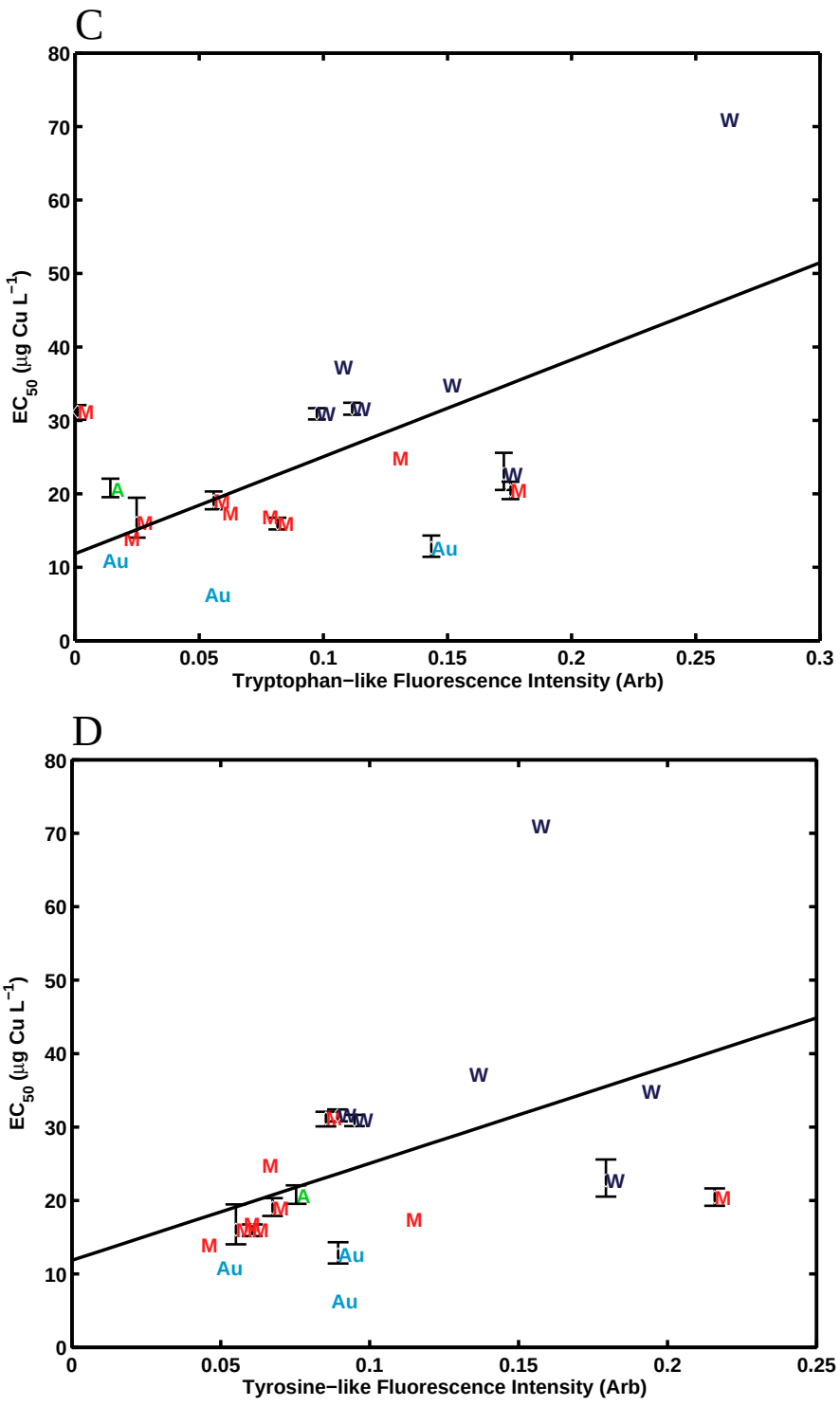

Figure 4.4: Plot of total dissolved copper EC_{50} as a function of fluorescent A) humic-, B) fulvic-, C) tryptophan-, and D) tyrosine-like concentrations on the samples measured in this study and from samples listed in Table 4.2. The plotted points are separated by source material in each sample: A=allochthonous, Au=autochthonous, W=wastewater, M=mixed source.

The fluorescent humic-like and fulvic-like fractions (Figure 4.4 A and B) appear to be good predictive measures of total copper toxicity in the tested coastal marine and estuarine samples. These findings agree with research by Nadella et al. (2009) where concentrations of fulvic material, estimated by fluorescence, displayed strong protective effects in marine water, suggesting a difference in protectiveness with DOM source. The fluorescent autochthonous fractions, Figure 4.4 C and D, did not influence copper toxicity to a significant extent. The association constants (log K) for 1:1 complex formation with tryptophan and tyrosine to Cu^{2+} are 8.29 and 7.81 $\pm$ 0.1 respectively (Martell and Smith, 1974). However, it is possible that the measured tryptophan and tyrosine fractions are embedded within dissolved proteins as peptide bonds and therefore not able to bind metal. Aluwihare et al. (1997) suggested that *in situ* organic matter may be predominantly found as clusters of proteins, carbohydrates, and lipids. If this is the case, then it is likely that the amine groups are not readily available to chelate free copper, despite the strong affinity of amines to Cu(II).

To further illustrate the difference in DOM quality in the water samples and the use of DOC as a good predictive measure, the quality index and SAC_{340} values were contrasted with the DOC-EC_{50} relationship from Figure 4.2. Comparisons in this manner would result in one of three observations: 1) quality index increases with DOC, suggesting that the fluorophore concentrations in these samples may be influenced by DOC concentrations and cannot be considered 'different' in DOM quality, 2) quality index is constant and independent of DOC concentrations, suggesting that the fluorophore concentrations may be linearly proportional to DOC concentrations and cannot be considered different in DOM quality, or 3) no significant correlation between quality index and DOC, suggesting that the samples collected can be considered different in DOM quality. Figure 4.5 contains five plots of the DOC-EC_{50} relationship (from Figure 4.2) on a linear scale, with quality index or SAC_{340} for each point indicated.

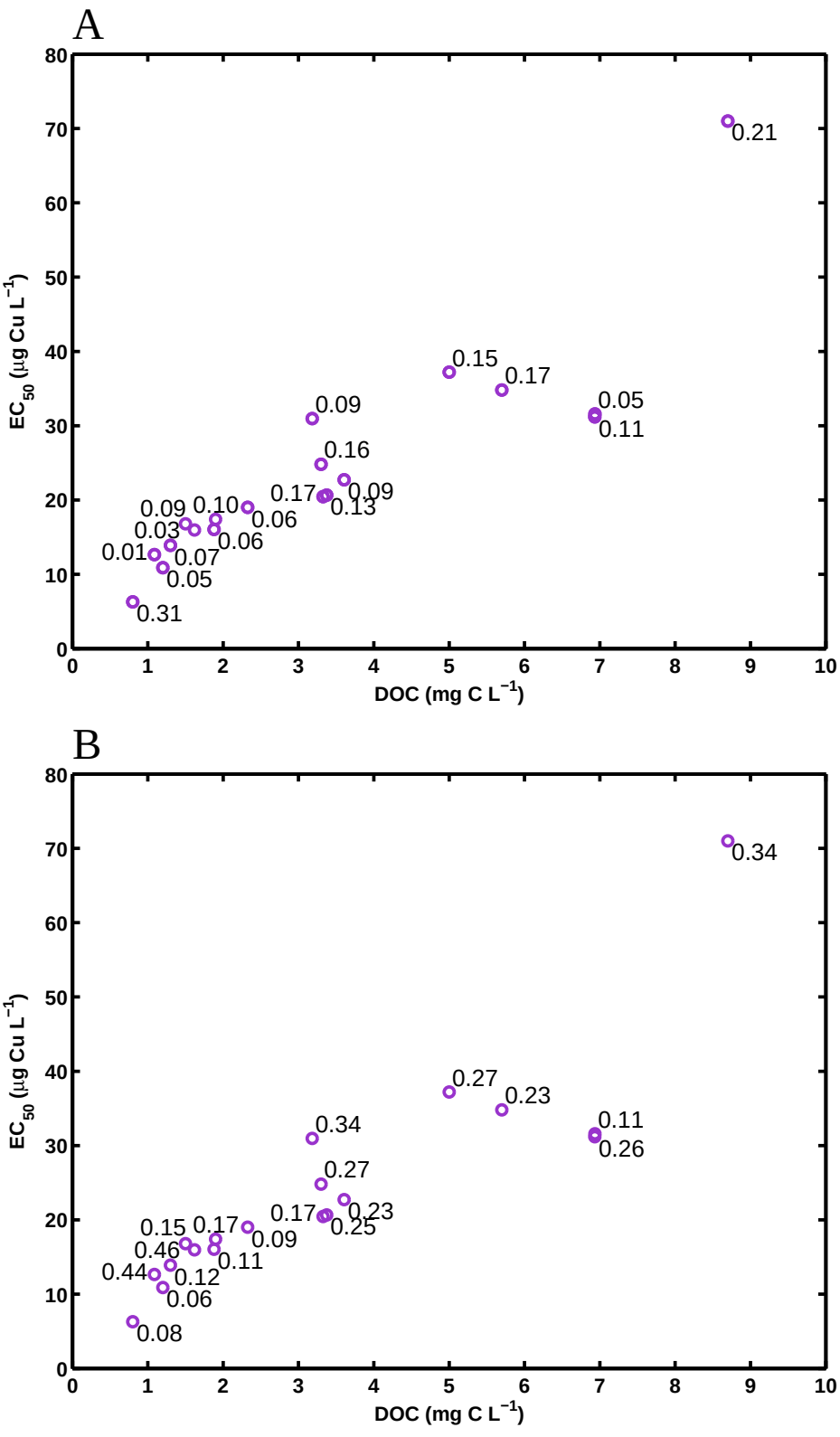
A
B
EC50 (µg Cu L−1)
DOC (mg C L−1)
0
10
20
30
40
50
60
70
80
0
1
2
3
4
5
6
7
8
9
10
0.21
0.15
0.17
0.09
0.05
0.11
0.16
0.17
0.09
0.13
0.09
0.10
0.06
0.03
0.06
0.01
0.07
0.05
0.31
0.34
0.27
0.23
0.34
0.11
0.26
0.27
0.17
0.23
0.25
0.15
0.17
0.09
0.46
0.11
0.44
0.12
0.06
0.08

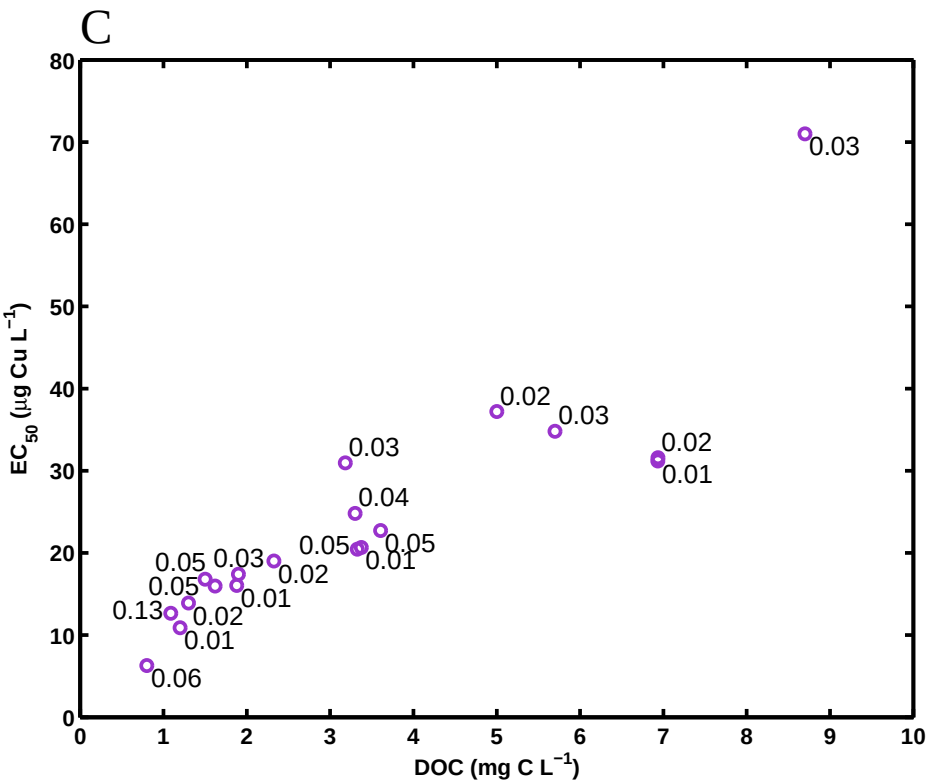
C
EC50 (µg Cu L−1)
DOC (mg C L−1)
0.03
0.02
0.03
0.02
0.01
0.03
0.04
0.05
0.05
0.01
0.05
0.03
0.02
0.05
0.01
0.13
0.02
0.01
0.06

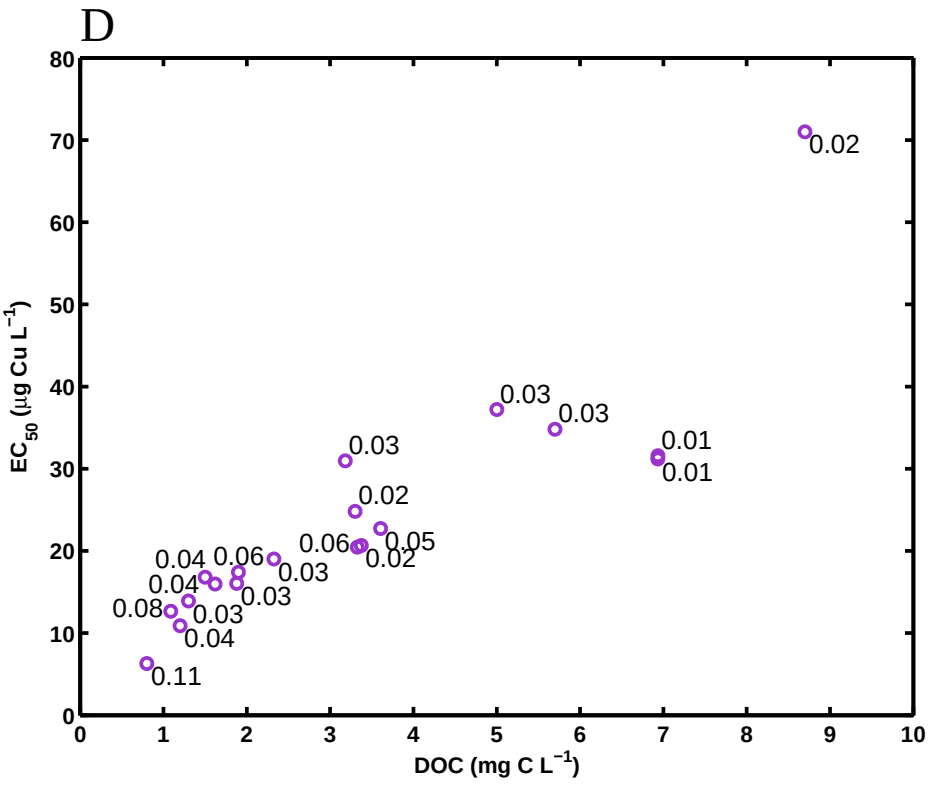
D
EC50 (µg Cu L−1)
DOC (mg C L−1)
0.02
0.03
0.03
0.01
0.01
0.03
0.02
0.06
0.05
0.02
0.04
0.06
0.03
0.04
0.03
0.08
0.03
0.04
0.11

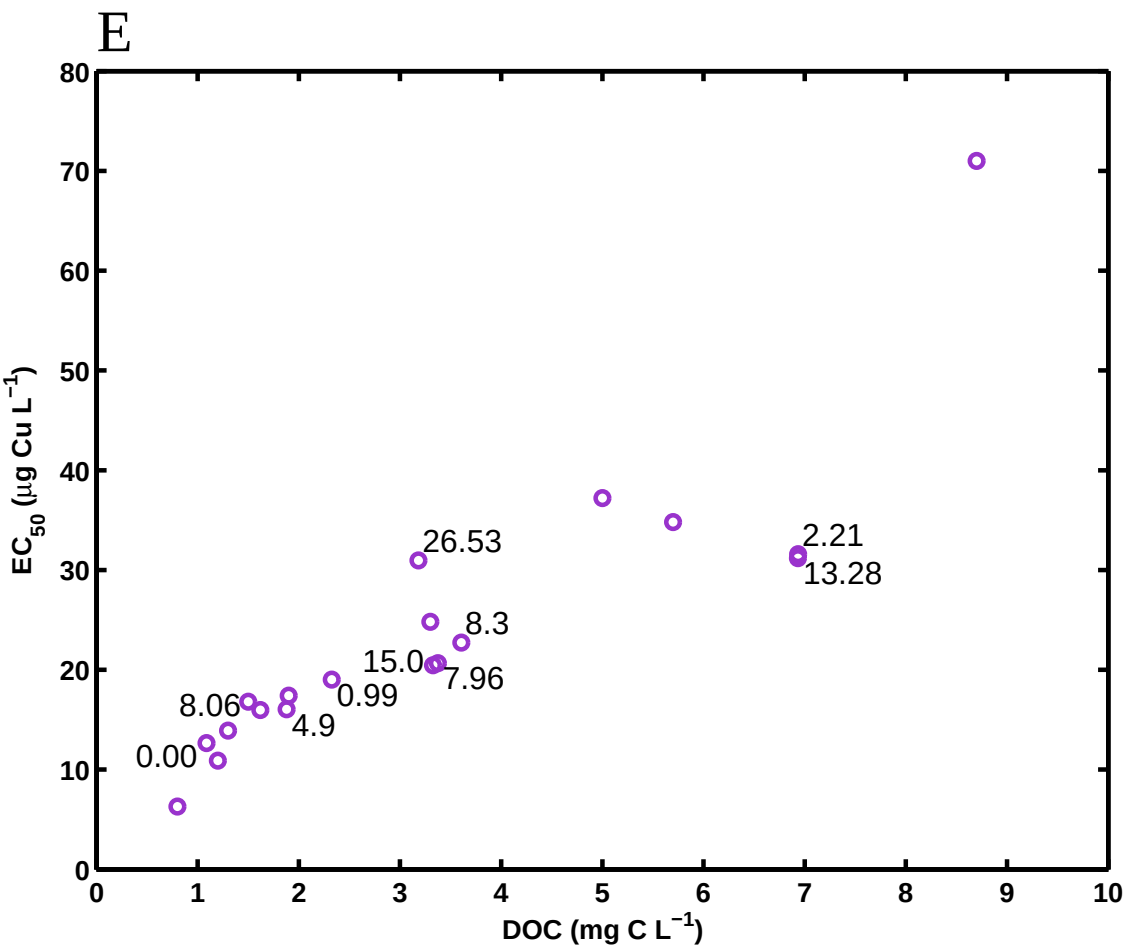

Figure 4.5: Plots of DOC vs. EC_{50}, as seen in Figure 4.2. The numeric values of each point in the plots refer to fluorescent A) humic index, B) fulvic index, C) tryptophan index , and D) tyrosine index. In plot E), the values are SAC_{340}.

Figure 4.5 illustrates that the estuarine samples used in the toxicity assays indeed varied in organic matter quality. More specifically, all the quality index values are randomly distributed when plotted against EC_{50}, expressed with low r^2 values (0.10, 0.12, 0.07, 0.29, and 0.28 for humic, fulvic, tryptophan, tyrosine, and SAC_{340} respectively) indicating no significant correlation between quality index and EC_{50}. For example, in Figure 4.5 B, the fulvic index measured at 0.44 and 0.46 near the low end of the EC_{50} scale, with values at 0.11, 0.26, and 0.34 at higher EC_{50}. In addition, in Figure 4.5 E there exists two points on the right hand side that overlap. These points are of Arthur Kill and Albemarle Sound

with SAC_{340} values of 2.21 and 13.28 respectively. They have approximately the same DOC concentration (see Section 4.3.1, Table 4.1) and EC_{50}, yet the SAC_{340} measurement is different by an order of magnitude. This variability in optical quality suggests that DOC is a very good predictive measure regardless of DOM quality.

The idea that CRS binds strongly to copper suggests that CRS may be protective towards copper toxicity and potentially predictive as well. To address this notion in coastal marine and estuarine waters, CRS and total copper EC_{50} were compared on a 1:1 plot using the same units (μM) for both measurements to identify whether CRS is a good predictive measure of copper toxicity. This plot is illustrated in Figure 4.6.

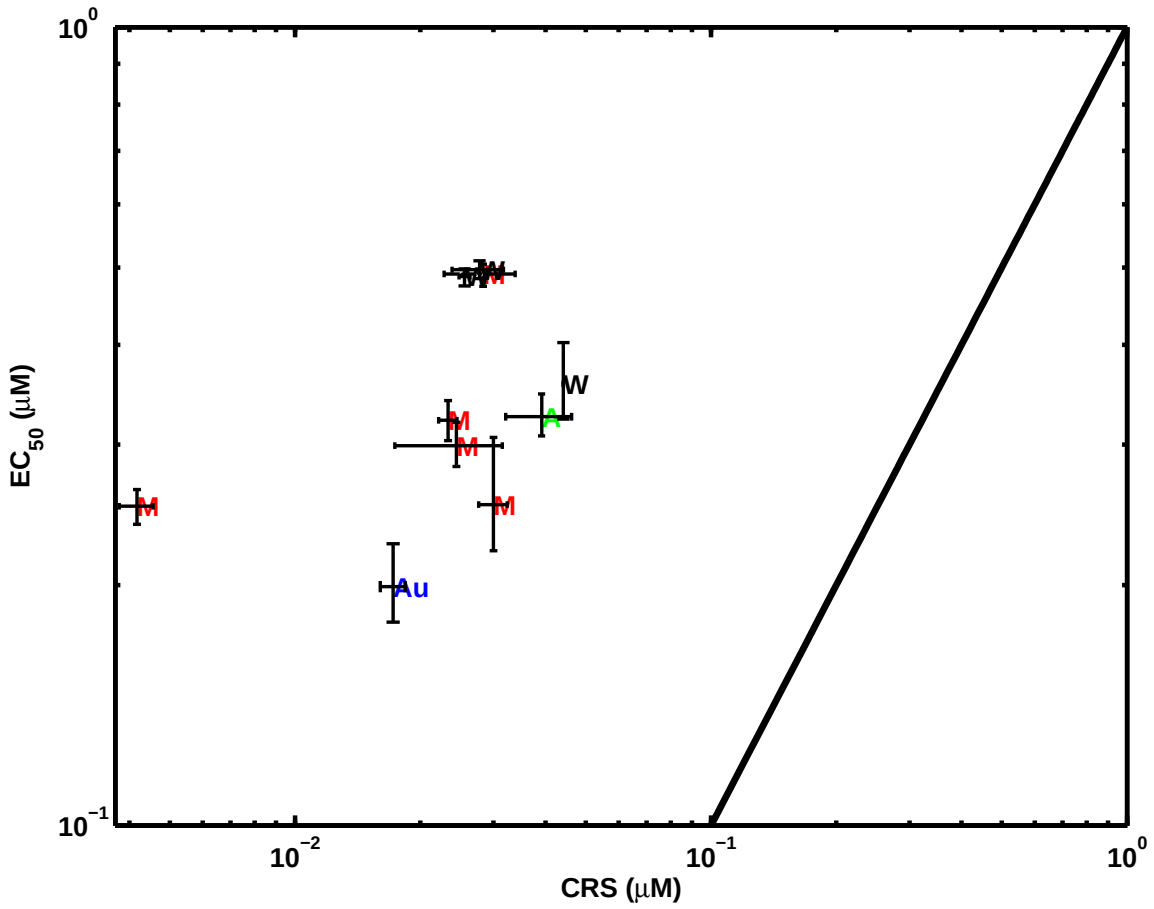

Figure 4.6: Plot of log EC_{50} as a function of dissolved CRS, both represented in μM. All the points appear above the 1:1 line (right side of the plot), which suggests CRS is a strong ligand for copper.

The 1:1 line in Figure 4.6 represents the toxicologically-relevant range of CRS concentrations. All the points are above the 1:1 line, suggesting that CRS contributes strong binding sites as described by Town and Filella (2000), and all CRS available binding sites for copper appear to be completely saturated before the EC_{50} concentration regime. The findings here imply that although CRS seems to be very protective of copper toxicity in coastal marine and estuaries, it may not be a useful predictive measure. However, the toxicity assays were performed on filtered samples, so in some cases a significant amount of CRS was filtered out or possibly lost during storage (Table 4.5). Unfiltered CRS may have a stronger influence on copper toxicity predictions.

Free, or bioavailable, copper concentrations were calculated at each EC_{50} based on total copper and DOC. A comparison between total copper EC_{50} and free copper EC_{50} is shown in Figure 4.7.

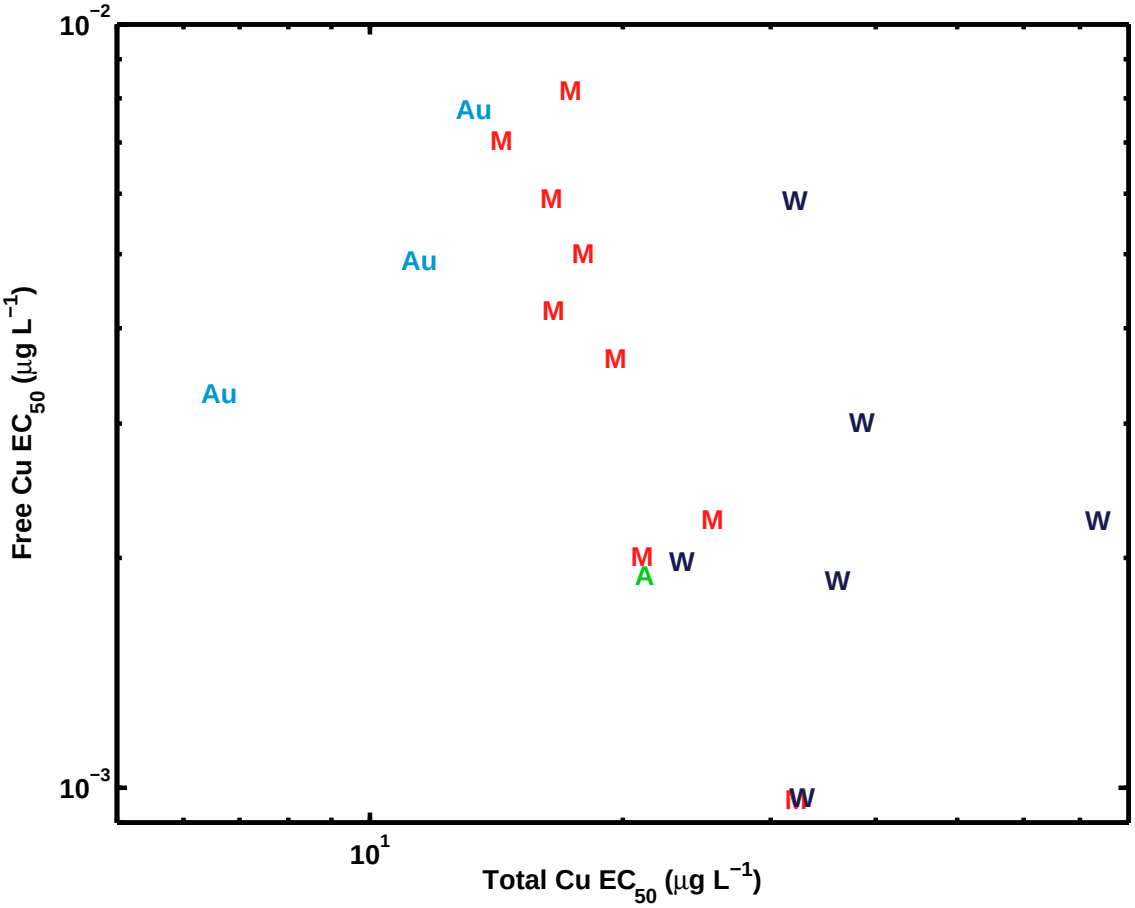

Figure 4.7: Comparison between total copper EC_{50} and free copper EC_{50}. The correlation between these two variables is not considered significant (r^2=0.26, p=0.03). The plotted points are separated by source material in each sample: allochthonous (A), autochthonous (Au), mixed source (M), and wastewater (W).

The free copper concentrations at the EC_{50} plotted in Figure 4.7, was approximately 3.85×10^{-3} μg·L^{-1} $\pm$ 2.21×10^{-3} μg·L^{-1}. A slight downwards slope was observed in in Figure 4.7, but is not considered a statistically significant trend (r^2=0.26, p=0.03). A decreasing trend suggests that higher total copper

results in less free copper required to elicit a toxic effect on the organisms, which is counterintuitive to the free-ion activity model (FIAM), where the free metal ion dictates the uptake and toxic effect in the test species (Morel, 1983; Campbell, 1995). However, other water chemistry measurements, such as calcium ion concentrations, are not expected to be the same in each water sample, and were not included in the calculations here. Although most ion concentrations are relatively constant in marine water, estuaries with relatively low salinity may express freshwater chemistry characteristics, such as variable Ca^{2+} concentrations, which would have an effect on the bioavailability of copper, as seen in freshwater (Erickson et al., 1996). Furthermore, Cu-humic complexes at higher concentrations may have toxic effects at the biotic ligand, which has been reported by Lorenzo et al. (2005) and Nadella et al. (2009), which are not included in the free copper EC_{50} calculations in Figure 4.7. It should also be noted that the model used to here calculate the free copper concentrations at the EC_{50} is not fitted to the measurements from this study, and is still in the early stages of development.

4.4 Conclusions

The findings in this study suggest that DOC is a very good predictive measure of copper toxicity in most coastal marine and estuarine environments and support the validity of the predictive equation found in Arnold et al. (2006) independent of source. The influence of DOM quality on copper toxicity appears to be marginal in comparison to the acceptable predictability for calculating toxicity. In addition, strong binding sites contributed from amine groups within autochthonous material appear to be unavailable for copper binding in the samples analyzed here as they are likely embedded within protein structures (i.e. peptide bonds).

Dissolved CRS concentrations contribute strong binding sites to copper,

but do not appear to be present in sufficient number of binding sites to reach toxicologically-relevant concentrations in coastal marine and estuarine environments. An important factor here is that toxicity assay protocol requires sample filtration prior to testing, which was assumed to greatly reduce the CRS concentrations in each sample. Comparisons should be made to CRS and EC_{50} values performed on unfiltered samples to identify its protective effects and possibly competition for binding sites to TOC.

Calculations of free copper at the EC_{50} did not result in a constant concentration as would be expected if DOC were the only factor contributing to protection. An average free copper concentration at the EC_{50} was calculated at 3.85×10^{-3} $\mu g{\cdot}L^{-1}$ $\pm$ 2.21×10^{-3} $\mu g{\cdot}L^{-1}$. The variability in this concentration suggested that other water chemistry measurements may have an influence on bioavailable copper in coastal marine and estuarine environments, especially in low salinity where water chemistry measurements may show similarities in ion variability as in freshwater. Furthermore, there is the possibility of toxicity from Cu-humic complexes, which are currently not included in the free copper calculations. The correlation between total copper EC_{50} and DOC is very strong and is sufficient to approximate copper toxicity in coastal marine and estuarine environments independent of other water chemistry measurements. Additional characteristic measures (i.e. fulvic-like, humic-like) do not dramatically improve predictive power.

Chapter 5

Summary and Conclusions

The goal of this thesis was to test the following hypotheses:

1. Fluorescence measurements in combination with PARAFAC would identify a reasonable set of operationally-defined DOM fractions that best describe DOM quality and their relative concentrations in each coastal marine and estuarine water sample.
2. Fluorescence measurements of DOM quality would contribute an improved approximation of copper EC_{50} from DOC, particularly the allochthonous fluorescent components, such as humic and fulvic material.
3. Optically-defined allochthonous carbon, through SAC_{340} measurements, would be more protective than autochthonous with respect to copper toxicity.
4. Reduced sulfur, through CRS measurements, would be protective of copper toxicity and a necessary input parameter for a marine-specific BLM.

Coastal marine and estuarine ambient water samples were collected from 71 sites along the east, west, and south coasts of North America. Including artificial seawater, a total of 72 samples were used in this study. Through communication with Ray Arnold and Scott Smith as well as aerial imagery (http://www.maps.google.ca), each sample was labelled based on primary DOM input including allochthonous, autochthonous, wastewater, or a mixture of

the three. DOM in each sample was first characterized by quantifying DOC concentrations. From hypothesis 1), fluorescence measurements in combination with PARAFAC provided good qualitative and quantitative measures of four operationally-defined fractions: humic, fulvic, tryptophan, and tyrosine. These four fluorescent fractions were successfully quantified via PARAFAC analysis, describing approximately 98% of the fluorescent data. Furthermore, calculations of FI (McKnight et al., 2001) and comparisons to fluorescent fractions confirmed the observations and primary source labels.

CRS measurements were performed on unfiltered aliquots of the 72 ambient water samples as well. CRS concentrations spanned six orders of magnitude from 0.07 nM to 7703 nM. On comparing CRS to DOC, there was no significant correlation between the two measurements. A correlation has been found between DOC and CRS in freshwater (Kramer et al., 2007). For regulatory purposes, a correlation between these two parameters would have been ideal so that CRS concentrations in coastal marine and estuarine waters could be estimated based on DOC measurements, however this was not the case. Further analysis identified a strong linear correlation between DOC and CRS from allochthonous-source samples only (r^2=0.79), similar to what was identified by Kramer et al. (2007) where terrestrially-derived DOM was likely the predominant contributor of DOC.

The quality index of each fluorophore, FI, and CRS were compared internally via Pearson correlation matrix to numerically identify linear correlations in DOM quality with varying input sources. Strong correlations were found between tryptophan and tyrosine index (r=0.72), followed by humic index and fulvic index (r=0.47). No strong correlations were found between quality index values and CRS, however humic, tryptophan, and tyrosine index values from allochthonous-source samples presented significant correlations. Humic index showed a significant positive correlation (r=0.83), while tryptophan index and tyrosine index showed

significant negative correlations of -0.76 and -0.73 respectively.

The toxicity findings in this study suggest that DOC is a very good predictive measure of copper toxicity in most estuarine environments and support the validity of the predictive equation found in Arnold et al. (2006). The toxicity data obtained here fell very close to their predicted values ($r^2 = 0.84$). From hypothesis 2) and 3) the influence of DOM quality on copper toxicity in the coastal marine and estuarine water samples appeared to be marginal in comparison to the acceptable predictability for calculating toxicity. However, humic and fulvic fractions were better correlated to EC_{50} on a linear scale than tryptophan and tyrosine fractions (r^2s of 0.84, 0.88, 0.40, and 0.21 respectively). This strong correlation between fulvic material eludes to the fact that copper may be predominantly bound to available phenolic and carboxylic groups. Furthermore, the amino acids (tryptophan and tyrosine) may be bound within proteins, resulting in embedded amine groups unavailable for copper binding. In regards to SAC_{340} measurements, there was no direct improvement to copper toxicity predictions ($r^2 = 0.52$). In fact, samples with the same DOC and SAC_{340} measurements different on an order of magnitude, resulted in the same total copper EC_{50}.

From hypothesis 4), the results from this study identified dissolved CRS as contributors of strong binding sites to copper, but do not seem to reach toxicologically-relevant concentrations in estuaries and so may not be significant predictive measures of copper toxicity. These findings give insight into the protectiveness of dissolved CRS on copper toxicity since only filtered samples were used. However further studies on unfiltered samples may identify particulate CRS as as relevant input for toxicity predictions.

Free copper at the EC_{50} was calculated based on DOC and total copper for each water sample. The high variability in free copper concentrations suggested

that other water chemistry measurements may have an influence on bioavailable copper in coastal marine and estuarine environments, especially in low salinity where water chemistry measurements may show similarities in ion variability as in freshwater. Furthermore, there is the possibility of toxicity from Cu-humic complexes, which are currently not included in the free copper calculations.

DOC appeared to be a good predictive measure of copper toxicity in most situations regardless of the source of DOM or other water chemistry measurements. For regulatory purposes, this measurement would be easy and reliable. Fluorescence spectroscopy may improve overall toxicity predictions, however these improvements may only be marginal. An important factor here is that toxicity assay protocol requires sample filtration prior to testing, which greatly reduced the CRS concentrations in each sample. Comparisons should be made to CRS and EC_{50} values performed on unfiltered samples to identify its protective effects and possibly competition for binding sites to total organic carbon.

APPENDICES

Appendix A

Matlab Scripts

A.1 Producing Contour Plots of FEEMs

A.1.1 summary_prelim_data.m

```
%%%%%%%%%%%%%%%%%%%%%%%%%%%%%%%%%%%%%%%%%%%%%%%%%%%%%%%%%%%%%%%%%%%%%%%%
% This script is designed to process the fluorescence data %
% and produce a contour plot                                %
%%%%%%%%%%%%%%%%%%%%%%%%%%%%%%%%%%%%%%%%%%%%%%%%%%%%%%%%%%%%%%%%%%%%%%%%

clear global; figure(1); close; figure(2); close;
colordef white

%Processes ASW_071508_ctrl.xls file to convert it into a FEEM
name='ASW_071508_ctrl';

%Calls preprocess_fluor_data_xls_file.m script
preprocess_fluor_data_xls_file(name);

%Produces FEEM
simplereport(name,[50 100 150 200 250 300 350 400 450...
 500 550 600 650 700 750 800 850 900 950 1000]);
```

A.1.2 preprocess_fluor_data_xls.m

```
%%%%%%%%%%%%%%%%%%%%%%%%%%%%%%%%%%%%%%%%%%%%%%%%%%%%%%%%%%%%%%%%%%%%%%%%
% This script is designed to remove Rayleigh light scattering %
%%%%%%%%%%%%%%%%%%%%%%%%%%%%%%%%%%%%%%%%%%%%%%%%%%%%%%%%%%%%%%%%%%%%%%%%
```

```
function II = preprocess_fluor_data_xls_file(name)

% start by loading the data from the xls file
txt=['data=xlsread(''',name,''');']; eval(txt);
[n,m]=size(data); em=data(2:n,1); ex=data(1,2:m); F=data(2:n,2:m)';

%% ----------- remove first artifact peak -----------------%
contour(em,ex,F,50,'k'); title('select lower limit')
[x,y]=ginput(10)
[Plow]=polyfit(x,y,3); ycalc=polyval(Plow,x);
plot(x,y,'ko',x,ycalc,'k'); pause

contour(em,ex,F,50,'k'); title('select upper limit')
[x,y]=ginput(10)
[Phigh]=polyfit(x,y,3); ycalc=polyval(Phigh,x);
plot(x,y,'ko',x,ycalc,'k'); pause

for i=1:size(ex,2)
    if ex(i)>=ex(1)
for j=1:size(em,1)
        lowerlimit=polyval(Plow,em(j));
        upperlimit=polyval(Phigh,em(j));
        if ex(i)>lowerlimit
if ex(i)<upperlimit
F(i,j)=NaN;
end
    end
    end
end
end

% ---- remove second artifact peak -----------------%
contour(em,ex,F,50,'k'); title('select lower limit')
[x,y]=ginput(10)
[Plow]=polyfit(x,y,3); ycalc=polyval(Plow,x);
plot(x,y,'ko',x,ycalc,'k'); pause

contour(em,ex,F,50,'k'); title('select upper limit')
[x,y]=ginput(10)
[Phigh]=polyfit(x,y,3); ycalc=polyval(Phigh,x);
plot(x,y,'ko',x,ycalc,'k'); pause

for i=1:size(ex,2)
    if ex(i)>=ex(1)
```

```
for j=1:size(em,1)
        lowerlimit=polyval(Plow,em(j));
        upperlimit=polyval(Phigh,em(j));
        if ex(i)>lowerlimit
if ex(i)<upperlimit
F(i,j)=NaN;
end
    end
    end
end
end

txt=['save ',name,'.mat']; eval(txt)
II=1;

end
```

A.1.3 simplereport.m

```
%%%%%%%%%%%%%%%%%%%%%%%%%%%%%%%%%%%%%%%%%%%%%%%%%%%%%%%%%%%%%%%%%%%%%%%%
% This script is designed to display the FEEM as a contour plot %
% with intensity contours, specified in summary_prelim_data.m   %
%%%%%%%%%%%%%%%%%%%%%%%%%%%%%%%%%%%%%%%%%%%%%%%%%%%%%%%%%%%%%%%%%%%%%%%%

function II=simplereport(name,vector)

txt=['load ',name,'.mat']; eval(txt);

figure(1); clf
[C,h]=contour(em,ex,F,vector,'k');
xlabel('em (nm)'); ylabel('ex (nm)');
set(h,'ShowText','on','TextStep',get(h,'LevelStep')*2)
txt=['print ',name,'.eps -depsc2']; eval(txt);
txt=['print ',name,'.png -dpng']; eval(txt);
txt=['print ',name,'.jpg -djpeg']; eval(txt);

figure(1)
```

A.2 Parallel Factor Analysis

A.2.1 PARAFAC_process_Sarah.m

```
%%%%%%%%%%%%%%%%%%%%%%%%%%%%%%%%%%%%%%%%%%%%%%%%%%%%%%%%%%%%%%%%%%%%%%%%%%%%
% This script is designed to calculate all the FEEMs simultaneously to     %
% identify the spectra of a defined number of components and their         %
% relative abundance, or 'concentration' in each sample, based on the FEEM %
%%%%%%%%%%%%%%%%%%%%%%%%%%%%%%%%%%%%%%%%%%%%%%%%%%%%%%%%%%%%%%%%%%%%%%%%%%%%

clear; clear global

%'ones(# mat files, type size(F) in command window to get other 2 numbers)'
Fnew=ones(120,26,351); Fnew=Fnew*NaN;

name='Tyr_5e-7M';txt=['load',name,'.mat'];eval(txt); Fnew(1,:,:)=F;
name='Trp_25e-8M';txt=['load',name,'.mat'];eval(txt); Fnew(2,:,:)=F;
name='SFBay1_071107';txt=['load',name,'.mat'];eval(txt); Fnew(3,:,:)=F;
name='SFBay2_071107';txt=['load',name,'.mat'];eval(txt); Fnew(4,:,:)=F;
name='GCML1_071107';txt=['load',name,'.mat'];eval(txt);  Fnew(5,:,:)=F;
name='GCML2_071107';txt=['load',name,'.mat'];eval(txt);  Fnew(6,:,:)=F;
name='Tyr_5e-7M';txt=['load',name,'.mat'];eval(txt); Fnew(7,:,:)=F;
name='Trp_25e-8M';txt=['load',name,'.mat'];eval(txt); Fnew(8,:,:)=F;
name='RA1_071307';txt=['load',name,'.mat'];eval(txt); Fnew(9,:,:)=F;
name='RA2_071807';txt=['load',name,'.mat'];eval(txt); Fnew(10,:,:)=F;
name='RA3_071807';txt=['load',name,'.mat'];eval(txt); Fnew(11,:,:)=F;
name='RA4_072807';txt=['load',name,'.mat'];eval(txt); Fnew(12,:,:)=F;
name='RA5_072807';txt=['load',name,'.mat'];eval(txt); Fnew(13,:,:)=F;
name='Tyr_5e-7M';txt=['load',name,'.mat'];eval(txt); Fnew(14,:,:)=F;
name='Trp_25e-8M';txt=['load',name,'.mat'];eval(txt); Fnew(15,:,:)=F;
name='RA6_072807';txt=['load',name,'.mat'];eval(txt);  Fnew(16,:,:)=F;
name='RA7_072807';txt=['load',name,'.mat'];eval(txt);  Fnew(17,:,:)=F;
name='RA8_081607';txt=['load',name,'.mat'];eval(txt);  Fnew(18,:,:)=F;
name='RA9_081607';txt=['load',name,'.mat'];eval(txt);  Fnew(19,:,:)=F;
name='RA10_081607';txt=['load',name,'.mat'];eval(txt); Fnew(20,:,:)=F;
name='Tyr_5e-7M';txt=['load',name,'.mat'];eval(txt); Fnew(21,:,:)=F;
name='Trp_25e-8M';txt=['load',name,'.mat'];eval(txt); Fnew(22,:,:)=F;
name='RA11_081607';txt=['load',name,'.mat'];eval(txt); Fnew(23,:,:)=F;
name='RA13_091007';txt=['load',name,'.mat'];eval(txt); Fnew(24,:,:)=F;
name='RA14_091007';txt=['load',name,'.mat'];eval(txt); Fnew(25,:,:)=F;
name='Tyr_5e-7M';txt=['load',name,'.mat'];eval(txt); Fnew(26,:,:)=F;
name='Trp_25e-8M';txt=['load',name,'.mat'];eval(txt); Fnew(27,:,:)=F;
name='RA15_091007';txt=['load',name,'.mat'];eval(txt); Fnew(28,:,:)=F;
name='RA16_091007';txt=['load',name,'.mat'];eval(txt); Fnew(29,:,:)=F;
```

```
name='RA17_091007';txt=['load',name,'.mat'];eval(txt); Fnew(30,:,:)=F;
name='RA18_091907';txt=['load',name,'.mat'];eval(txt); Fnew(31,:,:)=F;
name='RA19_091907';txt=['load',name,'.mat'];eval(txt); Fnew(32,:,:)=F;
name='Tyr_5e-7M';txt=['load ',name,'.mat'];eval(txt); Fnew(33,:,:)=F;
name='Trp_25e-8M';txt=['load ',name,'.mat'];eval(txt); Fnew(34,:,:)=F;
name='RA20_091907';txt=['load',name,'.mat'];eval(txt); Fnew(35,:,:)=F;
name='RA21_091907';txt=['load',name,'.mat'];eval(txt); Fnew(36,:,:)=F;
name='RA22_091907';txt=['load',name,'.mat'];eval(txt); Fnew(37,:,:)=F;
name='RA23_091907';txt=['load',name,'.mat'];eval(txt); Fnew(38,:,:)=F;
name='RA24_092407';txt=['load',name,'.mat'];eval(txt); Fnew(39,:,:)=F;
name='RA25_092407';txt=['load',name,'.mat'];eval(txt); Fnew(40,:,:)=F;
name='Tyr_5e-7M';txt=['load',name,'.mat'];eval(txt); Fnew(41,:,:)=F;
name='Trp_25e-8M';txt=['load',name,'.mat'];eval(txt); Fnew(42,:,:)=F;
name='RA26_092407';txt=['load',name,'.mat'];eval(txt); Fnew(43,:,:)=F;
name='RA27_092407';txt=['load',name,'.mat'];eval(txt); Fnew(44,:,:)=F;
name='RA28_092407';txt=['load',name,'.mat'];eval(txt); Fnew(45,:,:)=F;
name='RA29_092507';txt=['load',name,'.mat'];eval(txt); Fnew(46,:,:)=F;
name='Tyr_5e-7M';txt=['load',name,'.mat'];eval(txt); Fnew(47,:,:)=F;
name='Trp_25e-8M';txt=['load',name,'.mat'];eval(txt); Fnew(48,:,:)=F;
name='RA30_092507';txt=['load',name,'.mat'];eval(txt); Fnew(49,:,:)=F;
name='RA31_092507';txt=['load',name,'.mat'];eval(txt); Fnew(50,:,:)=F;
name='RA32_092507';txt=['load',name,'.mat'];eval(txt); Fnew(51,:,:)=F;
name='RA33_092507';txt=['load',name,'.mat'];eval(txt); Fnew(52,:,:)=F;
name='RA34_101107';txt=['load',name,'.mat'];eval(txt); Fnew(53,:,:)=F;
name='Tyr_5e-7M';txt=['load',name,'.mat'];eval(txt); Fnew(54,:,:)=F;
name='Trp_25e-8M';txt=['load',name,'.mat'];eval(txt); Fnew(55,:,:)=F;
name='RA35_101107';txt=['load',name,'.mat'];eval(txt); Fnew(56,:,:)=F;
name='RA36_101107';txt=['load',name,'.mat'];eval(txt); Fnew(57,:,:)=F;
name='RA37_101107';txt=['load',name,'.mat'];eval(txt); Fnew(58,:,:)=F;
name='RA38_101107';txt=['load',name,'.mat'];eval(txt); Fnew(59,:,:)=F;
name='RA39_101107';txt=['load',name,'.mat'];eval(txt); Fnew(60,:,:)=F;
name='Tyr_5e-7M';txt=['load',name,'.mat'];eval(txt);  Fnew(61,:,:)=F;
name='Trp_25e-8M';txt=['load',name,'.mat'];eval(txt); Fnew(62,:,:)=F;
name='RA40_101607';txt=['load',name,'.mat'];eval(txt); Fnew(63,:,:)=F;
name='RA41_101607';txt=['load',name,'.mat'];eval(txt); Fnew(64,:,:)=F;
name='RA42_101707';txt=['load',name,'.mat'];eval(txt); Fnew(65,:,:)=F;
name='RA43_101707';txt=['load',name,'.mat'];eval(txt); Fnew(66,:,:)=F;
name='RA44_101707';txt=['load',name,'.mat'];eval(txt); Fnew(67,:,:)=F;
name='Tyr_5e-7M';txt=['load',name,'.mat'];eval(txt); Fnew(68,:,:)=F;
name='Trp_25e-8M';txt=['load',name,'.mat'];eval(txt); Fnew(69,:,:)=F;
name='RA45_101807';txt=['load',name,'.mat'];eval(txt); Fnew(70,:,:)=F;
name='RA46_101807';txt=['load',name,'.mat'];eval(txt); Fnew(71,:,:)=F;
name='RA47_101807';txt=['load',name,'.mat'];eval(txt); Fnew(72,:,:)=F;
name='RA48_101807';txt=['load',name,'.mat'];eval(txt); Fnew(73,:,:)=F;
name='RA49_102207';txt=['load',name,'.mat'];eval(txt); Fnew(74,:,:)=F;
```

```
name='Tyr_5e-7M';txt=['load',name,'.mat'];eval(txt);  Fnew(75,:,:)=F;
name='Trp_25e-8M';txt=['load',name,'.mat'];eval(txt); Fnew(76,:,:)=F;
name='RA50_102307';txt=['load',name,'.mat'];eval(txt); Fnew(77,:,:)=F;
name='RA51_010808_dil';txt=['load',name,'.mat'];eval(txt);
      Fnew(78,:,:)=F*2;
name='RA52_102307';txt=['load',name,'.mat'];eval(txt); Fnew(79,:,:)=F;
name='RA53_102307_dil';txt=['load',name,'.mat'];eval(txt);
      Fnew(80,:,:)=F*2;
name='RA54_102307';txt=['load',name,'.mat'];eval(txt); Fnew(81,:,:)=F;
name='Tyr_5e-7M';txt=['load',name,'.mat'];eval(txt); Fnew(82,:,:)=F;
name='Trp_25e-8M';txt=['load',name,'.mat'];eval(txt); Fnew(83,:,:)=F;
name='RA55_102407';txt=['load',name,'.mat'];eval(txt); Fnew(84,:,:)=F;
name='RA56_102407';txt=['load',name,'.mat'];eval(txt); Fnew(85,:,:)=F;
name='RA57_102407';txt=['load',name,'.mat'];eval(txt); Fnew(86,:,:)=F;
name='RA58_121207';txt=['load',name,'.mat'];eval(txt); Fnew(87,:,:)=F;
name='RA59_121307';txt=['load',name,'.mat'];eval(txt); Fnew(88,:,:)=F;
name='RA60_121307';txt=['load',name,'.mat'];eval(txt); Fnew(89,:,:)=F;
name='Tyr_5e-7M';txt=['load',name,'.mat'];eval(txt);  Fnew(90,:,:)=F;
name='Trp_25e-8M';txt=['load',name,'.mat'];eval(txt); Fnew(91,:,:)=F;
name='RA61_121307';txt=['load',name,'.mat'];eval(txt); Fnew(92,:,:)=F;
name='RA62_121307';txt=['load',name,'.mat'];eval(txt); Fnew(93,:,:)=F;
name='SS1_090707';txt=['load',name,'.mat'];eval(txt);  Fnew(94,:,:)=F;
name='SS2_090707';txt=['load',name,'.mat'];eval(txt);  Fnew(95,:,:)=F;
name='Tyr_5e-7M';txt=['load',name,'.mat'];eval(txt); Fnew(96,:,:)=F;
name='Trp_25e-8M';txt=['load',name,'.mat'];eval(txt); Fnew(97,:,:)=F;
name='SS3_090707';txt=['load',name,'.mat'];eval(txt); Fnew(98,:,:)=F;
name='SS4_090707';txt=['load',name,'.mat'];eval(txt); Fnew(99,:,:)=F;
name='SS5_090707';txt=['load',name,'.mat'];eval(txt); Fnew(100,:,:)=F;
name='SS6_090707';txt=['load',name,'.mat'];eval(txt); Fnew(101,:,:)=F;
name='Tyr_5e-7M';txt=['load',name,'.mat'];eval(txt); Fnew(102,:,:)=F;
name='Trp_25e-8M';txt=['load',name,'.mat'];eval(txt); Fnew(103,:,:)=F;
name='RA1_071608_ctrl';txt=['load',name,'.mat'];eval(txt); Fnew(104,:,:)=F;
name='RA4_062608_ctrl';txt=['load',name,'.mat'];eval(txt); Fnew(105,:,:)=F;
name='RA5_071608_ctrl';txt=['load',name,'.mat'];eval(txt); Fnew(106,:,:)=F;
name='RA19_070208_ctrl';txt=['load',name,'.mat'];eval(txt);Fnew(107,:,:)=F;
name='Tyr_5e-7M';txt=['load',name,'.mat'];eval(txt); Fnew(108,:,:)=F;
name='Trp_25e-8M';txt=['load',name,'.mat'];eval(txt); Fnew(109,:,:)=F;
name='RA25_070808_ctrl';txt=['load',name,'.mat'];eval(txt); Fnew(110,:,:)=F;
name='RA33_070208_ctrl';txt=['load',name,'.mat'];eval(txt); Fnew(111,:,:)=F;
name='RA60_070808_ctrl_dil';txt=['load',name,'.mat'];eval(txt);
      Fnew(112,:,:)=F*2;
name='ASW_071508_ctrl';txt=['load',name,'.mat'];eval(txt);  Fnew(113,:,:)=F;
name='Tyr_5e-7M';txt=['load',name,'.mat'];eval(txt); Fnew(114,:,:)=F;
name='Trp_25e-8M';txt=['load',name,'.mat'];eval(txt); Fnew(115,:,:)=F;
name='RA34_072308_ctrl';txt=['load',name,'.mat'];eval(txt); Fnew(116,:,:)=F;
```

```
name='RA54_072308_ctrl';txt=['load',name,'.mat'];eval(txt); Fnew(117,:,:)=F;
name='Tyr_5e-7M';txt=['load',name,'.mat'];eval(txt); Fnew(118,:,:)=F;
name='Trp_25e-8M';txt=['load',name,'.mat'];eval(txt);Fnew(119,:,:)=F;
name='Tyr_5e-7M_Trp_25e-8M_041208';txt=['load',name,'.mat'];eval(txt);
      Fnew(120,:,:)=F;

f=dataset(Fnew);

f.author='Sarah DePalma';
f.axisscale{1}=[1:1:120]; %last number = number of mat files
f.axisscale{2}=ex;
f.axisscale{3}=em;
f.axisscalename{1}='Sample number';
f.axisscalename{2}='Emission wavelength';
f.axisscalename{3}='Excitation wavelength';
f.title{1}='Sample mode';
f.title{2}='Emission mode';
f.title{3}='Excitation mode';

numberofcomponents=4;
options=parafac('options');
options.stopcrit(4)=103600*5;

for i=1:3 %three dimensions
    istr=num2str(i);
    txt=['options.constraints{',istr,'}.nonnegativity=1;'];
    eval(txt);
end

model=parafac(f,numberofcomponents,options)

for i=1:numberofcomponents
    istr=num2str(i);
    txt=['emspec',istr,'=(model.loads{2}(:,',istr,'));'];eval(txt)
    txt=['exspec',istr,'=(model.loads{3}(:,',istr,'));'];eval(txt)
    txt=['conc',istr,'=(model.loads{1}(:,',istr,'));'];eval(txt)
    txt=['surf',istr,'=emspec',istr,'*exspec',istr,''';'];eval(txt)
end

if numberofcomponents==4; save four; end
```

A.2.2 PARAFAC_summary_of_4_components.m

```
clear; clear global
```

```
load four.mat;

figure(1);
subplot(221);contour(em,ex,surf1,3,'k');
xlabel('emission'); ylabel('excitation'); title('component 1')
subplot(222);contour(em,ex,surf2,3,'k');
xlabel('emission'); ylabel('excitation'); title('component 2')
subplot(223);contour(em,ex,surf3,3,'k');
xlabel('emission'); ylabel('excitation'); title('component 3')
subplot(224);contour(em,ex,surf4,3,'k');
xlabel('emission'); ylabel('excitation'); title('component 4')
name=['parafac_4_components'];
figure(1)

txt=['print ',name,'.eps -depsc2']; eval(txt);
txt=['! ps2pdf -dEPSCrop ',name,'.eps']; eval(txt);

figure(2);
subplot(221); plot(conc1,'ko');
xlabel('site'); ylabel('conc'); title('component 1')
subplot(222); plot(conc2,'ko');
xlabel('site'); ylabel('conc'); title('component 2')
subplot(223); plot(conc3,'ko');
xlabel('site'); ylabel('conc'); title('component 3')
subplot(224); plot(conc4,'ko');
xlabel('site'); ylabel('conc'); title('component 4')
name=['plots_4_components'];
figure(2)

txt=['print ',name,'.eps -depsc2']; eval(txt);
txt=['! ps2pdf -dEPSCrop ',name,'.eps']; eval(txt);
```

Appendix B

Water Chemistry Measurements of 72 Coastal Marine and Estuarine Samples

Table B.1: Water chemistry measurements of all seventy-two estuarine water samples. Measurements of pH, salinity, DOC, CRS, and fluorescence were made. FI represents fluorescence index, calculated using Equation 2.6.

				DOC			Fluorescence Intensity			
	ID	pH	‰	(mg C·L^{-1})	CRS (nM)	HA (Arb)	FA (Arb)	Trp (Arb)	Tyr (Arb)	FI
1	SFBay-1	7.74	26.7	5.700	7736.11 ± 648.18	0.9935	1.3252	0.1481	0.1914	1.490
2	SFBay-2	7.77	27.0	5.000	7702.78±98.21	0.7355	1.3396	0.1043	0.1335	1.554
3	GCML-1	7.49	38.3	1.200	0.07±0.82	0.2398	0.0642	0.0521	0.0871	1.836
4	GCML-2	7.51	38.0	0.800	0.01±0.78	0.0610	0.0721	0.0110	0.0485	1.575
5	RA-1	7.40	27.3	6.936	75.00±9.43	0.3040	0.7510	0.1153	0.0960	1.435
6	RA-2	7.74	32.4	9.502	43.33±11.78	0.3141	0.4372	0.1061	0.1090	1.388
7	RA-3	7.75	22.4	2.260	98.33±0.00	0.6296	0.8922	0.1298	0.1227	1.376
8	RA-4	7.45	11.6	4.759	1880.00±575.11	0.2725	1.1714	1.0429	0.3704	1.398
9	RA-5	7.84	10.7	3.183	75.00±11.78	0.3868	0.6722	0.1322	0.0899	1.459
10	RA-6	8.40	24.9	4.500	301.67±54.21	0.7797	1.1461	0.1757	0.0944	1.363
11	RA-7	7.66	9.1	2.917	158.33±91.92	0.4877	0.9197	0.0654	0.0819	1.480
12	RA-8	7.73	32.0	1.588	66.67±21.21	0.1956	0.2308	0.0483	0.0637	1.602
13	RA-9	7.87	32.0	1.746	106.67±87.21	0.2012	0.2782	0.0428	0.0650	1.334
14	RA-10	7.85	33.1	1.700	86.67±44.78	0.1707	0.2023	0.0713	0.0766	1.534
15	RA-11	7.63	30.6	2.921	90.00±21.21	0.2685	0.4408	0.1467	0.1123	1.356
16	RA-13	8.10	37.2	1.585	39.17±4.32	0.1011	0.1456	0.0350	0.0607	1.333
17	RA-14	7.93	18.0	5.358	58.61±6.68	0.7318	1.2311	0.0943	0.0691	1.432
18	RA-15	8.19	7.8	6.664	343.33±33.00	1.4115	1.8796	0.0755	0.0519	1.521
19	RA-16	7.83	9.7	5.325	2155.42±483.39	0.8463	1.4371	0.2063	0.1031	1.420
20	RA-17	7.60	4.0	5.765	179.17±0.39	1.2175	1.9694	0.1723	0.1023	1.522
21	RA-18	8.07	37.2	2.052	443.89±5.50	0.1854	0.3370	0.0608	0.0720	1.495
22	RA-19	8.03	38.0	2.188	1483.61±36.14	0.1479	0.3143	0.0711	0.0789	1.398
23	RA-20	7.98	35.7	1.348	145.28±7.86	0.1263	0.1953	0.0428	0.0630	1.486
24	RA-21	8.00	24.5	4.004	354.17±1.18	0.4166	0.9422	0.2814	0.2406	1.595
25	RA-22	7.83	35.0	1.443	14.72±5.11	0.1412	0.2431	0.0450	0.0852	1.641
26	RA-23	8.20	36.5	2.180	1216.39±217.63	0.3386	0.3903	0.0461	0.0640	1.451
27	RA-24	7.78	20.0	2.623	695.83±22.00	0.3624	0.6038	0.0661	0.0707	1.462
28	RA-25	7.80	33.1	3.180	116.94±20.03	0.4668	0.6990	0.0281	0.0567	1.297
29	RA-26	8.04	35.7	1.664	159.72±7.46	0.1215	0.1359	0.0276	0.0559	1.491
30	RA-27	7.82	35.0	1.587	216.67±7.86	0.1883	0.2683	0.0301	0.0572	1.478
31	RA-28	7.79	35.7	1.192	270.28±10.61	0.0952	0.1636	0.0480	0.0484	1.766
32	RA-29	7.84	4.2	2.261	48.61±3.14	0.2269	0.2890	0.0646	0.0740	1.480
33	RA-30	7.74	28.8	2.354	184.72±22.39	0.3199	0.3612	0.0253	0.0597	1.404
34	RA-31	7.28	28.8	1.461	56.39±3.14	0.1580	0.2319	0.0632	0.0646	1.337
35	RA-32	7.46	24.9	1.199	30.56±8.25	0.1021	0.1523	0.0148	0.0505	1.554
36	RA-33	7.62	29.5	1.646	27.50±1.18	0.1161	0.2004	0.0248	0.0551	1.449
37	RA-34	7.65	31.3	1.619	25.83±3.14	0.1213	0.1893	0.0459	0.0565	1.370
38	RA-35	8.07	30.2	2.024	18.06±0.00	0.1817	0.2713	0.0500	0.0615	1.415
39	RA-36	7.99	34.3	2.108	17.92±2.36	0.2047	0.3225	0.0658	0.0720	1.699
40	RA-37	7.87	30.2	1.302	28.33±0.98	0.0847	0.1178	0.0452	0.0596	1.385
41	RA-38	7.74	29.9	2.353	35.28±8.25	0.1507	0.2621	0.0527	0.0743	1.372
42	RA-39	7.63	8.8	2.787	323.06±21.61	0.5485	0.5742	0.0346	0.0686	1.393
43	RA-40	7.52	14.3	5.894	126.94±1.57	0.8360	1.3668	0.1269	0.0725	1.343
44	RA-41	7.69	19.7	6.215	1233.06±101.35	0.9820	1.5787	0.2745	0.1961	1.424
45	RA-42	7.91	12.3	4.595	463.61±34.57	0.8558	1.1510	0.1156	0.0932	1.773
46	RA-43	8.27	30.6	2.665	171.39±47.14	0.2898	0.4537	0.0427	0.0552	1.252
47	RA-44	8.18	36.1	2.508	239.44±18.07	0.2612	0.3946	0.0390	0.0603	1.306
48	RA-45	7.90	29.5	5.724	573.61±56.18	0.8836	1.3517	0.1571	0.1578	1.375
49	RA-46	8.24	31.0	5.500	331.94±33.39	0.8661	1.1496	0.0381	0.0610	1.384
50	RA-47	8.22	35.7	3.545	292.78±1.57	0.3603	0.6168	0.0461	0.0639	1.409
51	RA-48	7.87	31.0	5.020	939.72±102.92	0.5343	1.0230	0.0774	0.0700	1.398
52	RA-49	8.06	32.0	4.331	1284.72±165.78	1.1233	1.2851	0.0000	0.0482	1.416
53	RA-50	7.99	30.6	12.380	134.72±12.18	0.9111	1.7172	0.0751	0.0706	1.523
54	RA-51	7.68	3.9	15.140	1735.56±8.25	3.5210	2.9766	0.0059	0.1025	1.238
55	RA-52	7.39	29.2	6.549	731.67±61.28	1.2210	1.5714	0.0000	0.0535	1.334
56	RA-53	7.19	2.7	20.660	1551.11±34.96	5.2787	2.6554	0.0000	0.0509	1.215
57	RA-54	7.58	3.6	6.934	112.22±7.07	0.8780	1.2700	0.1275	0.0939	1.459
58	RA-55	7.98	11.0	15.010	83.33±5.50	1.3237	1.8232	0.0941	0.0801	1.332
59	RA-56	7.42	24.9	7.431	296.25±35.36	1.4091	1.7224	0.0223	0.0765	1.515
60	RA-57	7.80	19.7	3.424	166.67±15.91	0.4206	0.6891	0.0478	0.0658	1.437
61	RA-58	7.55	25.9	1.587	30.28±3.54	0.1321	0.1519	0.0154	0.0337	1.407
62	RA-59	7.58	27.7	1.807	21.39±4.32	0.1308	0.1562	0.0075	0.0420	1.380
63	RA-60	7.44	21.1	3.011	23.33±0.78	0.3845	0.3688	0.0138	0.1179	1.333
64	RA-61	7.69	24.9	1.795	9.72±0.39	0.1627	0.2077	0.0189	0.0378	1.438
65	RA-62	7.68	25.2	1.799	19.58±0.59	0.1738	0.2424	0.0293	0.0406	1.422
66	SS-1	7.88	32.0	2.429		0.1692	0.2533	0.0483	0.0620	1.362
67	SS-2	7.22	1.9	5.229	20.42±2.95	0.9041	0.8390	0.1378	0.1179	1.255
68	SS-3	7.70	17.6	3.983	17.92±2.36	0.5595	0.6193	0.0329	0.0553	1.331
69	SS-4	7.38	27.7	2.014	18.06±0.00	0.2278	0.6132	0.0698	0.0587	1.575
70	SS-5	7.49	29.9	1.961	25.83±3.14	0.2070	0.2730	0.1009	0.0895	1.391
71	SS-6	7.78	31.3	1.924		0.1745	0.2347	0.0880	0.0759	1.604
72	ASW	7.80	30.0	1.087	17.22±1.18	0.0000	0.4750	0.1435	0.0894	1.960

Appendix C

Fluorophore Concentration Calculations

The following is a list of approximated concentrations of each fluorophore, defined by PARAFAC, in each water sample. The concentration (C) of a fluorophore in solution is linearly proportional to its fluorescent abundance value (F) defined by PARAFAC such that $F = kC$ where k is an experimentally-determined linear proportionality constant that is unique to the molecular identity and quantum efficiency of that fluorophore. In this study, PARAFAC was used to identify four fluorescent fractions in DOM from coastal marine and estuarine waters. Two of the fractions were defined as humic-like and fulvic-like based on their molecular weight difference, described by Wu et al. (2003). The other two fractions were defined as tryptophan-like and tyrosine-like based on comparisons with FEEMs of pure tryptophan (Trp) and tyrosine (Tyr) standard solutions.

Although the molecular structures of these four fluorescent DOM fractions are not known, they have similar structures to common standard material, where Suwanee River Fulvic Acid (SRFA) can be used to approximate the concentrations of the humic and fulvic material in SRFA equivalents, and pure Trp and Tyr standards can be used to approximate the concentrations of the tryptophan and

tyrosine material in Trp and Tyr equivalents, respectively. In order to approximate the concentrations in this manner, the fluorophore abundance values must be normalized to DOC (fluorophore abundance per mg DOC, referred to as 'quality index') so that comparisons between components in natural samples to standards can be achieved on a per mg basis.

Spectral deconvolution of the FEEMs from 72 water samples was performed simultaneously with the three standards (SRFA, Trp, and Tyr) in PARAFAC. Table C.1 presents the concentrations, fluorophore abundance values, and calculated k of the three standards.

Table C.1: Determination of linear proportionality constants for Trp, Tyr, humic and fulvic acid based on spectral deconvolution by PARAFAC.

	Concentration		Fluorophore	k
Standard	mmol·L^{-1}	mg C·L^{-1}	Abundance (Arb)	(L·mg^{-1} cm^{-1})
Trp	5.10×10^{-2}	3.30×10^{-2}	0.6182	18.73
Tyr	9.08×10^{-2}	5.40×10^{-2}	3.938	7.293
HA_{SRFA}	n/a	20	0.2940	0.0147
FA_{SRFA}	n/a	20	0.0512	0.0030

Dividing the fluorescence index by the appropriate linear proportionality constants, the concentrations of each fluorophore can be approximated, as seen in Table C.2. Note that the units of each concentration are represented as equivalents of their representative standards. For example, a humic acid concentration of 2 represents 2 SRFA equivalents.

Table C.2: Approximations of the fluorophore component concentrations. The concentrations of fluorescent humic (HA) and fulvic (FA) fractions are both represented in SRFA equivalents. The concentrations of fluorescent tryptophan (Trp) and tyrosine (Tyr) are represented in Trp and Tyr equivalents respectively.

	[HA]	[FA]	[Trp]$\times 10^{-3}$	[Tyr]$\times 10^{-3}$
SRFA	1.0	1.0	0.0	0.0
Trp	0.0	0.0	1.0	0.0
Tyr	0.0	0.0	0.0	1.0
SFB-1	11.86	89.42	1.39	4.60
SFB-2	10.01	103.05	1.11	3.66
GCML-1	13.59	20.58	2.32	9.96
GCML-2	5.19	34.66	0.73	8.32
RA-1	2.98	41.64	0.89	1.90
RA-2	2.25	17.70	0.60	1.57
RA-3	18.95	151.84	3.07	7.45
RA-4	3.90	94.67	11.7	10.7
RA-5	8.27	81.22	2.22	3.87
RA-6	11.79	97.96	2.08	2.88
RA-7	11.37	121.27	1.20	3.85
RA-8	8.38	55.90	1.62	5.50
RA-9	7.84	61.28	1.31	5.11
RA-10	6.83	45.77	2.24	6.18
RA-11	6.25	58.04	2.68	5.27
RA-13	4.34	35.33	1.18	5.25
RA-14	9.29	88.37	0.94	1.77
RA-15	14.41	108.48	0.61	1.07
RA-16	10.81	103.80	2.07	2.66
RA-17	14.37	131.39	1.60	2.43
RA-18	6.15	63.17	1.58	4.81
RA-19	4.60	55.25	1.73	4.95
RA-20	6.37	55.72	1.69	6.41
RA-21	7.08	90.51	3.75	8.24
RA-22	6.66	64.80	1.66	8.10
RA-23	10.57	68.86	1.13	4.02
RA-24	9.40	88.54	1.35	3.69
RA-25	9.99	84.54	0.47	2.44
RA-26	4.97	31.41	0.88	4.60
RA-27	8.07	65.02	1.01	4.94
RA-28	5.43	52.79	2.15	5.57
RA-29	6.83	49.16	1.53	4.49
RA-30	9.24	59.02	0.57	3.48
RA-31	7.36	61.05	2.31	6.07
RA-32	5.79	48.85	0.66	5.78
RA-33	4.80	46.83	0.80	4.59
RA-34	5.10	44.97	1.51	4.79
RA-35	6.11	51.55	1.32	4.16
RA-36	6.61	58.84	1.67	4.68
RA-37	4.43	34.80	1.85	6.27
RA-38	4.36	42.84	1.20	4.33
RA-39	13.39	79.24	0.66	3.37
RA-40	9.65	89.19	1.15	1.69
RA-41	10.75	97.70	2.36	4.33
RA-42	12.67	96.34	1.34	2.78
RA-43	7.40	65.48	0.86	2.84
RA-44	7.08	60.51	0.83	3.30
RA-45	10.50	90.83	1.47	3.78
RA-46	10.71	80.39	0.37	1.52
RA-47	6.91	66.92	0.69	2.47
RA-48	7.24	78.38	0.82	1.91
RA-49	17.64	114.12	0.00	1.53
RA-50	5.01	53.35	0.32	0.78
RA-51	15.82	75.62	0.02	0.93
RA-52	12.68	92.29	0.00	1.12
RA-53	17.38	49.43	0.00	0.34
RA-54	8.61	70.44	0.98	1.86
RA-55	6.00	46.72	0.34	0.73
RA-56	12.90	89.15	0.16	1.41
RA-57	8.36	77.41	0.74	2.64
RA-58	5.66	36.81	0.51	2.91
RA-59	4.92	33.25	0.22	3.18
RA-60	8.69	47.11	0.24	1.78
RA-61	6.17	44.50	0.56	2.88
RA-62	6.57	51.82	0.87	3.10
SS-1	4.74	40.11	1.06	3.50
SS-2	11.76	61.71	1.41	3.09
SS-3	9.56	59.80	0.44	1.90
SS-4	7.69	117.10	1.85	3.99
SS-5	7.18	53.54	2.75	6.26
SS-6	6.17	46.92	2.44	5.41

Appendix D

Pearson Correlation Matrices

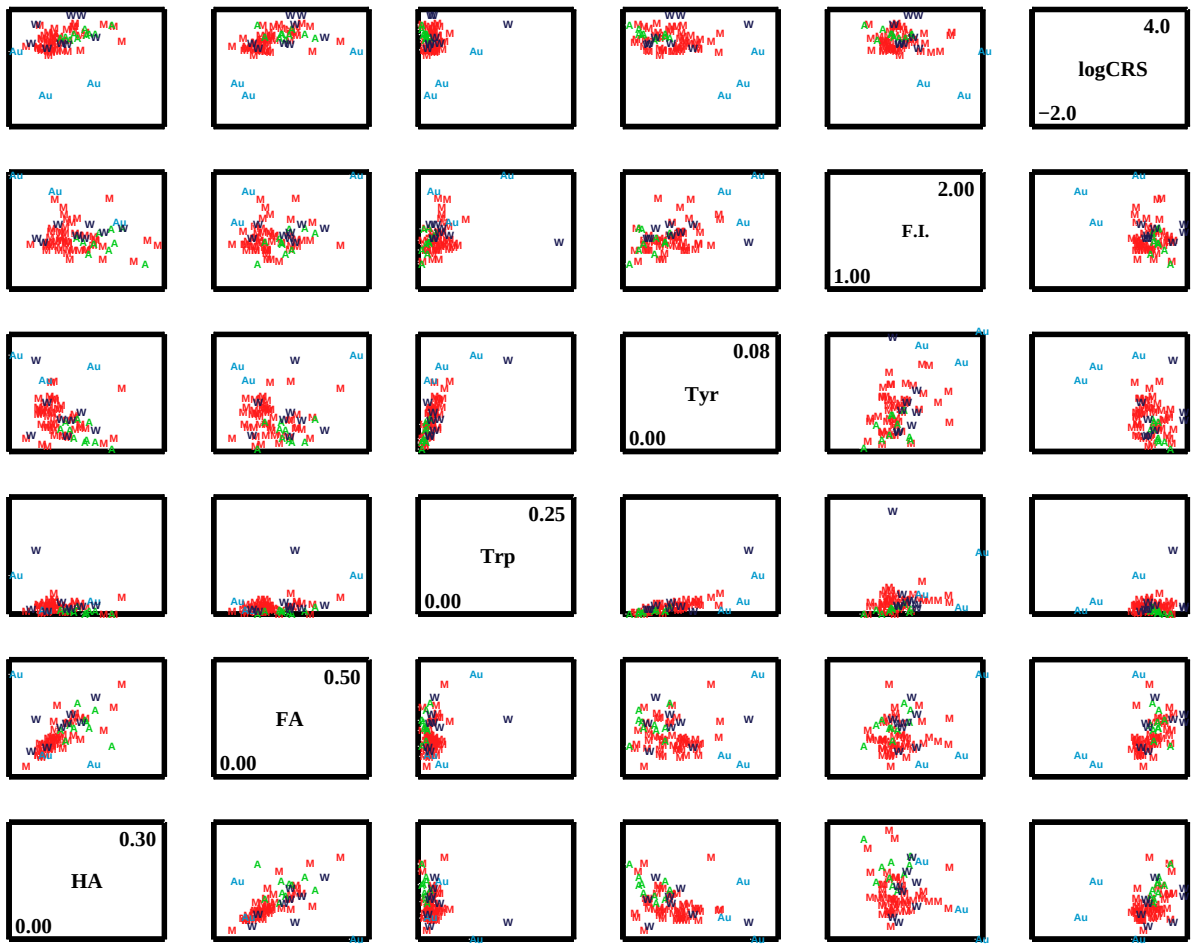

Figure D.1: Scatterplot matrix of the following 6 variables: humic index (HA), fulvic index (FA), tryptophan (Trp) index, tyrosine index (Tyr), fluorescent index (FI), and logCRS. Each cell of the scatterplot matrix represents a separate scatterplot where the x-axis is indicated by the labelled cell in the same column and the y-axis is indicated by the labelled cell in the same row.

Table D.1: Correlation matrix for fluorescent DOM and CRS based on values obtained from allochthonous-source samples only (sample set of 11). Values are correlation coefficients and probability, listed as r(p). HA=humic index, FI=fulvic index, Trp=tryptophan index, Tyr=tyrosine index, FI=fluorescent index, CRS=chromium(II) reducible sulfide.

	HA	FA	Trp	Tyr	FI	CRS
HA	1.0	0.10(0.1)	-0.49(>0.1)	-0.62(0.05)	-0.26(0.05)	0.83(0.003)
FA	0.10(0.1)	1.0	0.50(0.1)	0.22(0.05)	0.65(0.04)	-0.37(>0.1)
Trp	-0.49(>0.1)	0.50(0.1)	1.0	0.82(0.003)	0.52(0.1)	-0.73(0.01)
Tyr	-0.62(0.05)	0.22(0.05)	0.82(0.003)	1.0	0.31(0.03)	-0.76(0.01)
FI	-0.26(0.05)	0.65(0.04)	0.52(0.1)	0.31(0.03)	1.0	-0.66(0.04)
CRS	0.83(0.003)	-0.37(>0.1)	-0.73(0.01)	-0.76(0.01)	-0.66(0.04)	1.0

Table D.2: Correlation matrix for fluorescent DOM and CRS based on values obtained from autochthonous-source samples only (sample set of 3).

	HA	FA	Trp	Tyr	FI	CRS
HA	1.0	-0.84(0.1)	-0.62(>0.1)	-0.31(>0.1)	-0.99(0.04)	0.61(>0.1)
FA	-0.84(0.1)	1.0	0.95(>0.1)	0.78(>0.1)	0.80(>0.1)	0.94(>0.1)
Trp	-0.62(>0.1)	0.95(>0.1)	1.0	0.94(0.05)	0.57(>0.1)	1.0(0.01)
Tyr	-0.31(>0.1)	0.78(>0.1)	0.94(0.05)	1.0	0.24(>0.1)	0.94(0.1)
FI	-0.99(0.04)	0.80(>0.1)	0.57(>0.1)	0.24(>0.1)	1.0	0.56(0.1)
CRS	0.61(>0.1)	0.94(>0.1)	1.0(0.01)	0.94(0.1)	0.56(0.1)	1.0

Table D.3: Correlation matrix for fluorescent DOM and CRS based on values obtained from wastewater-source samples only (sample set of 8).

	HA	FA	Trp	Tyr	FI	CRS
HA	1.0	0.77(0.02)	-0.40(>0.1)	-0.41(>0.1)	0.48(>0.1)	0.28(>0.1)
FA	0.77(0.02)	1.0	0.20(>0.1)	0.02(>0.1)	0.15(0.01)	0.45(0.1)
Trp	-0.40(>0.1)	0.20(>0.1)	1.0	0.87(0.005)	-0.58(0.1)	0.31(>0.1)
Tyr	-0.41(>0.1)	0.02(>0.1)	0.87(0.005)	1.0	-0.25(>0.1)	0.36(0.1)
FI	0.48(>0.1)	0.15(0.01)	-0.58(0.1)	-0.25(>0.1)	1.0	0.11(>0.1)
CRS	0.28(>0.1)	0.45(0.1)	0.31(>0.1)	0.36(0.1)	0.11(>0.1)	1.0

Table D.4: Correlation matrix for fluorescent DOM and CRS based on values obtained from mixed-source samples only (sample set of 50).

	HA	FA	Trp	Tyr	FI	CRS
HA	1.0	0.81(<0.001)	0.06(>0.1)	-0.15(0.05)	-0.04(>0.1)	0.44(0.002)
FA	0.81(<0.001)	1.0	0.35(0.01)	0.02(>0.1)	0.14(0.1)	0.49(<0.001)
Trp	0.06(>0.1)	0.35(0.01)	1.0	0.78(<0.001)	0.24(0.09)	0.07(0.1)
Tyr	-0.15(0.05)	0.02(>0.1)	0.78(<0.001)	1.0	0.25(0.08)	-0.17(0.1)
FI	-0.04(>0.1)	0.14(0.1)	0.24(0.09)	0.25(0.08)	1.0	0.03(0.1)
CRS	0.44(0.002)	0.49(<0.001)	0.07(0.1)	-0.17(0.1)	0.03(0.1)	1.0

Appendix E

Application of a Significance Test for Comparison of the Means of Two Samples

The goal here is to assess whether variations between the toxicity data collected in this study and published data from Arnold (2005) and Arnold et al. (2006) are significant at a 95% confidence limit. The significance test (t-test) can be used here, as suggested by Miller and Miller (1993). Tables E.1 and E.2 are measured results of acute toxicity tests performed on the listed subset of samples by Ray and myself respectively.

Table E.1: Measured DOC and EC_{50} results from Arnold et al. (2006).

#	ID	DOC	EC_{50}	EC_{50}/mg DOC
R1	RA-22	1.9	17.4	9.1579
R2	RA-33	1.3	13.9	10.6923
R3	RA-11	1.5	16.8	11.2000
R4	SFBay-2	5	37.2	7.4400
R5	RA-16	3.3	24.8	7.5152
R6	SFBay-1	5.7	34.8	6.1053
R7	RA-17	8.7	71	8.1609
R8	GCML-1	0.8	6.3	7.8750
R9	GCML-2	1.2	10.9	9.0833
			Mean	8.5811
		Standard Deviation		1.62

Table E.2: Measured DOC and EC_{50}s from my experimental results.

#	ID	DOC	EC_{50}	EC_{50}/mg DOC
S1	ASW	1.087	12.656	11.6431
S2	RA-4B	3.606	22.719	6.3003
S3	RA-19	2.326	19.008	8.1720
S4	RA-25	3.374	20.665	6.1248
S5	RA-33	1.880	16.037	8.5303
S6	RA-60	3.327	20.451	6.1470
S7	RA-1	6.936	31.576	4.5525
S8	RA-5	3.183	30.964	9.7279
S9	RA-34	1.619	15.959	9.8573
S10	RA-54	6.934	31.186	4.4975
			Mean	7.555
		Standard Deviation		2.40

A plot of the two data sets is illustrated in Figure E.1.

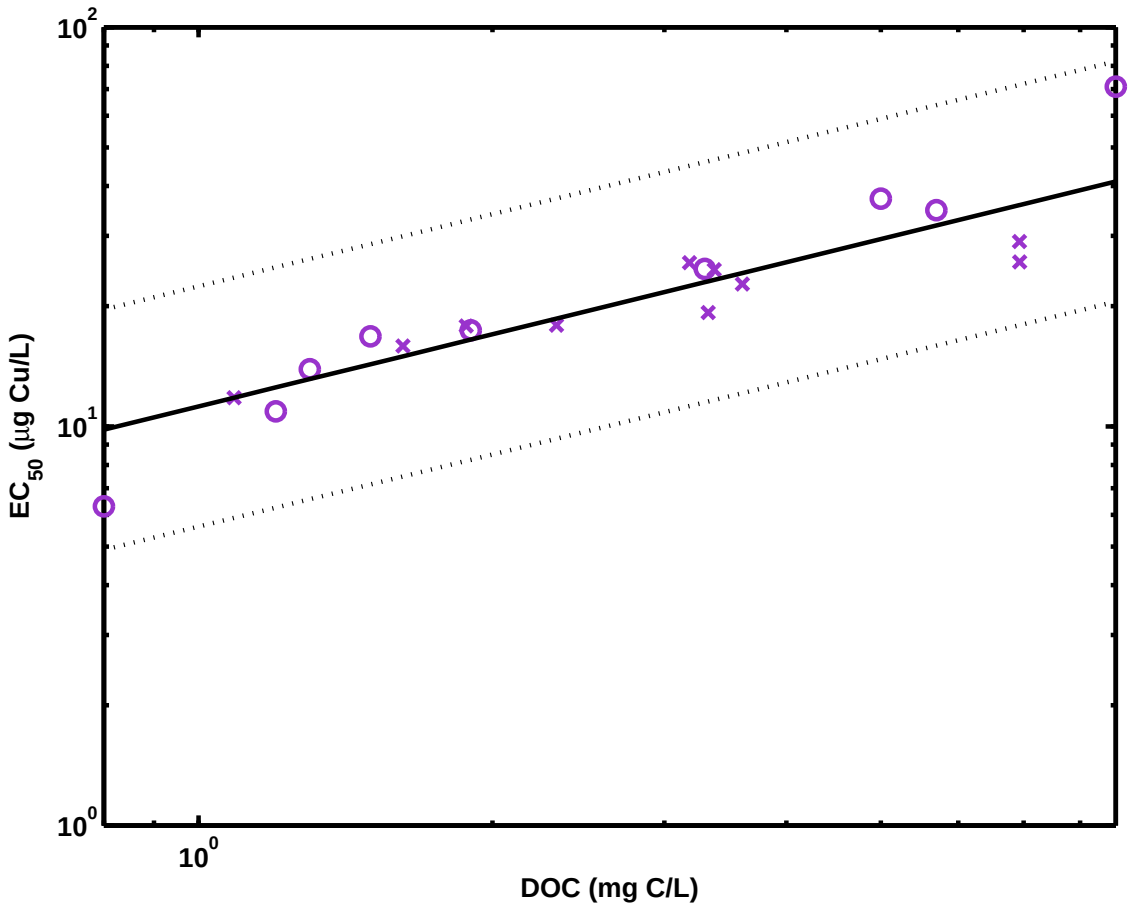

Figure E.1: Plot of total copper EC_{50} with respect to DOC. Data sets from Tables E.1 and E.2 are plotted in O and X respectively. The solid line represents the predictive equation EC_{50}=11.22 $DOC^{0.6}$, determined by linear regression on a dataset of sample size n=75 (Arnold et al., 2006).

The equation of the line for the data plotted as X in Figure E.1 is EC_{50}=12.44 $DOC^{0.5}$ (r^2=0.86, p=0.002, n=10) whereas O is EC_{50}=9.52 $DOC^{0.9}$ (r^2=0.92, p=0.001, n=9). The equation of the line for all the points is EC_{50}=10.27 $DOC^{0.7}$ (r^2=0.89, p=0.001, n=19) (Figure E.1). Given that the plot of the two data sets shows them to be almost overlapping and that the difference in means (1.03) is small, initial observations show that the toxicity data is very similar. However, a t-test was used to statistically show whether the variation between the data could be attributed to random error. In order to compare the two data sets in Tables E.1 and E.2, the EC_{50} values were normalized to DOC. This removes the change in EC_{50} with respect to DOC, resulting in comparisons between intensive values as

opposed to extensive. Intensive values allow for statistical comparisons since the average and standard deviation can now be calculated between each data set.

The null hypothesis for the t-test states that there is no significant difference between the two data sets, other than that which can be attributed to random variation (Miller and Miller, 1993). A pooled estimate of the standard deviation was calculated from the two individual standard deviations using Equation E.1, followed by application of a calculated t value (Equation E.2) where t has $n_1 + n_2 - 2$ degrees of freedom:

$$s_{pooled} = \sqrt{\frac{s_1^2(n_1 - 1) + s_2^2(n_2 - 1)}{n_1 + n_2 - 2}} \tag{E.1}$$

$$t_{calc} = \frac{\mid \bar{x}_1 - \bar{x}_2 \mid}{s_{pooled}} \sqrt{\frac{n_1 n_2}{n_1 + n_2}} \tag{E.2}$$

where x is the sample mean, s is the standard deviation, and n is the sample size of *1* and *2* data sets of Rays and my data respectively. The results of the t-test are found in Table E.3.

Table E.3: Results from the t-test as a comparison of the means of two samples.

df	17
s_{pooled}	2.191
t_{calc}	0.774
t_{95}	2.11

The calculated value of t was less than the critical value (P = 0.05), and so the null hypothesis was retained. Since the data points overlapped in Figure E.1 and the t-test showed no evidence of a difference, the results obtained in this study were

significantly similar to the data published in Arnold et al. (2006) and differences between the two data sets can be attributed to random variation.

Appendix F

Toxicity Data

Table F.1: Water chemistry measurements and toxicity results samples from Arnold (2005) and Arnold et al. (2006) (1 - 9) and from this study (10 - 19). DOC is reported in mg C·L^{-1}. Toxicity data is reported as total dissolved copper (in μg Cu·L^{-1}) with p=0.05 lower and upper confidence limits. Calculated toxicity data is based on the equation $EC_{50} = 11.22DOC^{0.6}$ (Arnold et al., 2006). Free copper concentrations were calculated by R. Santore at HydroQual© and reported in μg Cu·L^{-1}.

	ID	DOC	CRS (nM)	HA (Arb)	FA (Arb)	Trp (Arb)	Tyr (Arb)	SAC_{340}	Calc EC_{50}	LCL	UCL	EC_{50}	LCL	UCL	Free Cu
1	RA-22	1.9	n/a	0.1859	0.3201	0.0593	0.1122	n/a	16.49	8.24	32.98	17.4	n/a	n/a	5.03×10^{-3}
2	RA-33	1.3	n/a	0.0917	0.1583	0.0196	0.0435	n/a	13.13	6.57	26.26	13.9	n/a	n/a	7.05×10^{-3}
3	RA-11	1.5	n/a	0.1379	0.2264	0.0753	0.0577	n/a	14.31	7.16	28.62	16.8	n/a	n/a	8.20×10^{-3}
4	SFBay-2	5.0	n/a	0.7355	1.3396	0.1043	0.1335	n/a	29.47	14.73	58.94	37.2	n/a	n/a	3.01×10^{-3}
5	RA-16	3.3	n/a	0.5245	0.8906	0.1278	0.0639	n/a	22.97	11.48	45.93	24.8	n/a	n/a	2.25×10^{-3}
6	SFBay-1	5.7	n/a	0.9935	1.3252	0.1481	0.1914	n/a	31.88	15.94	63.76	34.8	n/a	n/a	1.87×10^{-3}
7	RA-17	8.7	n/a	1.8373	2.9720	0.2600	0.1544	n/a	41.09	20.54	82.17	71	n/a	n/a	2.24×10^{-3}
8	GCML-1	0.8	n/a	0.2398	0.0642	0.0521	0.0871	n/a	9.81	4.91	19.63	6.3	n/a	n/a	3.29×10^{-3}
9	GCML-2	1.2	n/a	0.0610	0.0721	0.0110	0.0485	n/a	12.52	6.26	25.03	10.9	n/a	n/a	4.91×10^{-3}
10	ASW	1.087	17.22±1.18	0.0000	0.4750	0.1435	0.0894	0.00	11.80	5.90	23.59	12.656	11.427	14.322	7.75×10^{-3}
11	RA-4B	3.606	44.17±0.00	0.3364	0.8314	0.1727	0.1793	8.30	24.22	12.11	48.44	22.719	20.524	25.587	1.98×10^{-3}
12	RA-19	2.326	24.44±7.07	0.1358	0.2044	0.0558	0.0674	0.99	18.62	9.31	37.24	19.008	17.9	20.331	3.66×10^{-3}
13	RA-25	3.374	39.17±7.07	0.4338	0.8340	0.0142	0.0753	7.96	23.27	11.64	46.55	20.665	19.55	22.065	1.90×10^{-3}
14	RA-33	1.880	30.00±2.36	0.1161	0.2004	0.0248	0.0551	4.90	16.39	8.19	32.77	16.037	14.038	19.467	4.23×10^{-3}
15	RA-60	3.327	23.33±1.18	0.5631	0.5741	0.1754	0.2158	15.00	23.08	11.54	46.16	20.451	19.285	21.652	2.01×10^{-3}
16	RA-1	6.936	27.78±3.93	0.3277	0.7785	0.1116	0.0892	2.21	35.86	17.93	71.73	31.576	30.771	32.391	9.72×10^{-4}
17	RA-5	3.183	25.56±0.78	0.2966	1.0958	0.0974	0.0949	26.53	22.47	11.24	44.945	30.964	30.132	31.654	5.89×10^{-3}
18	RA-34	1.619	4.17±0.39	0.0425	0.7403	0.0815	0.0606	8.06	14.98	7.49	29.96	15.959	15.15	16.749	5.92×10^{-3}
19	RA-54	6.934	28.33±5.50	0.7716	1.7987	0.0000	0.0853	13.28	35.86	17.93	71.72	31.186	30.098	32.073	9.66×10^{-4}

References

Al-Farawati, R., van den Berg, C. M., 1999. Metal-sulfide complexation in seawater. Marine Chemistry 63, 331–352.

Allen, H., 1993. The significance of trace metal speciation for water, sediment, and soil quality standards. Science of the Total Environment 134, 23.

Allen, H., Hansen, S., 1996. The importance of trace metal speciation to water quality criteria. Water Environment Research 68, 42–54.

Aluwihare, L. I., Repeta, D. J., Chen, R. F., 1997. A major biopolymeric component to dissolved organic carbon in surface seawater. Nature 387, 166–169.

Andreae, T., Cutter, G., Hussain, N., Radford-Knoery, J., Andreae, M., 1991. Hydrogen sulfide and radon in and over the western north-atlantic ocean. Journal of Geophysical Research 96, 18753–18760.

Arnold, W. R., 2005. Effects of dissolved organic carbon on copper toxicity: Implications for saltwater criteria. Integrated Environmental Assessment and Management 1, 34–39.

Arnold, W. R., Cotsifas, J. S., Corneille, K., 2006. Validation and update of a model used to predict copper toxicity to the marine bivalve *Mytilus sp.* Environmental Toxicology 21, 65–70.

Arnold, W. R., Cotsifas, J. S., Winter, A. R., Klinck, J. S., Smith, D. S., Playle, R. C., 2007. Effects of using synthetic sea salts when measuring and modeling

copper toxicity in saltwater toxicity tests. Environmental Toxicology and Chemistry 26 (5), 935–943.

A.S.T.M. International, 2004. Standard guide for conducting static acute toxicity tests starting with embryos of four species of saltwater bivalve molluscs. Tech. Rep. E 724-98, ASTM International, West Conshohocken, PA.

Baker, A., 2001. Fluorescence excitation-emission matrix characterization of some sewage-impacted rivers. Environmental Science and Technology 35, 948–953.

Bianchini, A., Bowles, K. C., 2002. Metal sulfides in oxygenated aquatic systems: Implications for the biotic ligand model. Comparative Biochemistry and Physiology Part C 133, 51–64.

Bowen, H., 1985. The Handbook of Environmental Chemistry: The natural environment and biogeochemical cycles. Vol. 1. Springer-Verlag, New York, NY.

Bowles, K. C., Bell, R. A., Ernste, M. J., Kramer, J. R., Manolopoulos, H., Ogden, N., 2002. Synthesis and characterization of metal sulfide clusters for toxicological studies. Environmental Toxicology and Chemistry 21 (4), 693–699.

Bowles, K. C., Ernste, M. J., Kramer, J. R., 2003. Trace sulfide determination in oxic freshwaters. Analytica Chimica Acta 477, 113–124.

Box, G. E., Hunter, W. G., Hunter, J. S., 1978. Statistics for Experiments: An Introduction to Design, Data Analysis, and Model Building. John Wiley, John & Sons, Incorporated.

Campbell, P. G., 1995. Metal Speciation and Bioavailability in Aquatic Systems. John Wiley, John & Sons, Incorporated, Chichester, NY.

Canfield, D., Raiswell, R., Westrich, J., Reaves, C., Berner, R., 1986. The use of chromium reduction in the analysis of reduced inorganic sulfur in sediments and shales. Chemical Geology 54, 149–155.

CCME, December 2007. Canadian water quality guidelines for the protection of aquatic life. Canadian Council of Ministers of the Environment, 6th Edition.

Cline, J., 1969. Spectrophotometric determination of hydrogen sulfide in natural waters. Limnology and Oceanography 14, 454–458.

Coble, P., 1996. Characterization of marine and terrestrial DOM in seawater using excitation-emission matrix spectroscopy. Marine Chemistry 51, 325–346.

Dafner, E. V., Wangersky, P. J., 2002a. A brief overview of modern directions in marine DOC studies Part I. Methodological aspects. Journal of Environmental Monitoring 4, 48–54.

Dafner, E. V., Wangersky, P. J., 2002b. A brief overview of modern directions in marine DOC studies Part II. Recent progress in marine DOC studies. Journal of Environmental Monitoring 4, 55–69.

Day, J. J., Hall, C., Kemp, W., Janez-Arancibia, A., 1989. Estuarine Ecology. John Wiley, John & Sons, Incorporated, New York, NY.

De Schamphelaere, K., Janssen, C., 2002. A biotic ligand model predicting acute copper toxicity for *Daphnia magna*: The effect of calcium, magnesium, sodium, potassium, and pH. Environmental Science and Technology 36, 48–54.

Dehnen, S., Schäfer, A., Ahlrichs, R., Fenske, D., 1996. An *ab initio* study of structures and energetics of copper sulfide clusters. Chemistry A European Journal 2, 429–435.

DiToro, D., Allen, H., Bergmen, H., Meyer, J., Paquin, P., Santore, R., 2001. Biotic ligand model of the acute toxicity of metals I: Technical basis. Environmental Toxicology and Chemistry 20, 2383–2396.

Du, H., Fuh, R. A., Li, J., Corkan, A., Lindsey, J. S., 1998. PhotochemCAD: A computer-aided design and research tool in photochemistry 68, 141-142, (1998). Photochemistry and Photobiology 68, 141–142.

Erickson, R. J., Benoit, D. A., Mattson, V. R., Nelson Jr., H. P., Leonard, E. N., 1996. The effects of water chemistry on the toxicology of copper to fathead minnows. Environmental Toxicology and Chemistry 15, 181–193.

Eriksen, R. S., Mackey, D. J., van Dam, R., Nowak, B., 2001. Copper speciation and toxicity in Macquarie Harbour, Tasmania: An investigation using a copper ion selective electrode. Marine Chemistry 74, 99–113.

Food and Nutrition Board, Institute of Medicine, 2001. Dietary Reference Intakes for Vitamin A, Vitamin K, Arsenic, Boron, Chromium, Copper, Iodine, Iron, Manganese, Molybdenum, Nickel, Silicon, Vanadium, and Zinc. National Academies of Sciences, Washington D.C.

Guilbault, G., 1973. Practical Fluorescence. Marcel Dekker, New York, NY.

Hall, G. J., Kenny, J. E., 2007. Estuarine water classification using EEM spectroscopy and PARAFAC-SIMCA. Analytica Chimica Acta 581, 118–124.

Hall, W. S., Bushong, S. J., Lenwood, W. H. J., Lenkevich, M. J., Pinkney, A. E., 2004. Monitoring dissolved copper concentrations in Chesapeake Bay, USA. Environmental Monitoring and Assessment 11, 33–42.

Harvey, G. R., Boran, D. A., Chesal, L. A., Tokar, J. M., 1983. The structure of marine fulvic and humic acids. Marine Chemistry 12, 119–132.

Hessen, D., Tranvik, L., 1998. Aquatic Humic Substances: Ecology and Biogeochemistry. Springer-Verlag, Berlin, Heidelberg, Germany.

Hoenicke, Rainer, D. J. A., Gunther, A., Mumley, T. E., Abu-Saba, K., Taberski, K., 2003. Effective application of monitoring information: The case of San Francisco Bay. Environmental Monitoring and Assessment 81, 15–25.

Jones, C., 1888. A rapid method for the reduction of ferric sulphate in volumetric analysis. Transactions of the American Institute of Mining, Metalurgical and Petroluem Engineers 17, 411.

Kramer, J. R., Bell, R. A., Smith, D. S., 2007. Determination of sulfide ligands and association with natural organic matter. Applied Geochemistry 22, 1606–1611.

Lenwood, W. H. J., Scott, M. C., Killen, W. D., 1998. Ecological risk assessment of copper and cadmium in surface waters of Chesapeake Bay watershed. Environmental Toxicology and Chemistry 17, 1172–1189.

Leppäkoski, E., Bonsdorff, E., 1989. Chemicals in the Aquatic Environment: Advanced Hazard Assessment. Springer-Verlag.

Long, E. R., Buchman, M. F., Bay, S. M., Breteler, R. J., Carr, S. R., Chapman, P. M., Hose, Jo Ellen, L. A. L., Scott, J., Wolfe, D. A., 1990. Comparative evaluation of five toxicity tests with sediments from San Francisco Bay and Tomales Bay, California. Environmental Toxicology and Chemistry 9, 1193–1214.

Lorenzo, J. I., Beiras, R., Mubiana, V. K., Blust, R., 2005. Copper uptake by *Mytilus edulis* in the presence of humic acids. Environmental Toxicology and Chemistry 24, 973–980.

Lorenzo, J. I., Nieto, O., Beiras, R., 2006. Anodic stripping voltammetry measures copper bioavailability for sea urchin larvae in the presence of fulvic acids. Environmental Toxicology and Chemistry 25, 36–44.

Luther, G. I., Tsamakis, E., 1989. Concentration and form of dissolved sulfide in the oxic water column of the ocean. Marine Chemistry 27, 165–177.

Ma, H., Allen, H., Yin, Y., 2001. Characterization of isolated fractions of dissolved organic matter from natural waters and a wastewater effluent. Water Research 35, 985–996.

Malcolm, R., 1990. The uniqueness of humic substances in each of soil, stream, and marine environments. Analytica Chimica Acta 232, 19–30.

Mantoura, R., Woodward, M., 1983. Conservative behaviour of riverine dissolved organic carbon in the Severn Estuary: Chemical and geochemical implications. Geochimica et Cosmochimica Acta 47, 1293–1309.

Martell, A. E., Smith, R. M., 1974. Critical Stability Constants Volume 1: Amino Acids. Plenum Press.

Martin, M., Ichikawa, G., Goetzl, J., DeLoris Reyes, M., Stephenson, M., 1984. Relationships between physiological stress and trace toxic substances in the bay mussel, *Mytilus edulis*, from San Francisco Bay, California. Marine Environmental Research 11, 91–110.

McDonald, S., Bishop, A., Prenzler, P., Robards, K., 2004. Analytical chemistry of freshwater humic substances. Analytica Chimica Acta 527, 105–124.

McGeer, J. C., Playle, R., Wood, C. M., Galvez, F., 2000. A physiologically-based biotic ligand model for predicting the acute toxicity of waterborne silver to rainbow trout in freshwaters. Environmental Science and Technology 34, 4199–4207.

McKnight, D. M., Boyer, E. W., Westerhoff, P. K., Doran, P. T., Kulbe, T., Anderson, D. T., 2001. Spectrofluorometric characterization of dissolved organic matter for indication of precursor organic material and aromaticity. Limnology and Oceanography 46 (1), 38–48.

Miller, J., Miller, J., 1993. Statistics for Analytical Chemistry, 3rd Edition. Ellis Horwood PTR Prentice Hall, West Sussex, Great Britian.

Millero, F. J., 2001. Physical Chemistry of Natural Waters. John Wiley, John & Sons, Incorporated.

Mopper, K., Schultz, C., 1993. Fluorescence as a possible tool for studying the nature and water column distribution of DOC components. Marine Chemistry 41, 229–238.

Morel, F., 1983. Principles of Aquatic Chemistry. Wiley-Interscience, New York, NY.

Nadella, S. R., Fitzpatrick, J. L., Franklin, N., Bucking, C., Smith, D. S., Wood, C. M., 2009. Toxicity of dissolved Cu, Zn, Ni, and Cd to developing embryos of

the blue mussel (*Mytilus trossolus*) and the protective effect of dissolved organic carbon. Comparative Biochemistry and Physiology Part C 149, 340–348.

Nahorniak, M. L., Booksh, K. S., 2003. Optimizing the implementation of the PARAFAC method for near-real time calibration of excitation-emission fluorescence analysis. Journal of Chemometrics 17, 608–617.

NOAA, 2004. Population trends along the coastal united states: 1980-2008. Tech. rep., National Oceanic and Atmospheric Administration: National Ocean Service.

Pagenkopf, G., 1983. Gill surface interaction model for trace-metal toxicity to fishes: Role of complexation, pH, and water hardness. Environmental Science and Technology 17, 342–347.

Pagenkopf, G., Russo, R., Thurston, R., 1974. Effect of complexation on toxicity of copper to fishes. Journal of the Fisheries Board of Canada 31, 462.

Paquin, P., Gorsuch, J., Apte, S., Graeme, E., Bowles, K. C., Campbell, P. G., Delos, C., DiToro, D. M., Dwyer, R., Galvez, F., Gensemer, R., Goss, G., Hogstrand, C., Janssen, C., McGeer, J. C., Naddy, R., Playle, R., Santore, R. C., Schneider, U., Stubblefield, W., Wood, C. M., Wu, K., 2002. The biotic ligand model: A historical overview. Comparative Biochemistry and Physiology Part C 133, 3–35.

Rozan, T., Lassman, M., Ridge, D., Luther, G., 2000. Evidence for multinuclear Fe, Cu, and Zn molecular sulfide clusters in oxic river waters. Nature 406, 879–882.

Santore, R., DiToro, D., Paquin, P., Allen, H., Meyer, J., 2001. Biotic ligand model of the acute toxicity of metals II: Application to acute copper toxicity in freshwater fish and *Daphnia*. Environmental Toxicology and Chemistry 20, 2397–2402.

Santore, R., Driscoll, C., 1995. Chemical equilibrium and reaction models. American Society of Agronomy, Madison, WI.

Santore, R. C., 2007. BLM - Biotic Ligand Model.
URL *http* : *//www.hydroqual.com/wr*$_b$*lm.html*

Schiff, K., Diehl, D., Valkirs, A., 2004. Copper emissions from antifouling paint on recreational vessels. Marine Pollution Bulletin 48, 371–377.

Schwartz, M., Curtis, P., Playle, R., 2004. Influence of natural organic matter source on acute copper, lead, and cadmium toxicity to rainbow trout (*Oncorhynchus mykiss*). Environmental Toxicology and Chemistry 23 (12), 2889–2899.

Sedlak, D. L., Phinney, J. T., Bedsworth, W. W., 1997. Strongly complexed Cu and Ni in wastewater effluents and surface runoff. Environmental Science and Technology 31, 3010–3016.

Sigleo, A., Means, J., 1990. Organic and inorganic components in estuarine colloids: Implications for sorption and transport of pollutants. Reviews of Environmental Contamination and Toxicology 112, 123–147.

Smith, D. S., Bell, R. A., Kramer, J. R., 2002. Metal speciation in natural waters with emphasis on reduced sulfur groups as strong metal binding sites. Comparative Biochemistry and Physiology Part C 133, 65–74.

Smith, D. S., Bell, R. A., Valliant, J., Kramer, J. R., 2004. Determination of strong ligand sites in sewage effluent-impacted waters by competitive ligand titration with silver. Environmental Science and Technology 38, 2120–2125.

Smith, D. S., Kramer, J. R., 1999. Fluorescence analysis for multi-site aluminium binding to natural organic matter. Environment International 25 (2/3), 295–306.

Stedmon, C. A., Markager, S., 2005. Resolving the variability in dissolved organic matter fluorescence in a termperate estuary and its catchment using PARAFAC analysis. Limnology and Oceanography 50 (2), 686–697.

Stedmon, C. A., Markager, S., Bro, R., 2003. Tracing dissolved organic matter in aquatic environments using a new approach to fluorescence spectroscopy. Marine Chemistry 82, 239–254.

Sunda, W., Gillespie, P., 1979. The response of a marine bacterium to cupric ion and its use to estimate cupric ion activity in seawater. Journal of Marine Research 37, 761–777.

Tang, D., Santschi, P. H., 2000. Sensitive determination of dissolved sulfide in estuarine water by solid-phase extraction and high-performance liquid chromatography of methylene blue. Journal of Chromatography A 883, 305–309.

Tang, D., Warnken, K. W., Santschi, P. H., 2002. Distribution and partitioning of trace metals (Cd, Cu, Ni, Pb, Zn) in Galveston Bay waters. Marine Chemistry 78, 29–45.

Tipping, E., 1994. WHAM - a chemical equilibrium model and computer code for waters, sediments, and soils incorporating a discrete site/electrostatic model of ion-binding by humic substances. Computers and Geosciences 20 (6), 973–1023.

Town, R. M., Filella, M., 2000. Dispelling the myths: Is the existence of L1 and L2 ligands necessary to explain metal ion speciation in natural waters? Limnology and Oceanography 45, 1341–1357.

U.S. EPA, April 1995a. Ambient water quality criteria - saltwater copper addendum. Office of Water, Washington, DC, Draft Edition.

U.S. EPA, 1995b. Short-term methods for estimating the chronic toxicity of effluents and receiving waters to west coast marine and estuarine organisms. Tech. Rep. EPA/600/R-95/136, Office of Water, Washington, D.C.

U.S. EPA, February 2007. Aquatic life ambient freshwater quality criteria - copper. Tech. Rep. EPA/822/R-07/01, Washington, D.C.

van Veen, E., Burton, N., Comber, S., Gardner, M., 2002. Speciation of copper in sewage effluents and its toxicity to *Daphnia magna*. Environmental Toxicology and Chemistry 21, 275–280.

Winter, A. R., Fish, T. A. E., Playle, R. C., Smith, D. S., Curtis, P. J., 2007. Photodegradation of natural organic matter from diverse freshwater sources. Aquatic Toxicology 84, 215–222.

Wood, C., Adams, W., Ankley, G., 1997. Reassessment of metal criteria for aquatic life protection: Priorities for research and implementation. SETAC Press, Pensacola, FL.

Wu, F., Evans, R., Dillon, P., 2003. Separation and characterization of NOM by high-performance liquid chromatography and on-line three-dimensional excitation emission matrix fluorescence detection. Environmental Science and Technology 37, 3687–3693.

Xie, W.-H., Shiu, W.-Y., Mackay, D., 1997. A review of the effect of salts on the solubility of organic compounds in seawater. Marine Environmental Research 44 (4), 429–444.